MARMARA UNIVERSITY
INSTITUTE FOR GRADUATE STUDIES
IN PURE AND APPLIED SCIENCES

COMPUTATIONAL STUDY ON THE INHIBITON MULTIDRUG RESISTANCE EFFLUX PUMPS

DUYGU ŞENTÜRK KARAGÖZ

MASTER THESIS
Department of Bioengineering

Thesis Supervisor
Prof. Dr. Berna SARIYAR AKBULUT

Thesis CO- Supervisor
Assoc. Prof. Dr. Pemra ÖZBEK SARICA

ISTANBUL, 2019

MARMARA UNIVERSITY
INSTITUTE FOR GRADUATE STUDIES
IN PURE AND APPLIED SCIENCES

COMPUTATIONAL STUDY ON THE INHIBITON MULTIDRUG RESISTANCE EFFLUX PUMPS

DUYGU ŞENTÜRK KARAGÖZ

(524216004)

MASTER THESIS
Department of Bioengineering

Thesis Supervisor
Prof. Dr. Berna SARIYAR AKBULUT

Thesis CO- Supervisor
Assoc. Prof. Dr. Pemra ÖZBEK SARICA

ISTANBUL, 2019

MARMARA UNIVERSITY
INSTITUTE FOR GRADUATE STUDIES IN PURE AND APPLIED SCIENCES

Duygu ŞENTÜRK KARAGÖZ, a Master of Science student of Marmara University Institute for Graduate Studies in Pure and Applied Sciences, defended her thesis entitled **"Computational Study on the Inhibition Multidrug Resistance Efflux Pumps"**, on Aug 20, 2019 and has been found to be satisfactory by the jury members.

Jury Members

Prof.Dr. Berna SARIYAR AKBULUT (Advisor)
Marmara University .....

Assoc.Prof. Pemra ÖZBEK SARICA (Co-Advisor)
Marmara University .....

Assoc.Prof. Kazım YALÇIN ARĞA (Jury Member)
Marmara University .....

Prof.Dr. Işıl AKSAN KURNAZ (Jury Member)
Gebze Tecnical University .....

Assist.Prof. Hilal TAYMAZ NİKEREL (Jury Member)
Istanbul Bilgi University .....

APPROVAL

Marmara University Institute for Graduate Studies in Pure and Applied Sciences Executive Committee approves that Duygu ŞENTÜRK KARAGÖZ be granted the degree of Master of Science in Department of Bioengineering, Bioengineering Program on 04.09.2019 (Resolution no: 2019/18-02)

Director of the Institute
Prof. Dr. Bülent EKİCİ

ACKNOWLEDGEMENTS

Foremost, I would like to express my sincere gratitude to my advisor Prof. Dr. Berna SARIYAR AKBULUT and my co-advisor Assoc. Prof. Dr. Pemra ÖZBEK SARICA for the continuous support during my master's work, for their patience, motivation, enthusiasm and immense knowledge. Their guidance helped me at all times of this thesis. I could not have imagined working with other advisors and mentors during my study.

I would also like to thank Onur SERÇİNOĞLU for his full support, patience, encouragement, insightful comments and hard questions. I am grateful to him.

My sincere thanks also go to all my friends who have worked with me in the Bioengineering Department since 2011. I thank my labmates of the computational lab: Elif Naz BINGOl, Asuman BUNSUZ and Metin YAZAR for the technical support and friendship and I thank Fatma Gizem Avcı and Fatma Ece Altınışık for their help in the experimental studies.

Last but not the least, I would like to thank my family: my parents Selattin ŞENTÜRK and Saliha ŞENTÜRK, for giving birth to me, in the first place, and supporting me spiritually throughout my life. Finally, I would like to thank my husband Mehmet KARAGÖZ who has always been there with his unending support and love.

ISTANBUL, JULY 2019 **Duygu ŞENTÜRK KARAGÖZ**

CONTENT

Page Number

ACKNOWLEDGEMENTS i

CONTENTS ii

ÖZET iv

ABSTRACT v

LIST OF SYMBOLS vi

LIST OF ABBREVIATIONS vii

LIST OF FIGURES ix

LIST OF TABLES xi

CHAPTER 1 – INTRODUCTION 1

1.1. Antibiotic History 1

1.2. Antimicrobial Resistance and Multidrug Resistant Efflux Pumps 2

1.3. ATP Binding Cassette (ABC) Drug Efflux Pumps 3

1.3.1. BmrA Multidrug Efflux Pumps 5

1.4. Molecular Docking 6

1.4.1. Theory 7

1.4.2. AutoDock Vina 8

1.5. Homology Modeling 9

CHAPTER 2 – MATERIALS AND METHODS 13

2.1. BmrA protein sequence 13

2.2. Homology Modelling Templates 13

2.3. Virtual Screening Libraries 14

2.4. Homology Modelling 15

2.4.1. Software 15

2.4.2. Method 15

2.5. Virtual Screening 17

2.5.1. Virtual Screening Preliminary Preparation 17

2.6. Docking Procedure 21

2.7. Docking Results Evaluation 21

CHAPTER 3 – RESULTS AND DISCUSSION ……. 25
3.1. Homology Modelling of BmrA Efflux Pump Protein 25
3.1.1. 3B5W as a template 25
3.1.2. Ec.full.cor.pdb as a template 28
3.1.3. Determination of BmrA model 30
3.2. Virtual Screening Studies 38
3.2.1. Virtual Screening Process Optimization 38
3.2.2. Chemotheca Library 41
3.2.3. Chimiothèque Nationale Library 51
CHAPTER 4 – CONCLUSION ……... 89
REFERENCES …….. 91
APPENDIX ……... 101
AUTOBIOGRAPHY

ÖZET

ÇOKLU İLAÇ DİRENÇLİLİĞİ SAĞLAYAN DIŞA ATIM POMPALARININ POTANSİYEL İNHİBİTÖRLERİ ÜZERİNE HESAPSAL ÇALIŞMA

İlaçların dışa atımı ile gelişen antimikrobiyel direnç, dünya çapında bir sağlık sorunu olarak görülmektedir. Antibakteriyel duyarlılığı geri kazanma ve mevcut antibiyotiklerin klinik etkinliklerini geri döndürme zorunluluğu, bu dışa atım pompalarının işlevlerinin engellenmesine yönelik çalışmaları yoğunlaştırmaktadır. Mevcut tez çalışmasında, ATP enerjisini kullanarak çalışan ve *Bacillus subtilus* mikroorganizmasında bulunup bir zincirinde 575 amino asite sahip, homodimer yapılı dışa atım BmrA ilaç atım pompasının inhibisyonunu sağlayacak inhibitor adaylarının keşfedilmesi hedeflenmiştir. İnhibisyonu hedeflenen BmrA membran proteinine ait deneysel olarak belirlenmiş bir yapının henüz bulunmamasından dolayı, bu çalışmada ilk olarak BmrA'nın homologları olan *Escherichia coli* EcMsbA (Tam koordinatlı yapısı) ve *Staphylococcus aureus* SAV1866 (PDB: 2HYD) yapıları kalıp olarak kullanılarak 'Modeller 9.19' programı ile BmrA'nın yapısı oluşturulmuştur. Sanal tarama, Chemotheca (http:// chemotheca.unicz.it/index.php.) ve Chimiothèque Nationale (http://chimiotheque- nationale.cn.cnrs.fr/?-Acces-utilisateurs-) kütüphaneleri ile AutoDock Vina 1.1.2 programı kullanılarak 5 tekrarlı olarak gerçekleştirilmiştir. Sanal tarama bağlanma enerji sonuçları, DruLiTo ile belirlenen ligandların ilaç benzerlikleri ve BmrA ile ligandların bağlanma etkileşimleriyle birlikte değerlendirilmiştir. Tüm kriterler göz önüne alındığında, Chemotheca kütüphanesinden 5 ve Chimiothèque Nationale kütüphanesinden 27 olmak üzere toplam 32 potansiyel inhibitör adayı belirlenmiştir. Belirlenen 32 adayın BmrA'ya bağlandıkları bölgeler karşılaştıklarında, bu bölgelerde büyük benzerlikler olduğu gözlemlenmiştir. Bu benzerlik, sonuçların tutarlı olduğunu gösterip çoklu ilaç dirençliliği sağlayan BmrA dışa atım pompasındaki hedef bölgedeki kalıntılara ait önemli ipuçları vermektedir.

ABSTRACT

COMPUTATIONAL STUDY ON THE POTENTIAL INHIBITORS OF MULTIDRUG RESISTANCE EFFLUX PUMPS

Drug efflux mediated antimicrobial resistance is seen as a worldwide health problem. Thereof, the necessity to restore antibacterial susceptibility and to return existing antibiotics into the clinic have made the inhibition of these efflux pumps the center of attention. In this thesis, the aim was to find new inhibitor candidates that target the *Bacillus subtilis* efflux pump BmrA, energized by ATP. This efflux pump is characterized as a homodimer of 575 residues in each chain. Since the structure of the BmrA pump is not available, homology modeling was first used to reconstitute its structure using *Escherichia coli* EcMsbA (Full coordinate model) and *Staphylococcus aureus* SAV1866 (PDB: 2HYD) as templates for the Modeller 9.19 program. For consistent results, virtual screening was repeated five times using Chemotheca (http://chemotheca.unicz.it/index.php.) and Chimiothèque Nationale (http://chimiotheque-nationale.cn.cnrs.fr/?-Acces-utilisateurs-) libraries with AutoDock Vina 1.1.2. Binding energies of virtual screening were evaluated using both the ligands' drug-likeness properties, determined by DruLiTo, and the interacting residues between the ligands and BmrA. When all criteria were taken into account, a total of 32 potential inhibitor candidates were identified, 5 from the Chemotheca library and 27 from Chimiothèque Nationale library. By comparatively analyzing the 32 inhibitor candidates, the residues that interacted with the identified ligands were found to be quite similar. These findings suggest that the results are consistent, and that the interacting residues of the BmrA multidrug efflux pump could be regarded as targets in inhibitor design.

LIST OF SYMBOLS

ΔG	Gibbs free energy
$\Delta G_{binding}$	Binding free energy
K_{eq}	Equilibrium constant
K_d	Binding affinity constant

LIST OF ABBREVIATIONS

ABC	ATP-binding cassette
ATP	Adenosine triphosphate
MFS	Major facilitator superfamily
MATE	Multidrug and toxin extrusion
SMR	Small multidrug resistance
RND	Resistance-nodulation-cell division
PACE	Proteobacterial antimicrobial compound efflux
NBD	Nucleotide binding domain
TMD	Transmembrane domain
R	Gas constant
T	Absolute temperature in Kelvin degree
Vina	AutoDock Vina
DOPE	Discrete optimized protein energy
RMSD	Root-mean-square deviation of atomic positions
ProSA	Protein Structure Analysis
3D	Three dimensional
COST	European Cooperation in Science and Technology
CNRS	Centre National de la Recherche Scientifique
FBE	Free binding energy
Avg	Average
DruLiTo	Drug-likeness tool
CMC	Comprehensive medicinal chemistry

MDDR	MDL drug data report
BBB	Blood-brain barrier
uwQED	Unweighted Quantitative Estimate of Drug-likeness
wQED	Weighted Quantitative Estimate of Drug-likeness
K	Lysine
Lys	Lysine
T	Threonine
Thr	Threonine
F	Phenylalanine
Phe	Phenylalanine
S	Serine
Ser	Serine
G	Glycine
Gly	Glycine
L	Leucine
Leu	Leucine

LIST OF FIGURES

Figure 1.1 A) Representative structure of a homodimeric ABC pumps Sav1866 (PDB: 2HYD), B) Schematic illustrations of NBDs showing Walker A and signature sequence when ATP is bound …… 3

Figure 1.2 Inward-facing and Outward-facing confirmation states of ABC transporter Sav1866 (PDB: 2HYD) from *Staphylococcus aureus* 4

Figure 1.3 Transport mechanism of ABC transporters 5

Figure 1.4 Representative image of BmrA which is obtained with HDX-MS 6

Figure 1.5 Representation of a homology modelling procedure 10

Figure 1.6 Sequence alignment programs that can be used for homology modelling.....11

Figure 1.7 Comparison of homology modelling tools 11

Figure 1.8 Programs that can used for evaluation and validation of the models created...11

Figure 2.1 The amino acid sequence is belonged to one chain of BmrA (Accession: O06967.1, GI: 81814872) 13

Figure 2.2. A) Representative image of *Escherichia coli* MsbA with full coordinates. B) Representative image of Staphylococcus aureus Sav1866(PDB: 2HYD) 14

Figure 2.3 The alignment result of BmrA and Ec_Full_Cor MsbA sequences is obtained by Align2d.py script. 16

Figure 2.4 Flowchart of Virtual screening results evaluation.....23

Figure 3.1. The Ramachandran Plot results of BmrA.Marun and BmrA_EcMsbA obtained by ProCheck program. 27

Figure 3.2 The superposition of BmrA_EcMsbA and BmrA.Marun generated by Modeller program.....27

Figure 3.3 The Ramachandran Plot results of BmrA044 and BmrA_EcMsbA obtained by ProCheck program. 29

Figure 3.4 The superposition of BmrA_EcMsbA and BmrA044 generated by Modeller program.....29

Figure 3.5 The graph showing average z-score of 2HYD-A which is homologous with BmrA protein 31

Figure 3.6 The representative image showing small and large drugrability regions of BmrA based on the PockDrug results.....40

Figure 3.7 The representation of BmrA ATP binding region.....43

Figure 3.8 Representation of NB592 bound to p-gp 44

LIST OF TABLES

Table 2.1 The list of structures used for re-docking studies…… 18

Table 2.2 Grid coordinates and the representation on BmrA pump for virtual screening. 20

Table 3.1 It is showed that DOPE scores from Modeller evaluation and the residues in most favoured region estimated from Ramachandran Plot. 26

Table 3.2 It is showed that DOPE scores from Modeller evaluation and the residues in most favoured region estimated from Ramachandran Plot. 28

Table 3.3 The results of ProSA evaluation. 33

Table 3.4 The results of Verify3D program evaluation. 36

Table 3.5 Binding free energies of the ligands calculated using AutoDock with different exhaustiveness values.. 38

Table 3.6 The drug-likeness properties of first 100 ligands within Chemotheca Library 41

Table 3.7 ATP Binding Sequences 43

Table 3.8 Residues of BmrA interacting with CM199 and CM174 45

Table 3.9 Residues of BmrA interacting with CM290 (Red: The residue is directly interacting with the ligand, Blue: The residue is not directly interacting with the ligand but is close to the ligand). 47

Table 3.10 The binding energy values of the ligands which were selected based the second strategy. 48

Table 3.11 DruLiTo assessment of the ligands which were selected based the second strategy. 48

Table 3.12 Residues of BmrA interacting with CM263 and 299 (Red: The residue is directly interacted with the ligand, Blue: The residue is not directly interacted with the ligand but is close to the ligand). 49

Table 3.13 Residues of BmrA interacting with CN52946, CN53203 and CN52560 (Red: The residue is directly interacting with the ligand, Blue: The residue is not directly interacting with the ligand but is close to the ligand).....52

Table 3.14 Residues of BmrA interacting with CN51357, CN52148, CN53019 and CN52716 (Red: The residue is directly interacting with the ligand, Blue: The residue is not directly interacting with the ligand but is close to the ligand).....55

Table 3.15 Overall assessment the of Chimiothèque Nationale library virtual screening 61

Table 3.16 Binding free energies of the ligands with a binding energy difference of 0 kcal/mol for the two NBDs, based on second strategy.....62

Table 3.17 DruLiTo assessment of the ligands with a binding energy difference of 0 kcal/mol for the two NBDs, based on the second strategy......62

Table 3.18 Residues of BmrA interacting with CN53952, CN52150, CN51977, CN53545 and CN48004 (Red: The residue is directly interacted with the ligand, Blue: The residue is not directly interacted with the ligand but is closely to the ligand).....63

Table 3.19 Binding free energies of the ligands with a binding energy difference between 0 – 0.02 kcal/mol for the two NBDs, based on second strategy.....68

Table 3.20: DruLiTo assessment of the ligands with a binding energy difference between 0 – 0.02 kcal/mol for the two NBDs, based on the second strategy.....69

Table 3.21 Residues of BmrA interacting with CN54268, CN52559 and CN53648 (Red: The residue is directly interacted with the ligand, Blue: The residue is not directly interacted with the ligand but is closely to the ligand).....70

Table 3.22 Residues of BmrA interacting with CN51349, CN52909, CN54733, CN54281, CN52713 and CN53219 (Red: The residue is directly interacted with the ligand, Blue: The residue is not directly interacted with the ligand but is closely to the ligand).. 73

Table 3.23 Binding free energies of the ligands with a binding energy difference between 0.02 – 0.04 kcal/mol for the two NBDs, based on second strategy.....79

Table 3.24 DruLiTo assessment of the ligands with a binding energy difference between 0.02 – 0.04 kcal/mol for the two NBDs, based on the second strategy..... 79

Table 3.25: Residues of BmrA interacting with CN52562, CN53026, CN53196 and CN50557 (Red: The residue is directly interacted with the ligand, Blue: The residue is not directly interacted with the ligand but is closely to the ligand)..... 80

Table 3.26 Residues of BmrA interacting with CN43843 and CN54231 (Red: The residue is directly interacted with the ligand, Blue: The residue is not directly interacted with the ligand but is closely to the ligand)..... 84

Table 3.27. It is shown that the interacted residues and/or closer residues of ligands selected from virtual screening 86

CHAPTER 1 – INTRODUCTION

1.1. Antibiotic History

Looking back to human infectious diseases, antibiotics have been used for their treatments for a long time, long before the development of modern medicine. Since ancient Egypt, wounds and burns have been treated with filamentous fungi, known to grow on bread. In the 19th century, Sir John Scott Burden – Sanderson became aware of the absence of bacteria in a liquid media enclosed with mold. Later, Joseph Lister explored *Penicillium glaucum's* inhibitory potential for bacterial growth and used *Penicillium glaucum* extracts in order to cure a nurse's injury. In 1877, Louis Pasteur and his colleague Jules Francois Joubert noticed that *Bacillus anthracis* was inhibited when it was co-cultivated with widespread aerobic bacteria [1-3].

First the word "antibiosis" which means one living organism inhibits the other to assure its own viability, was introduced in 1889 by Jean Paul Vuillemin. Before Fleming, in 1897, Ernest Duchesne found out the inhibition of *Escherichia coli* by *Penicillium glaucum*. Although various competitions were known between microorganisms, no antimicrobial molecule was available until, arsphenamine, the first antimicrobial discovered by Pual Ehrlich in 1909. It was then marketed under the name Salvarsan® then Mapharsen® [4].

In 1928, Fleming noticed that *Penicillium notatum* fungus contamination in culture dishes inhibited *Staphylococcus aureus* growth. This finding has lead to the identification of the first substance that could inhibit another microorganism's growth. This compound's purification, isolation and structure has been established and it was named as penicillin. It was used for many wounded soldiers during World War II. In 1930, the antibiotic effects of sulphanilamide was explored by Gerhard Domagk and it was commercialized under the name Protonsil® in 1935 [4-6].

In the 1940s, Selman Walksman conducted a systematic study of the antimicrobial activity of soil bacteria, especially of the members of *Streptomyces* and *Streptomycetes* and then introduced the platform ("Walksman platform") in order to investigate the antagonism between microorganisms. By screening *Streptomycetes* with Walksman platform, the first effective compound against tuberculosis and the first aminoglycoside were discovered.

After these developments, pharmaceutical industry used Walksman Platform and the major antibiotics classes were generated over the next 20 years [7-9].

During this impressive period, 23 classes of antibiotics were identified from 19 bacterial species and 7 fungi. These include nitrofuran in 1953, quinolone in 1960, sulphonamide in 1961 and oxazolidinones in 1987. After the discovery of the antibiotics classes in the 1980s, there was a long recession in discovery [4,10].

Consequently, the importance of antibiotics became evident. The greatest generators are identified as bacteria and fungi. Currently, *Streptomyces* genus produces approximately half of the antimicrobial compounds used in human infections [2].

1.2. Antimicrobial Resistance and Multidrug Resistant Efflux Pumps

Multidrug resistant bacteria withstand a wide range of antimicrobial substances, thereby this decreases treatment choices and enhances mortality. Antimicrobial resistance is of great concern worldwide. Infectious diseases continue to increase in developing countries where antibiotics utilization is high. Therefore, the World Health Organization has forced the evaluation strategies to overcome and control the spread of antimicrobial resistant microorganisms [11].

The major resistance to antibiotics is caused by membrane bound transporters that actively efflux drugs from the cells. All organisms possess these membrane transporter proteins. The genes, which encode these transporters, can be found either on the chromosomes or plasmids [12].

Based on the number of their membrane spanning regions, energy sources, substrates and sequence similarities, currently bacterial efflux pumps are classified into five families; ATP-binding cassette (ABC) family, the only family directly utilizing Adenosine triphosphate (ATP) as the energy source, major facilitator superfamily (MFS), multidrug and toxin extrusion (MATE) family, small multidrug resistance (SMR) family, and resistance-nodulation-cell division (RND) superfamily.

Very recently a new class, the proteobacterial antimicrobial compound efflux (PACE) family, which includes secondary active transporters that use electrochemical energy captured in transmembrane ion gradients, has been found [13-15].

1.3. ATP Binding Cassette (ABC) Drug Efflux Pumps

ABC efflux pumps, which exist in every form of life, perform efflux of toxins, metabolites and drugs from cells as an omnipresent membrane system. ABC exporters are classified as homodimeric and heterodimeric groups, which generally consist of two cytoplasmic nucleotide binding domains (NBDs) and two hydrophobic transmembrane domains (TMDs). Homodimeric ABC pumps have highly homologous NBDs that are fused to TMDs. In these efflux pumps, drug identification and transport are executed by TMDs while NBDs are liable for ATP hydrolysis in order to provide energy for the efflux system [16, 17].

The NBD subunits possess the preserved P-loop or Walker A motif (GXXXGXGK(S/T)), the Walker B motif (XXXXD, where X is a hydrophobic amino acid), and the ABC signature motif (LSGGQ) which is a prerequisite for an ABC pump. A representative image of an ABC type efflux pump is given in Figure 1.1 [18-19].

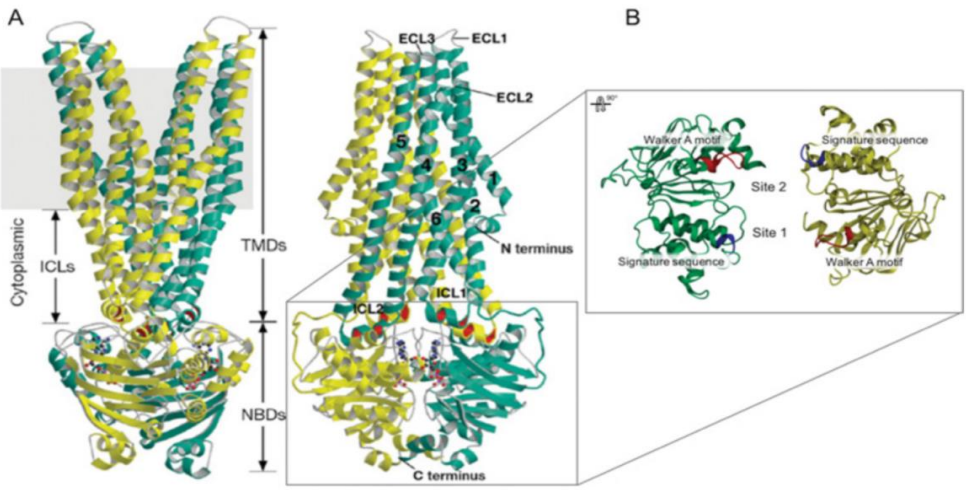

Figure 1.1 A) Representative structure of a homodimeric ABC pump SAV1866 (PDB: 2HYD), B) Schematic illustration of NBDs showing Walker A and signature sequence when ATP is bound [19].

Although these pumps have various cellular functions, their fundamental role is to transport compounds that are important for the cells. During the transport process, TMDs of the ABC transporters accomplish two conformations, one inward-facing and one outward-facing, in order to enable substrate binding or release, respectively [18, 20].

The representative conformations are given in Figure 1.2.

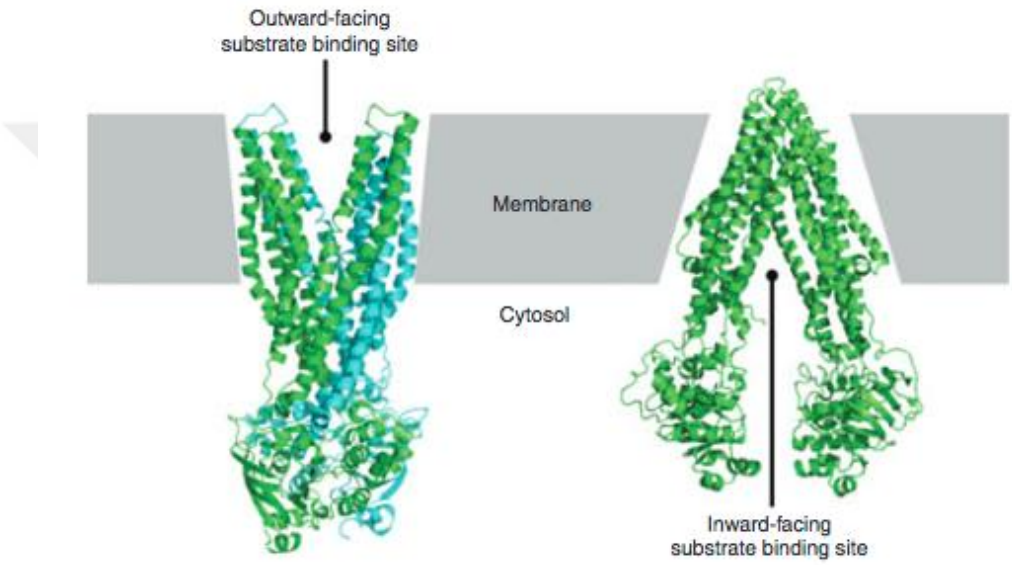

Figure 1.2 Inward-facing and Outward-facing confirmation states of ABC transporter SAV1866 (PDB: 2HYD) from *S. aureus* [21]

Efflux is realized with conformational changes. Conformational changes occur successively with NBD dimerization and dissociation powered by ATP binding or hydrolysis. Nucleotides can be switched, and the substrate binding region fronts towards the cytosol when NBDs are open. In the meantime, TMDs are switched simultaneously from the inward-facing to the outward-facing position during the transportation when connections of NBDs are induced by ATP binding, as seen in Figure 1.3 [22, 23].

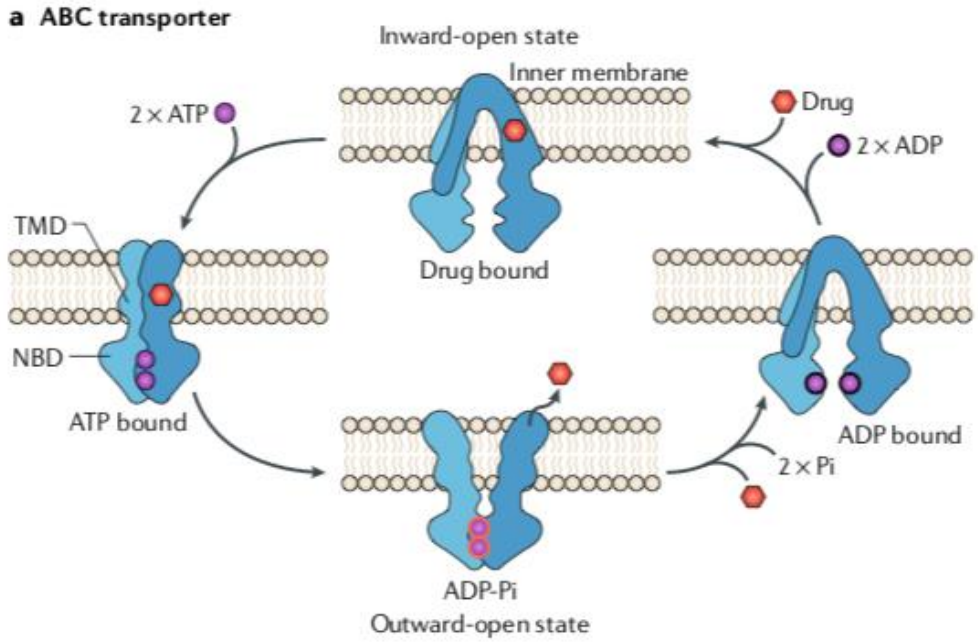

Figure 1.3 Transport mechanism of ABC transporters [23].

1.3.1. BmrA Multidrug Efflux Pump

BmrA, previously called as YvcC, was defined as a half-size ABC type transporter from *Bacillus subtilis* involved in multidrug resistance. BmrA, which is a 130 kDa membrane protein, contains 589 amino acids in one chain and has a homodimeric structure [24-26]. It consists of a total of four domains: two transmembrane domains with six predicted α-helices each, and two nucleotide binding domains, as seen in Figure 1.4. Moreover, the BmrA membrane protein is homologous with LmrA from *Lactococcus lactis*, eukaryotic P-glycoprotein (P-gp), SAV1866 from *S. aureus* MsbA from *E. coli* and *Vibrio cholerae*. BmrA transporter possess the advantage of being overproduced in *E. coli* with high yields. This advantage serves as an important starting point for the structural identification of membrane proteins [27-32].

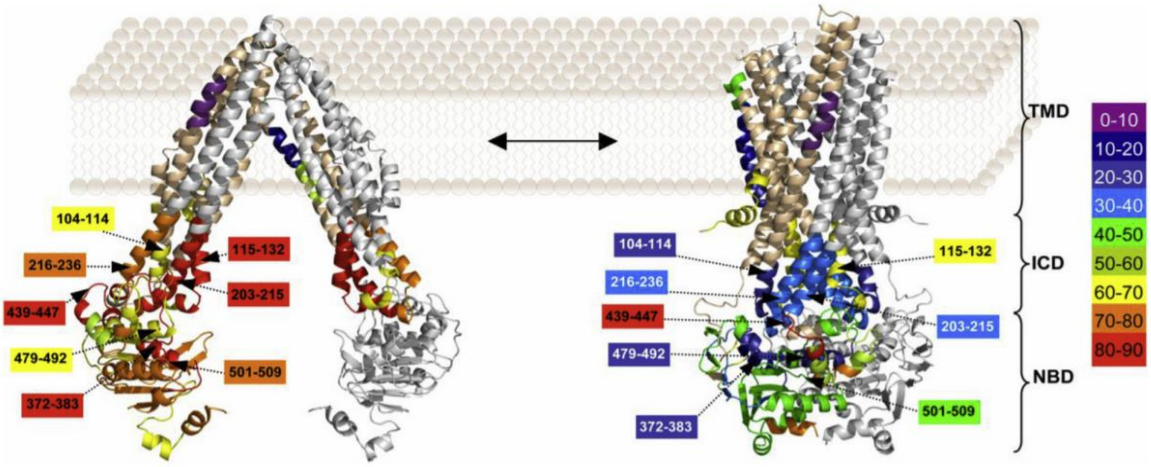

Figure 1.4 Representative image of BmrA which is obtained with HDX-MS [31].

In this study, the aim is to find new potential inhibitors for the BmrA multidrug efflux pump, based on virtual screening.

1.4. Molecular Docking

Proteins, which impose their functions through binding other molecular partners, play critical roles in almost all types of biological processes. Ligand-protein interactions are situated in the heart of many biological processes. Therefore, pharmaceutical community has been giving a lot of effort to comprehend protein-protein/ligand interaction mechanisms that will elucidate how proteins interact. This will eventually help the progress in drug design and discovery [33-35].

Molecular docking is an approach that undertakes the effort to estimate the noncovalent interactions of a receptor (macromolecule) and a small molecule (ligand), either beginning from the native state, if availbale, or from structures derived from molecular dynamic simulations or homology modeling etc. [36]. The small molecule, which is named as the ligand, usually interacts with the active sites of the protein. Active sites of proteins are known as the parts that are involved in the generation of the protein-ligand complex. There are many potential conformational areas where there is a possible binding. Each possible conformation is called a binding mode.

Molecular docking is generally applied to estimate binding conformations and energy of the intermolecular complex to calculate the binding affinity between the molecules using scoring functions [33, 37].

1.4.1. Docking Theory

Docking consists of two parts, the search algorithm and the scoring function.

The search algorithm attempts to form the optimum number of configurations that also cover binding modes determined experimentally. The algorithm can be systematic or stochastic. Stochastic algorithm is based on the elements' randomness so that the result changes. Systematic algorithm is preferred where freedom is only six degrees. In rigid protein-protein docking, systematic search methods are used with the programs such as DOT, GRAMM and ZDOCK etc. However, higher dimensional structures like flexible protein-ligand docking requires more satisfactory methods which are stochastic such as MCSA, Gas and hybrid global local [38, 39].

Scoring function method estimates the binding affinity, which is called the non-covalent interactions' power between the complex after the docking process has been performed. The results obtained from docking are ranked according to the scoring function. Scoring functions are generally divided into three main categories, which are force field, knowledge based, and empirical [40].

Force field-based functions are composed of the sum of energies from a force field and it usually takes into consideration the complex interaction energies and the internal ligand energy where continuum solvation methods such as Poisson-Boltzmann or Generalized Born compute the Solvation energy. DOCK and DockThor programs are examples of force field-based scoring functions [39].

Knowledge-based scoring functions rely on statistical evaluation of three-dimensional structures showing atom pairs interacting in protein-ligand complexes.

Pseudopotential is a mean force potential and identifies protein-ligand pairwise atom geometries, which are preferred. Therefore, pairwise atoms data information is transformed into pseudopotential in knowledge-based scoring function models such as DrugScore and PMF programs [40, 41].

Experimental scoring functions are improved to replicate experimental affinity data based on the hypothesis that it is probable to associate the binding free energy to cleared variables. The functional coefficients are acquired by regression evaluation utilizing binding affinity data obtained from experimentally identified structures [42, 43]. LUDI, ChemScore, GlideScore etc. are examples of knowledge-based categories [39]. In addition to these examples, some docking programs such as DockTScore (empirical and force-field based), SMoG2016 (empirical and knowledge-based), GalaxyDock BP2 Score (empirical, knowledge-based and force-field based) have a mixture of scoring functions [44-46].

1.4.2. AutoDock Vina

AutoDock, which was first published in 1990, is one of the many molecular docking programs available. It is based on empirical free energy force field and rapid Lamarckian genetic algorithm search method. The significant advantage of AutoDock is its high reproducibility rate [47, 48].

AutoDock Vina (Vina) is a turnkey computational docking software for drug discovery, molecular docking and virtual screening. It is published in 2010 by Dr. Oleg Trott from the group that developed AutoDock. Vina offers a high-performance rate and improved accuracy without constraint usage. The other important advantage of Vina that serves a multi-faceted capability, is its ability to run docking process in parallel with multiple cores in a machine. Vina has an influential optimization algorithm that relies on a new fully empirical scoring function and a rapid gradient-optimization conformational search for prediction of protein-ligand complex affinities and potential binding modes. Its scoring function includes Gaussian steric interaction terms, a finite repulsion term, piecewise linear hydrophobic and hydrogen-bond interaction terms and entropic term proportional to the number of rotatable bonds [49, 50].

Vina tries to estimate the approximate standard chemical potential of the system by using a scoring function. Gibbs free energy (ΔG) is the thermodynamic potential that calculates the capacity of the system to perform the maximum or reversible work under constant conditions, like temperature and pressure. This means that Gibbs free energy represents thermodynamical favorableness. For example; binding interaction is thermodynamically favorable if Gibbs free energy of the system is negative. The Gibss free energy of the system is calculated using equation 1.1a [51, 52];

$$\Delta G = \Delta G_{Binding} + RT \ln(K_{eq}) \quad (1.1a)$$

where T is the absolute temperate in Kelvins, K_{eq} is the equilibrium constant (equals to Kd which is binding affinity constant), R is the gas constant (R=1.99 cal mol-1 K-1) and $\Delta G_{Binding}$ is Gibbs free energy change of interactions. ΔG is 0 when the system reaches thermodynamic equilibrium and then the equation can be arranged as equation 1.1b [51, 53];

$$\Delta G_{Binding} = RT\ln(K_d) \quad (1.1b)$$

1.5. Homology Modeling

Three-dimensional structures of biological molecules give valuable information about their function on a molecular level and help to understand a broad spectrum of functions in life science studies. Therefore, homology modeling has become an attractive technique for computational biology in order to study protein structures with known sequences . This approach relies on the observation that proteins with similar sequences tend to possess similar three-dimensional conformations [54-56].

Chothia and Lesk reported that when 32 pairs of homologous proteins were investigated to explain the relationship between sequence conservation and structural similarity, the results showed that close models were obtained when the sequence identity was greater than 50 % and significant structural differences were generated when the sequence similarity was less than 20%. But, the active sites can still possess highly similar structures even if protein models are different [57].

Homology modeling approach is generally performed in four steps, which are defining a proper template whose structure is proved experimentally, performing a suitable target-template alignment, building the model and validation of the model (Figure 1.5) [58].

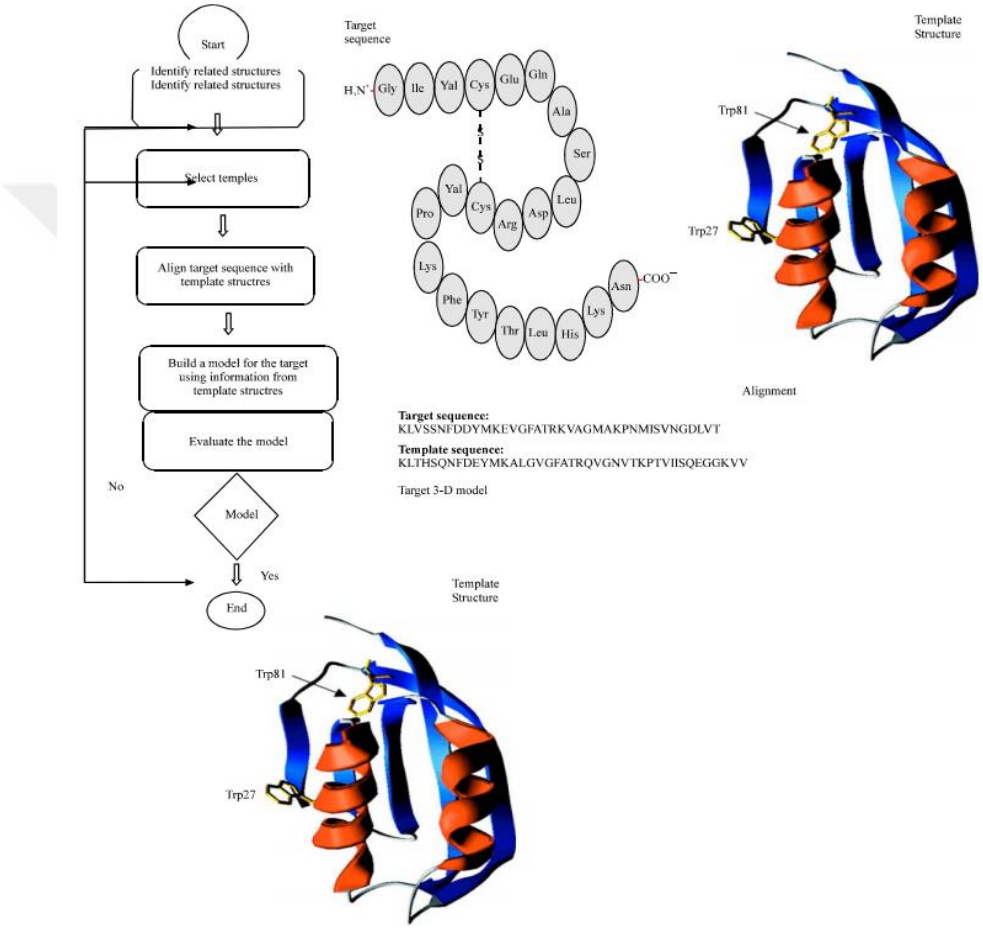

Figure 1.5 Representation of a homology modeling procedure [60].

For homology modeling, there are many free fully automated workflows, servers and programs, which do not require computational expertise in order to perform the procedure. Using the tool that is suitable to the target unknown protein, the researcher can generate reliable models with his/her visualization and interpretation. The examples of programs that are utilized effectively are given in Figures 1.6-1.8 [59, 60];

Program	Internet address
Expresso	http://www.tcoffee.org/
PROMALS3D	http://prodata.swmed.edu/promals3d/
3D-Coffee	http://igs-server.cnrs-mrs.fr/Tcoffee/tcoffee_cgi/index.cgi
MUSCLE	http://www.drive5.com/muscle/
PROBCONS	http://probcons.stanford.edu/
PRALINE	http://ibivu.cs.vu.nl/programs/pralinewww/
VAST, Cn3D	http://www.ncbi.nlm.nih.gov/Structure
ClustalW	http://www.ebi.ac.uk/clustalw/
SAM	http://www.cse.ucsc.edu/research/compbio/sam.html
GENEWISE	http://www.sanger.ac.uk/Software/Wise2/
MAFFT	http://align.bmr.kyushu-u.ac.jp/mafft/online/server/
T-Coffee	http://www.tcoffee.org/
PROMALS	http://prodata.swmed.edu/promals/
SPEM	http://sparks.informatics.iupui.edu/Softwares-Services_files/spem.htm
PROBE	ftp://ncbi.nlm.nih.gov/pub/neuwald/probe1.0/
BLOCKS	http://www.blocks.fhcrc.org/
PSI-BLAST	http://www.ncbi.nlm.nih.gov/BLAST/newblast.html

Figure 1.6 Sequence alignment programs that can be used for homology modelling [61].

Modeling program	Potential energy	Search method	Description
MODELLER	CHARMM	Spatial restraints	Modeling by satisfying spatial restraints
SwissModel	GROMOS	Rigid-body assembly	Web server using rigid-body assembly with loop modeling
COMPOSER		Rigid-body assembly	Use of multiple template structures for building homology model
3D-JIGSAW	Mean-field minimization methods	Rigid-body assembly	Web server using rigid-body assembly with loop modeling
PrISM		Rigid-body assembly	Most appropriate template is used for each segment of the target to be built
CONGEN	CHARMM	Rigid-body assembly	Distance constraints derived from known structure and alignment.

Figure 1.7 Comparison of homology modelling tools [61].

Program	Internet address
PROCHECK	http://www.biochem.ucl.ac.uk/~roman/procheck/procheck.html
WHATCHECK	http://www.sander.embl-heidelberg.de/whatcheck/
ProsaII	http://www.came.sbg.ac
VERIFY3D	http://www.doe-mbi.ucla.edu/Services/Verify_3D/
ERRAT	http://www.doe-mbi.ucla.edu/Services/Errat.html
ANOLEA	http://www.fundp.ac.be/pub/ANOLEA.html
Probe	http://kinemage.biochem.duke.edu/software/probe.php

Figure 1.8 Programs that can be used for evaluation and validation of the models created [61]

CHAPTER 2 – MATERIALS AND METHODS

2.1. BmrA protein sequence

BmrA is a homodimer, meaning that it consists of two chains with the same amino acid sequence. One chain possesses 589 amino acids, the sequence of which is given in Figure 2.1 (NCBI database);

```
  1 mptkkqksks klkpffalvr rtnpsygkla falalsvvtt lvsllipllt kqlvdgfsms
 61 nlsgtqigli alvffvqagl sayatyalny ngqkiisglr ellwkklikl pvsyfdtnas
121 getvsrvtnd tmvvkelitt hisgfitgii svigsltilf imnwkltllv lvvvplaali
181 lvpigrkmfs isretqdeta rftgllnqil peirlvkasn aedveygrgk mgisslfklg
241 vreakvqslv gplislvlma alvavigygg mqvssgelta galvafilyl fqiimpmgqi
301 ttfftqlqks igatermiei laeeeedtvt gkqienahlp iqldrvsfgy kpdqlilkev
361 savieagkvt aivgpsgggk ttlfkllerf ysptagtirl gdepvdtysl eswrehigyv
421 sqesplmsgt irenicygle rdvtdaeiek aaemayalnf ikelpnqfdt evgergimls
481 ggqrqriaia rallrnpsil mldeatssld sqseksvqqa levlmegrtt iviahrlstv
541 vdadqllfve kgeitgrgth helmashgly rdfaeqqlkm nadlenkag
```

Figure 2.1 Amino acid sequence of a single chain of BmrA (Accession: O06967.1, GI: 81814872) [62].

2.2. Homology Modeling Templates

There exist structures of different proteins, which are homologous with the BmrA. However, the best structure of BmrA was obtained when *E. coli* MsbA with full coordinates (kindly provided by Geoffrey Chang) and *S. aureus* SAV1866 (PDB: 2HYD) were used as models. The structures of the templates are given in Figure 2.2;

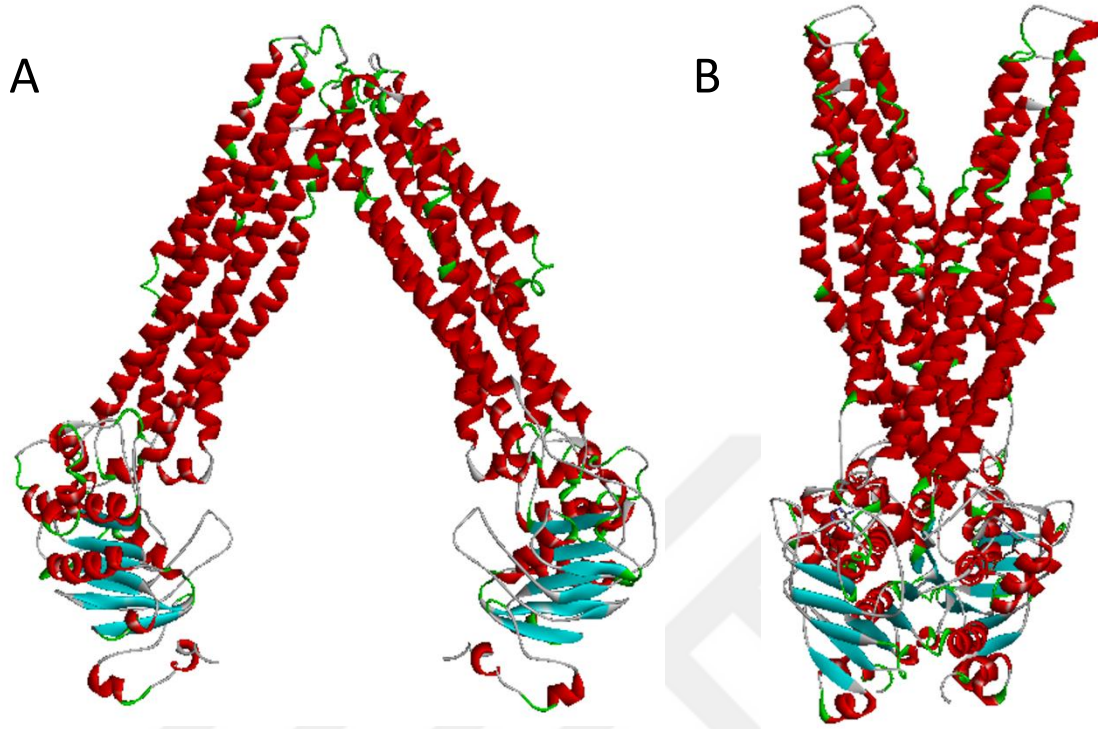

Figure 2.2. A) The representative image of *E. coli* MsbA with full coordinates. B) The representative image of *S. aureus* SAV1866 (PDB: 2HYD) [63]

2.3. Virtual Screening Libraries

Two completely independent libraries were used for virtual screening in this study; Chemotheca from a COST project (CA15135) [64] and Chimiothèque Nationale from CNRS (Centre National de la Recherche Scientifique) [65]. While the former library contains 844 ligands, the latter one includes 70889 ligands. All these ligands were investigated for docking.

2.4. Homology Modelling

2.4.1. Software

MODELLER v9.19 [66] (downloaded and installed from https://salilab.org/modeller/old_releases.html) program was used for homology modeling. It does not have a Graphical User Interface (GUI) and it is controlled from the command-line by executing the input scripts [66].

2.4.2. Method

1. The first step in comparative modeling is to identify one or more template structures that have significant similarity with the target. This identification was achieved by scanning the sequence of BmrA against a library of sequences extracted from known protein structures in the Protein Data Bank. This step was performed using the build_profile.py file as seen in Appendix 1 Figure I.

2. Second step is sequence-structure alignment. It was performed with the align2d () module of MODELLER. It is different from the standard sequence-sequence alignment methods because it takes into account the structural information from the template when constructing an alignment. This step was performed using the align2d.py file. This script reads the structure of the chosen template (3B5W, 3B60, 2HYD etc.) and the target sequence (BmrA), calls the align2d() module to perform the alignment. The script is given in Appendix 1 Figure II and the result of the alignment is given in Figure 2.3.

3. After the sequence-structure alignment was obtained, the target sequence was homology modeled by using model-multichain-sym.py script file given in Appendix 1 Figure III. This file contains the information about the homodimer, template structures and secondary structure restraints for constructing the best model.



Figure 2.3 Alignment of BmrA and Ec_Full_Cor MsbA sequences obtained by the Align2d.py script.

4. The final step of the MODELLER program is models' evaluations. The log files produced by each of the model building procedures contain a summary of each calculation at the bottom of the file. This summary includes discrete optimized protein energy (DOPE), pseudo-energy value. This score is crucial to select the most accurate model. It is accepted that the best model has the lowest DOPE and the constructed models were evaluated based on these rules.
5. After the most accurate model was determined, residue based pseudo-energy profile was generated using evaluate_model.py script given in Appendix 1 Figure IV, to compare target and template structures based on the residues.
6. In addition to the MODELLER evaluation profile, PROCHECK [67], Protein Structure Analysis (ProSA) [77, 78], and Verify3D [79, 80] programs were used for the assessment of the model quality and accuracy.

2.5. Virtual Screening

2.5.1. Virtual Screening Preliminary Preparation

Before initiating virtual screening, process parameters and process conditions were optimized. In this section, the preprocessing approaches have been summarized.

2.5.1.1. Re-docking Studies

Re-docking studies were conducted to choose the best scoring function for the most accurate evaluation of the docked protein-ligand complexes. As a template structure, P-glycoprotein (P-gp) was selected since it is a BmrA homolog and in PDB there are many P-gp structures bound to different ligands and inhibitors [68]. Details of the P-gp structures and the bound ligands' are given in Table 2.1. In order to choose the program to be used in this study, three different scoring functions; AutoDock Vina [49], DrugScore [69] and LigScore [70] were tested. The scoring program was chosen based on the accurate prediction percentage of the docked complexes.

Table 2.1 The list of structures used for re-docking studies.

	PDB ID	Ligand Name
1	4Q9L	QZ-Phe 1
2	4Q9L	QZ-Phe 2
3	4Q9K	QZ-Leu
4	4Q9J	QZ-Val 1
5	4Q9J	QZ-Val 2
6	4Q9J	QZ-Val 3
7	3G61	2J8 1
8	3G61	2J8 2
9	3G60	OJZ
10	4M2S	QZ59-RRR
11	4M2T	QZ59-SSS 1
12	4M2T	QZ59-SSS 2
13	4F4C	0SA 1
14	4F4C	0SA 2

2.5.2.2 AutoDock Vina Process Parameter Optimization: Exhaustiveness

For virtual screening, there are two main parameters to be considered: these are exhaustiveness and time. Exhaustiveness is a parameter found in AutoDock Vina and is used to control the amount of computational effort used during a docking run [71]. Furthermore, time is crucial in the screening of large libraries. Rising the value of exhaustiveness leads to long simulation times. Therefore, exhaustiveness should be optimized without altering the reliability of the results.

The value of the exhaustiveness was optimized between 10 and 900 based on the results of a preliminary screening study using the ligands boldine, bulbocapnine and roemerine ligands. These three alkaloids have quite similar structures; nevertheless, only roemerine binds BmrA.

2.5.2.3. Macromolecule preparation

3D structure of the BmrA protein was obtained from homology modeling and the obtained model was further used for virtual screening. For the macromolecule preparation, AutoDockTools version 1.5.6 [72] was used. All water molecules were deleted from the structure and all polar hydrogens were added to the structure. Finally, the prepared structure was saved in pdbqt format.

2.5.2.4. Grid Generation

In this work, drugrability regions of the BmrA protein were examined using PockDrug: Pocket Drugrability Prediction server system [73] to select the sites for docking. Representative images showing the potential drug binding sites are given in Figure 3.5.

According to potential drug binding sites evaluation by PockDrug system [73], and available ligand bound structures of P-gp in PDB, virtual screening was performed using three binding regions: the cavity, and the right and left NBS to find potential inhibitors of BmrA. Three grid sites were carefully constituted using AutoDockTools 1.5.6. [72]. The details of the grid sites are given in Table 2.2.

Table 2.2 Grid coordinates and the representation on BmrA for virtual screening.

The Representation	Grid Coordinates on AutoDock Tool
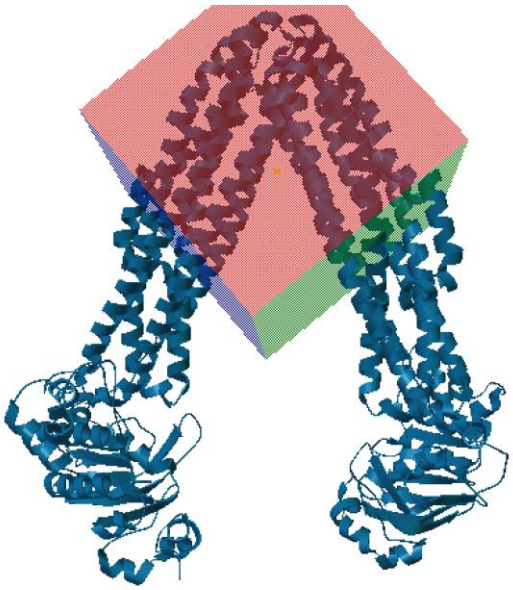	Spacing (angstrom): 1.000 Center Grid Box X center: -105 Y center: -110 Z center: -135 Dimension X-dimension: 50 Y-dimension: 50 Z-dimension: 50
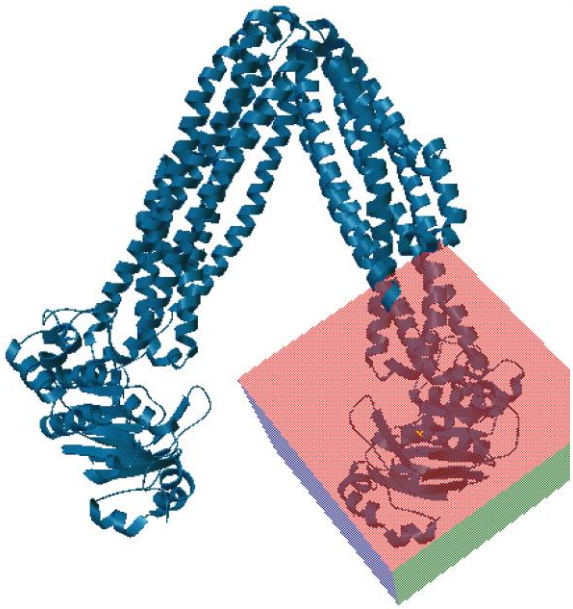	Spacing (angstrom): 1.000 Center Grid Box X center: -78 Y center: -48 Z center: -125 Dimension X-dimension: 56 Y-dimension: 48 Z-dimension: 50

Table 2.2 Grid coordinates and the representation on BmrA pump for virtual screening. (continue)

The Representation	Grid Coordinates on AutoDock Tool
	Spacing (angstrom): 1.000 Center Grid Box X center: -94 Y center: -85 Z center: -70 Dimension X-dimension: 54 Y-dimension: 56 Z-dimension: 38

2.6. Docking Procedure

AutoDock Vina version 1.1.2. was used for the repeated virtual screening processes. After all the molecules were prepared, a script was constituted in order to command docking of each ligand to BmrA. Docking of each ligand was performed five times for reliable results. All scripts, which were used in the Linux system to run the process, are given in Appendix 1, Figures V and VI.

2.7. Evaluation of the Docking Results

To evaluate the docking results, two different strategies were applied to both libraries. The first strategy used the binding energies of the ligands when docked to the cavity and the right and left NBD subunits. The ligand with the lowest binding energy is the molecule with the highest affinity for the macromolecule.

The binding affinities of the ligands were estimated by taking the average of the five runs. Following the preliminary ligand selection based on binding affinities, the selected ligands were further refined according to their drug-likeness properties. This was performed to eliminate inhibitor candidates that were not suitable to be a real drug. Drug-likeness Tool (DruLiTo) [74], which is an open source virtual screening tool, is used for this purpose. Its calculation is based on various drug-likeness rules such as Lipinski's, MDL drug data report (MDDR) like, Veber, Ghose filter, Blood-brain barrier (BBB), Comprehensive medicinal chemistry 50 (CMC-50) like, and Quantitative Estimate of Drug-likeness (QED). After the ligands were further filtered based on their drug-likeness, interactions between BmrA and the selected ligands were investigated by Discovery Studio version 1.5 [75]. Potential inhibitors with drug-likeness properties were investigated for their binding poses and the interacting residues with ATP binding sites of NBD domains. Although virtual screening was conducted for the cavity region of BmrA as well, analysis for the interacting residues was not performed for binding to this region. This is because of the absence of structures of homologs bound with their ligands/inhibitors. Since we believe that the accuracy of the results would be reduced without experimentally available interaction data, the thesis focused only on the detailed analysis of the ligands bound to the NBDs.

The second strategy was based on the binding energies and the binding energy differences between the two NBD subunits. In this strategy, ligands with a binding energy -9 kcal/mol or lower were selected. Then the ligands with a difference of 0.5 kcal/mol and 0.04 kcal/mol in their binding free energies with the two NBDs were selected from Chemotheca and Chimiothèque Nationale, respectively.

The choice of these threshold values ere explained in Results, Sections 3.2.2.2 and 3.2.3.2. After ligands were selected based on the second strategy, they were analyzed by DruLiTo [74] and Discovery Studio version 1.5 [75], as in the first strategy.

A flowchart explaining the methodology used in the analysis is given in Figure 2.4.

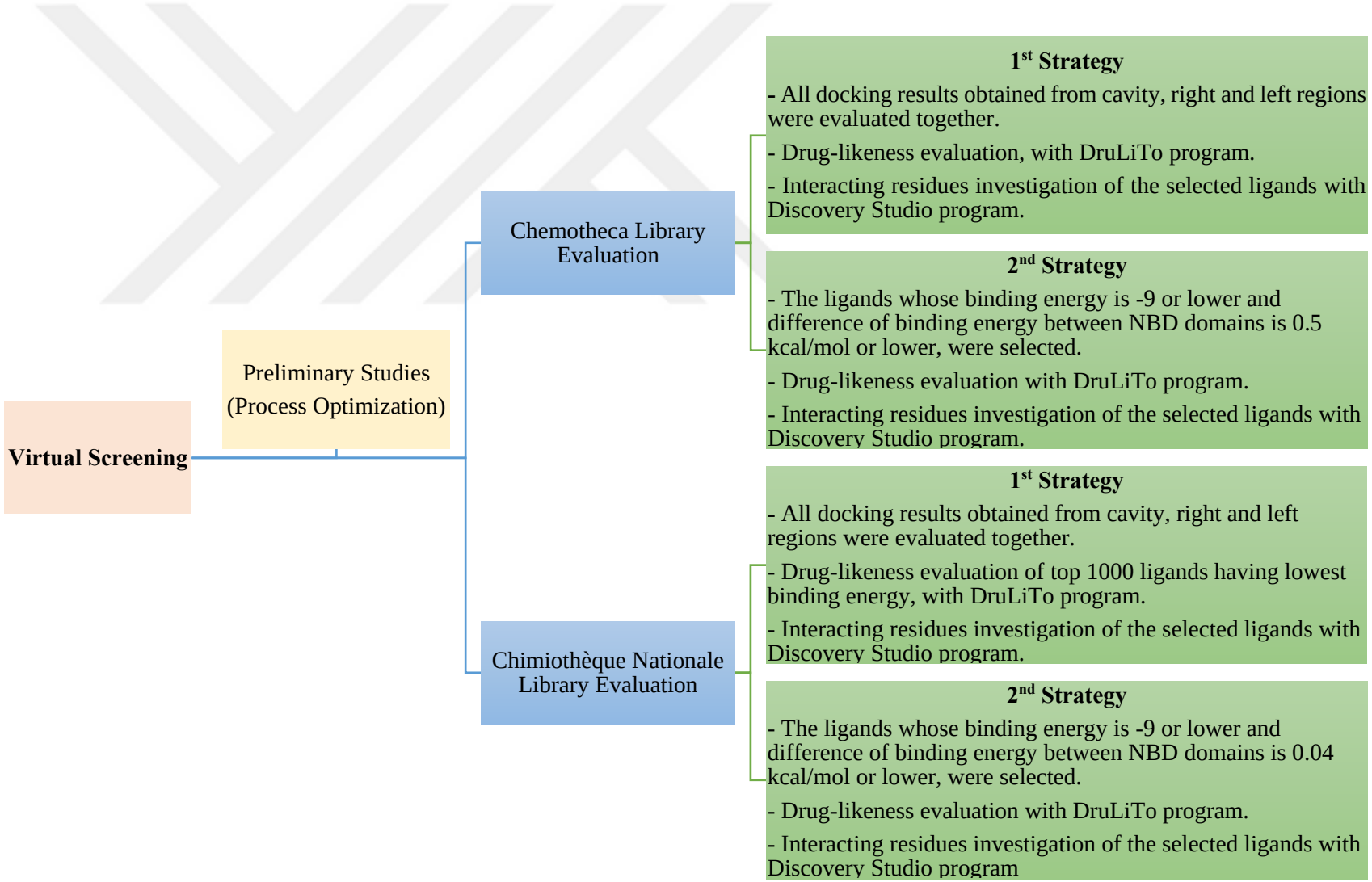

Figure 2.4 Flowchart of Virtual screening results evaluation.

CHAPTER 3 – RESULTS AND DISCUSSION

3.1. Homology Modelling of BmrA Efflux Pump Protein

In the current study, initial effort was the search for the homologs of the BmrA efflux pump for the construction of the most appropriate structure. It is found that MsbA of *E. coli*, SAV1866 of *S. aureus,* and the human P-gp were the commonly known homolog proteins of the BmrA protein. The structures of these proteins were found in the Protein Data Bank and used for further homology modeling studies.

The structure of BmrA was modeled using different parameters such as different modeling modes, different templates, and different tools. Models were generated for each parameter, and five models were selected based on their DOPE scores and they are assessed with Ramachandran plots using PROCHECK [67] program. Ramachandran plots show the relationship between phi and psi angles of the protein referring to dihedral angles between the N and the C-alpha and the C-alpha and the C-beta. The omega angle between the C-beta and the N tends to be fixed due to pi-pi interactions. Therefore, it assisted in constraining structure prediction simulations and helped with defining energy functions. The models, which were selected based on their DOPE scores and Ramachandran plots, were compared with each other and with the previously constructed BmrA model [76]. Finally, the most reliable model was selected after evaluation with ProSa [77, 78] and Verify3D [79, 80] modeling tools.

The two studies, which gave the best models, are given in the thesis.

3.1.1. 3B5W used as the template

The protein with the PDB ID 3B5W [81]is the *E. coli* MsbA efflux protein that belongs to the ABC superfamily. It is also a homodimer, like BmrA, and consists of 582 residues in one chain. However, not all coordinates of 3B5W [81] were available in PDB. The conditions when this protein was used as the template for modeling were;

Main Template: 3B5W [81]

Secondary Structure Template: 2HYD [82]

Name of the Homology Model Structure: BmrA.Marun.pdb

Name of the BmrA model constituted in 2009: BmrA_EcMsbA.pdb

The homology modeled structure was named as Bmr.Marun and the model published in 2009 was named as BmrA_EcMsbA. According to the preliminary results with BmrA.Marun and BmrA_EcMsbA, energy levels were found to be close to each other. The results indicated that the modeled BmrA.Marun structure could be slightly better because of its lower DOPE score, as seen in Table 3.1.

Table 3.1 It is showed that DOPE scores from Modeller evaluation and the residues in most favoured region estimated from Ramachandran Plot.

	DOPE Score	Residues in Most Favoured Region
BmrA. Marun	-71962.171875	% 89.6
BmrA_EcMsbA	-68704.1641	% 88.7

The amino acid distributions were also found to be similar based on the Ramachandran plot, as seen in Figure 3.1, The BmrA.Marun structure could be seen to be slightly more favorable because of a higher percentage of residues in the most preferred region. The models were found to be similar to each other when the obtained structures were aligned using VMD version 1.9.3 [83]. The superimposed structure is shown in Figure 3.2.

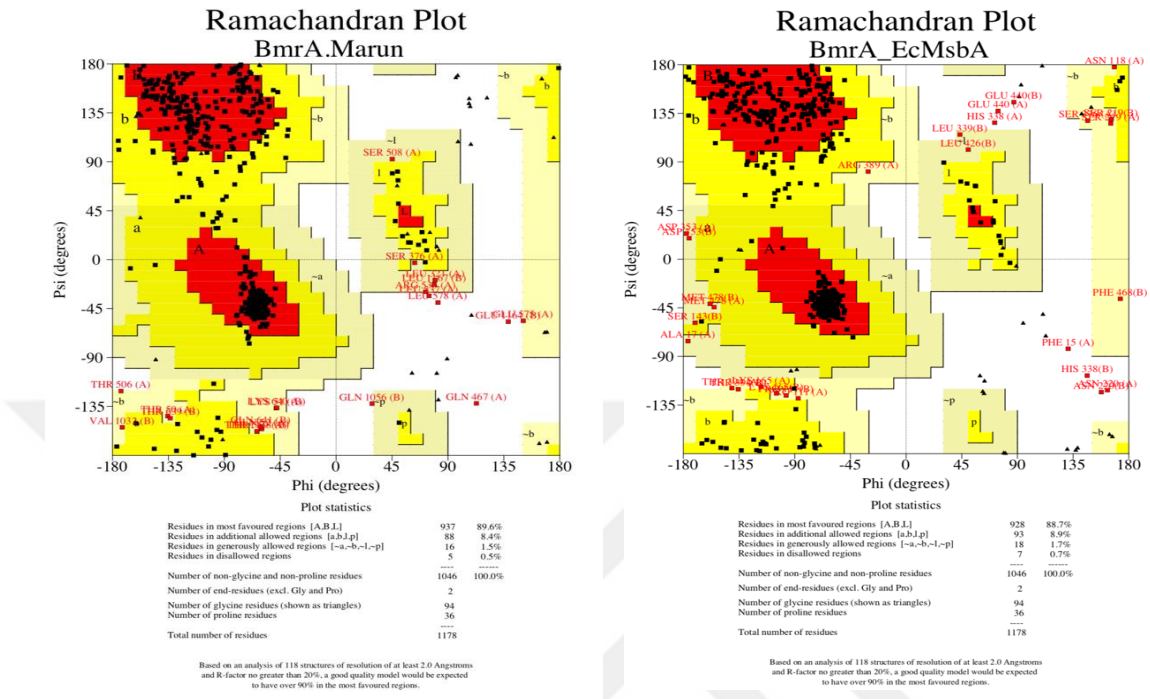

Figure 3.1. The Ramachandran Plot of BmrA.Marun and BmrA_EcMsbA obtained by ProCheck program.

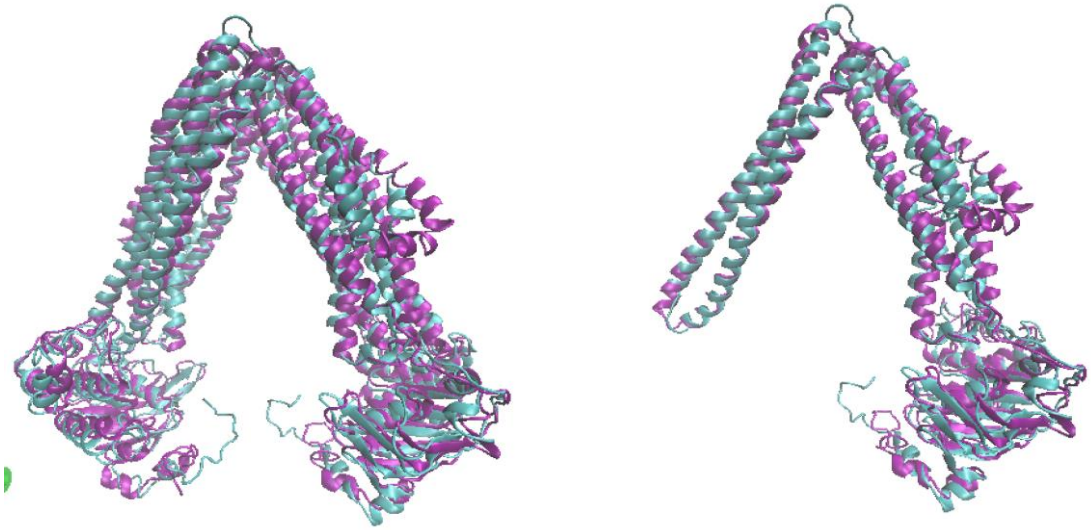

RMSD: 4.99 **RMSD:** 4.97

Figure 3.2 The superposition of BmrA_EcMsbA and BmrA.Marun generated by Modeller program. (Green is BmrA_EcMsbA and Purple is BmrA.Marun).

3.1.2. Ec.full.cor.pdb used as the template

Ec.full.cor. is an *E. coli* MsbA efflux protein like 3B5W but with full coordinates (kindly provided by Geoffrey Chang). It was used since the available MsbA structure in PDB did not have all the coordinates.

The Ramachandran plots and docking results with Ec.full.cor. are given in Figure 3.3 and Table 3.2. The homology modeled structure was constituted based on Ec.full.cor and 2HYD templates and named as BmrA044. The model published in 2009 was named as BmrA_EcMsbA, as before. The conditions when Ec.full.cor. was used as the template for modeling were;

Main Template: Ec.full.cor.

Secondary Structure Template: 2HYD

Name of the Homology Model Structure: BmrA044.pdb

Name of the BmrA model constituted in 2009: BmrA_EcMsbA.pdb

Table 3.2 It is showed that DOPE scores from Modeler evaluation and the residues in most favoured region estimated from Ramachandran Plot.

	DOPE Score	Residues in Most Favoured Region
BmrA044	-69677.046875	% 90.8
BmrA_EcMsbA	-68704.1641	% 88.7

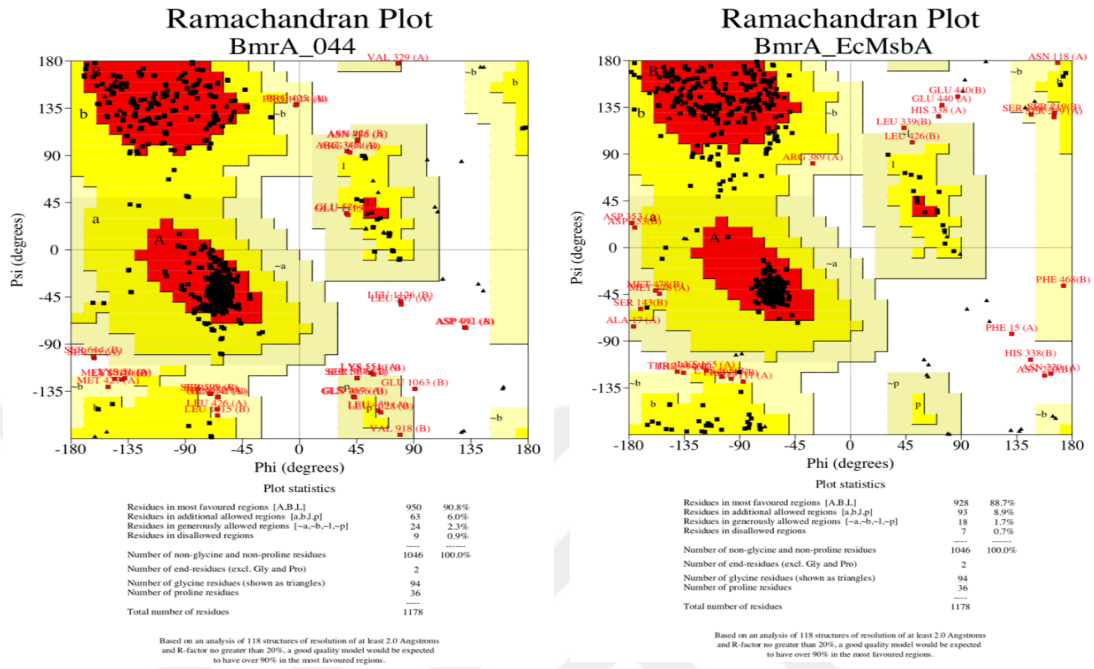

Figure 3.3 The Ramachandran plot of BmrA044 and BmrA_EcMsbA obtained by ProCheck program.

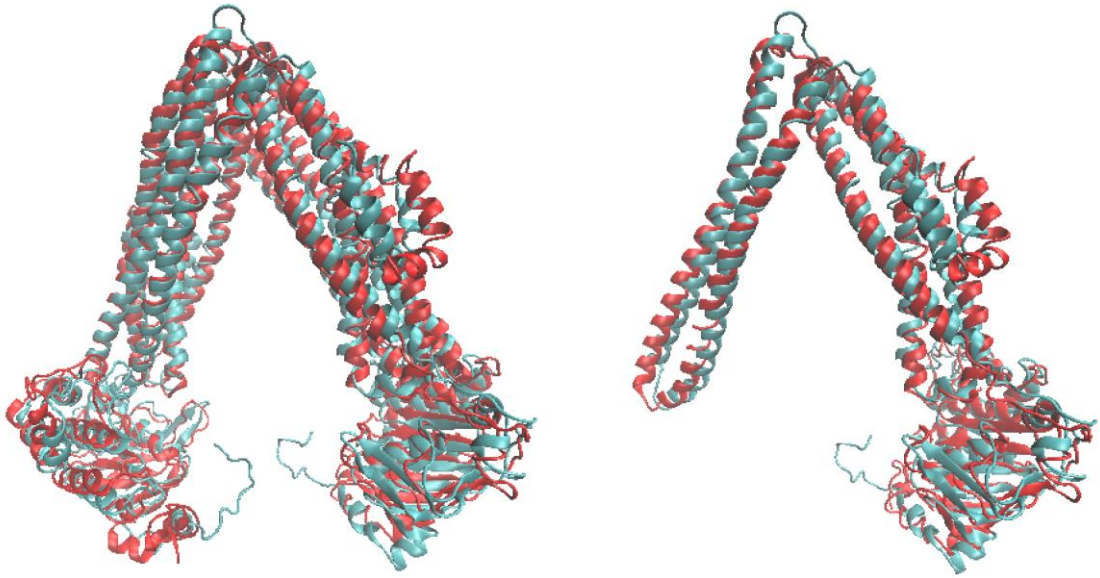

RMSD: 5.45 **RMSD:** 5.00

Figure 3.4 The superposition of BmrA_EcMsbA and BmrA044 generated by the Modeller program (Green is BmrA_EcMsbA and Red is BmrA044).

3.1.3. Determination of the BmrA model

According to the preliminary results, energy levels of BmrA.Marun, BmrA044, BmrA_EcMsbA structures were very close to each other. In addition, findings on the Ramachandran plot indicated that the amino acid distributions in Psi versus Phi plots were highly similar for these models. However, it seemed that the modeled BmrA044 structure using MsbA with the full coordinates could be slightly better because of a higher percentage of residues in the most preferred regions. The modeled structures were pretty similar to each as seen in the superimposed structure. VMD version 1.9.3 was used for superimposing the structures.

In order to select the most accurate BmrA model to be used for Virtual Screening, these three models were evaluated repeatedly with ProSa [77, 78] and Verify3D [79, 80] tools. ProSa and Verify3D results are given in Tables 3.3 and 3.4, respectively.

ProSA, which calculates the overall quality score for a specific model, is commonly applied in order to validate the protein model structure. This tool needs the atomic coordinates of the structure for this estimation. In addition, ProSA takes only the C-alpha atoms of the input model into account. Based on the energies obtained from atomic coordinates of C-alpha atoms, ProSA gives two important outputs to compare models; the z-score and residue energies plot [77]. The z-score points out the overall quality of the structure by measuring the total energy fluctuation of the model in accordance with an energy distribution generated from random conformations. For this, native protein characteristics should be considered. Z-scores, which do not lie in the range of native proteins' characteristics, is an indication of failed structures. Using ProSA principles, the z-scores of the BmrA.Marun and BmrA_044 models were evaluated based on the scores of BmrA_EcMsbA and the plot which contains similar size proteins' score, is given in Figure 3.5.

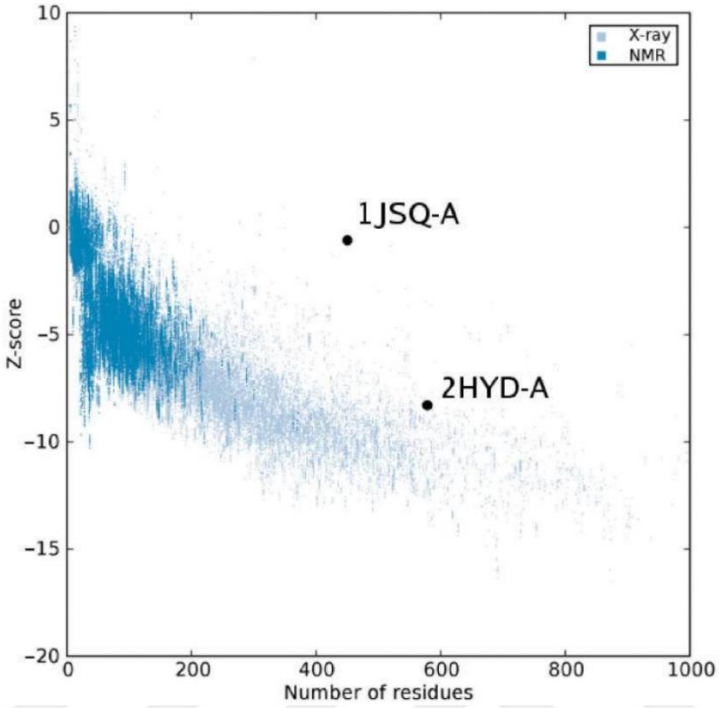

Figure 3.5 The graph showing average z-score of 2HYD-A which is homologous with BmrA protein [78]

In the first part of this study, homology modeling was performed using the homolog proteins. In order to evaluate z-scores of the modeled structures, information in literature on the z-scores of MsbA, SAV1866 and P-gp, were investigated. In a publication with the SAV18866 efflux pump (2HYD) a z-score was reported and this was accepted as a baseline for ProSA results' evaluations. Furthermore, the BmrA_EcMsbA structure constructed in 2009 was also analyzed by ProSA and it was also accepted as another important criteria. According to BmrA.EcMsbA and 2HYD-A's z-scores, our model's z-score was determined to be at least -5.0 and the model having a lower z-score, was said to be a better model. When two modeled BmrA models were compared based only on the z-scores, both models z-scores were found to be below -5. The BmrA.Marun model had a z-score of -6.06 while the BmrA_044 model has a z-score of -6.01, as seen in Table 3.3. Thus, z-scores of the models were pretty closer to each other.

Another evaluation criteria of ProSA is the residue energies plot. The energy plot gives the local model quality by evaluating the energies plot as a function of amino acid sequence and position. Generally, problematic parts or failures in the structure are determined by the corresponding positive values. When two modeled structures and the BmrA_EcMsbA structure were compared based on the residue energies plot, the positive and negative patterns of all were seen to be very similar. Therefore, ProSA results did not provide any further information to compare the quality of the models.

Table 3.3 The results of ProSA evaluation.

Model Name	Overall Model Quality	Local Model Quality
BmrA_EcMsbA	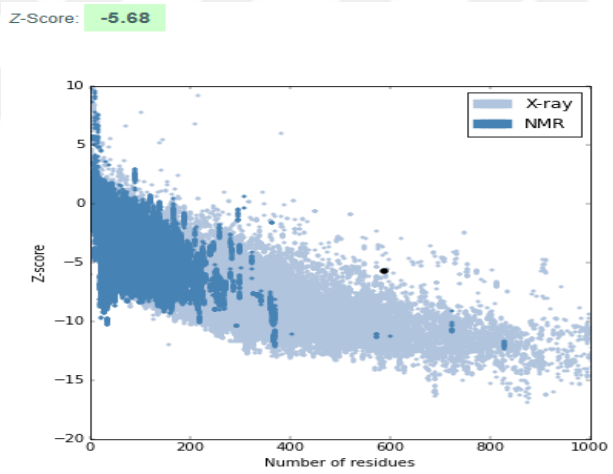	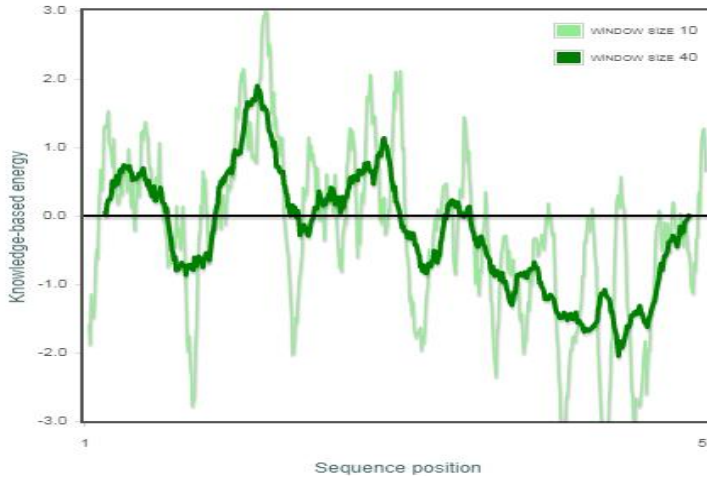
BmrA.Marun	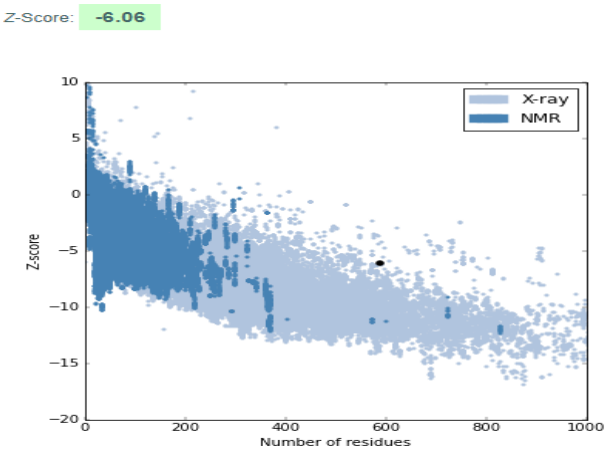	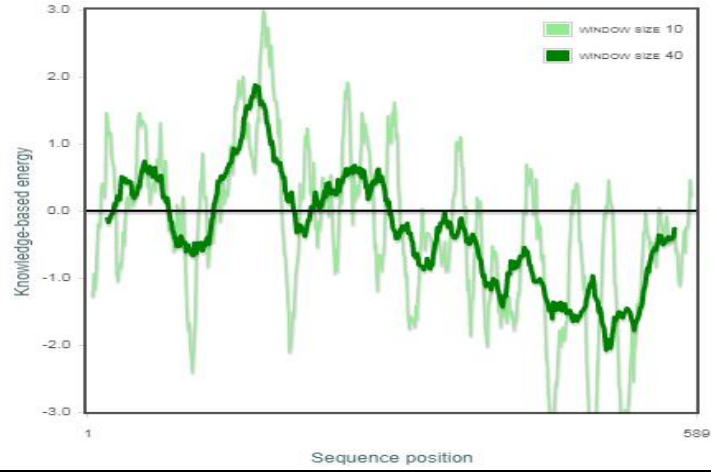

Table 3.3 The results of ProSA evaluation (Continued)

Model Name	Overall Model Quality	Local Model Quality
BmrA_044	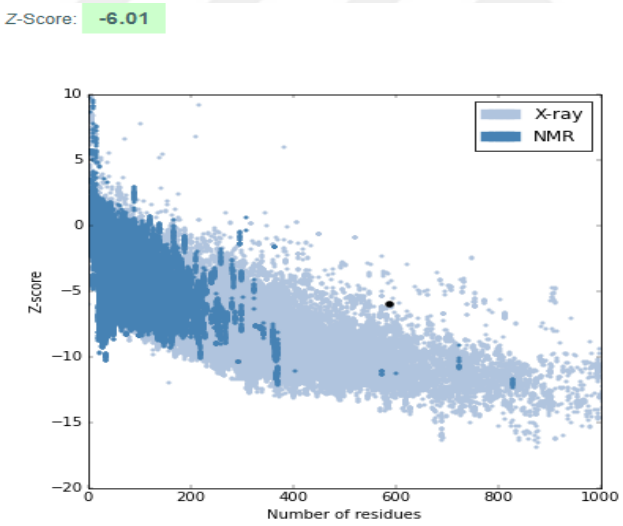	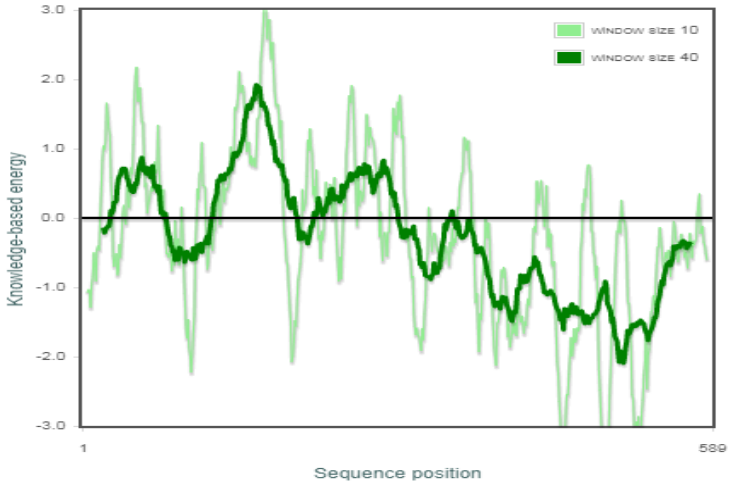

Verify3D tool [79, 80] establishes the congeniality of a protein model with its own amino acid sequence by constituting a 3D profile. It operates by specifying a structural cluster based on the -ground and environment of each amino acid position and then matching the results with the verified models. According to the tool theory, 3D profile of a correct protein structure has a high percentage score as it pairs with its own residues. Hence, the protein structure model with the highest 3D profile score among all the constructs should be selected as the main protein structure to be used for further study [79, 80]

To evaluate the quality of our models, which were constructed by Modeller 9.19, the BmrA_EcMsbA model was also analyzed using Verify3D and the results are shown in Figure 4.1-3. The comparative analysis has shown that BmrA.Marun and BmrA_044 models gave higher scores than BmrA_EcMsba. This meant that these models are better and closer to the real BmrA native structure, although the difference between the scores was quite small. BmrA_044 had higher score than BmrA.Marun by approximately 2%. Therefore, BmrA_044 model was used for further virtual screening studies.

Table 3.4 The results of Verify3D program evaluation.

Model Name	Overall Model Quality	Local Model Quality
BmrA_EcMsbA	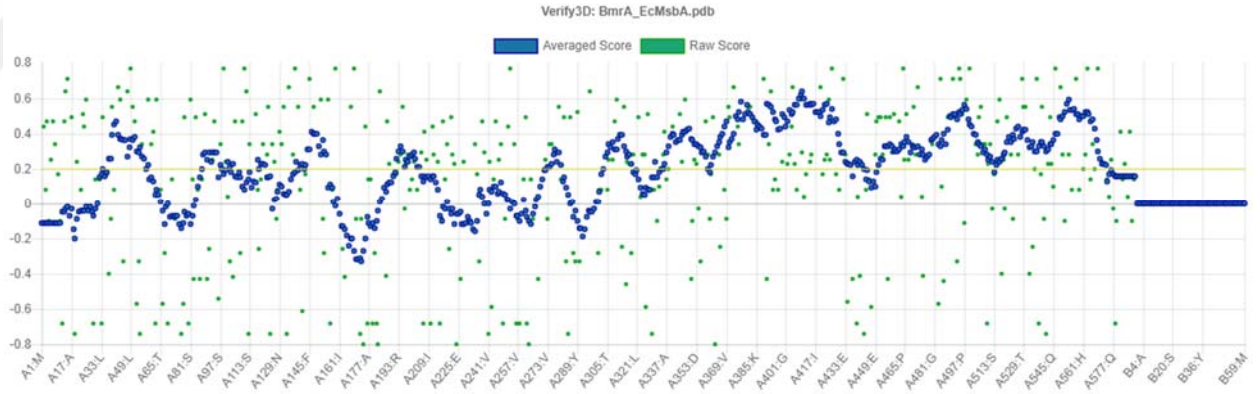	50.31 %
BmrA.Marun	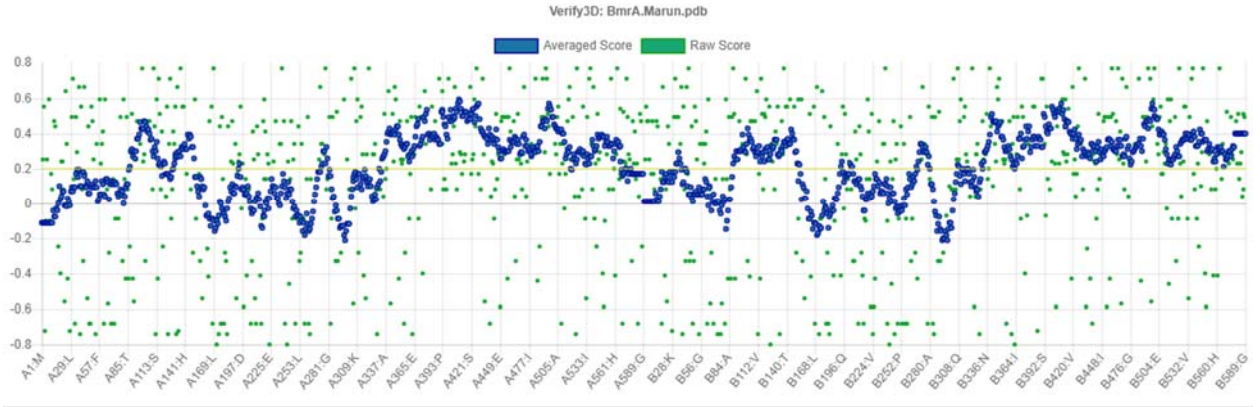	55.69 %

Table 3.4 The results of Verify3D program evaluation (Continued).

Model Name	Overall Model Quality	Local Model Quality
BmrA_044	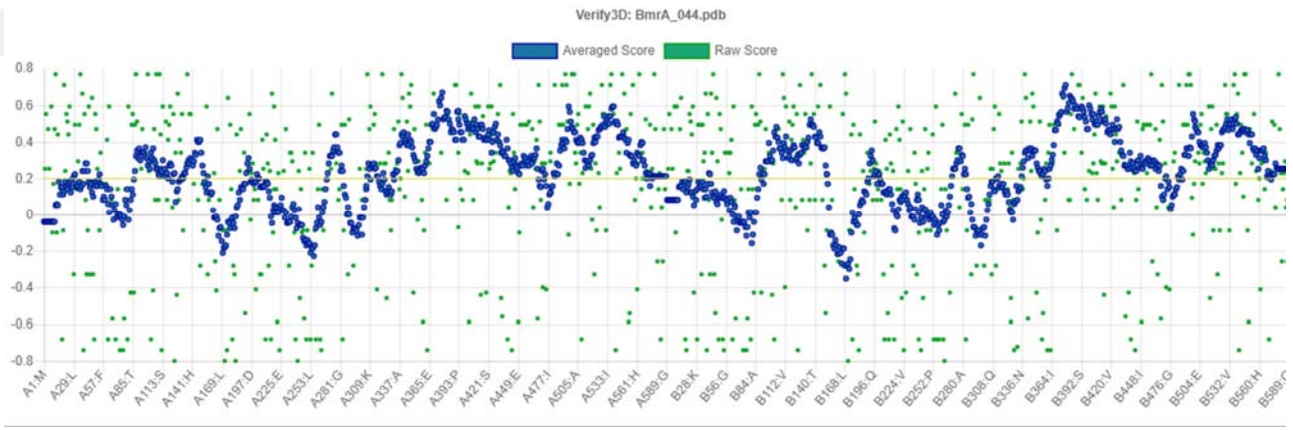	57.13 %

To sum up, Modeler 9.19 program was suitable for homology modeling of proteins with a high number of residues and dimeric structures like membrane proteins, such as BmrA. First screening was performed based on the Modeler DOPE score function between thousands of constructed models and the models with the lowest DOPE scores were further chosen for Ramachandran plot analysis. ProSA and Verify3D tools were then executed in order to select the structure for virtual screening of the macromolecules. The results of these three models were comparatively evaluated, and BmrA_044 protein model was selected as the main structure based on its high percentage of residues in the most preferred region, its lowest z-score and its higher 3D profile score.

3.2. Virtual Screening Studies

3.2.1. Virtual Screening Process Optimization

The docking program and exhaustiveness value for virtual screening were selected based on re-docking and AutoDock optimization studies. Based on the results from re-docking, AutoDock Vina 1.1.2 was chosen for virtual screening. After that, screening was performed to determine the optimum value of the exhaustiveness parameter. Screening studies were performed at exhaustiveness values between 10 to 900 with boldine, bulbocapnine and roemerine as ligands in right and left NBD subunits.

Table 3.5 Binding free energies of the ligands calculated using AutoDock with different exhaustiveness values.

Exhaustiveness	Boldine		Bulbocapnine		Roemerine	
	Right FBE (kcal/mol)	Left FBE (kcal/mol)	Right FBE (kcal/mol)	Left FBE (kcal/m)	Right FBE (kcal/mol)	Left FBE (kcal/mol)
10	-7.5	-7.4	-8.2	-7.6	-8.2	-7.9
10	-7.5	-7.4	-8	-7.6	-8.2	-7.9
10	-7.4	-7.4	-8.2	-8.3	-8.2	-7.9
10	-7.3	-7.4	-8.2	-8.3	-8.2	-7.9
10	-7.5	-7.4	-8.2	-8.3	-8.2	-7.9
50	-7.5	-7.4	-8.2	-8.3	-8.2	-7.9
50	-7.5	-7.4	-8.3	-8.3	-8.2	-7.9
50	-7.5	-7.4	-8.3	-8.3	-8.2	-7.9
50	-7.5	-7.4	-8.2	-8.3	-8.2	-8
50	-7.5	-7.4	-8.2	-8.3	-8.2	-7.9
100	-7.5	-7.4	-8.3	-8.3	-8.2	-7.9
100	-7.5	-7.4	-8.2	-8.3	-8.2	-7.9
100	-7.5	-7.4	-8.3	-8.3	-8.2	-7.9
100	-7.5	-7.4	-8.2	-8.3	-8.2	-7.9
100	-7.5	-7.4	-8.2	-8.3	-8.2	-7.9
500	-7.5	-7.4	-8.2	-8.3	-8.2	-7.9
500	-7.5	-7.4	-8.2	-8.3	-8.2	-7.9
500	-7.5	-7.4	-8.2	-8.3	-8.2	-7.9
500	-7.5	-7.4	-8.2	-8.3	-8.2	-7.9
500	-7.5	-7.4	-8.2	-8.3	-8.2	-7.9

Table 3.5 The Binding free energies of the ligands calculated using AutoDock with different exhaustiveness values (continued).

Exhaustiveness	Boldine		Bulbocapnine		Roemerine	
	Right FBE (kcal/mol)	Left FBE (kcal/mol)	Right FBE (kcal/mol)	Left FBE (kcal/m)	Right FBE (kcal/mol)	Left FBE (kcal/mol)
700	-7.5	-7.4	-8.2	-8.3	-8.2	-7.9
700	-7.5	-7.4	-8.2	-8.3	-8.2	-7.9
700	-7.5	-7.4	-8.2	-8.3	-8.2	-7.9
700	-7.5	-7.4	-8.2	-8.3	-8.2	-8.0
700	-7.5	-7.4	-8.2	-8.3	-8.2	-7.9
900	-7.5	-7.4	-8.2	-8.3	-8.2	-7.9
900	-7.5	-7.4	-8.2	-8.3	-8.2	-7.9
900	-7.5	-7.4	-8.2	-8.3	-8.2	-7.9
900	-7.5	-7.4	-8.2	-8.3	-8.2	-7.9
900	-7.5	-7.4	-8.2	-8.3	-8.2	-7.9

Roemerine is a known BmrA efflux pump inhibitor, its inhibition affect was proven with experimental data [84]. Therefore, it was selected for screening to obtain energy data on protein-inhibitor binding. The other ligands were boldine and bulbocapnine that were structurally very similar to roemerine, but which were not binders. They were also selected for screening to evaluate their binding. The calculated binding free energies are given in Table 3.5. It was seen that, the values of the exhaustiveness parameter did not significantly affect the docking of the selected ligands to BmrA, so the least value was selected for virtual screening to decrease run time.

Once the process parameters were optimized, the grid boxes that indicate the regions on the protein where ligands could to bind were determined based on the BmrA macromolecule druggability regions. The druggable regions determined by PockDrug are given in Figure 3.6.

BmrA efflux pump was found to possess many small or large druggable regions but many of these regions were located on the TMDs embedded in membrane, therefore binding to these sites was not possible. According to the druggable region evaluation, 3 regions, the cavity, right NBD and left NBD, were selected for the generation of the grid box. The coordinates of the grid boxes were defined by AutoDock Tools 1.5.6 for virtual screening.

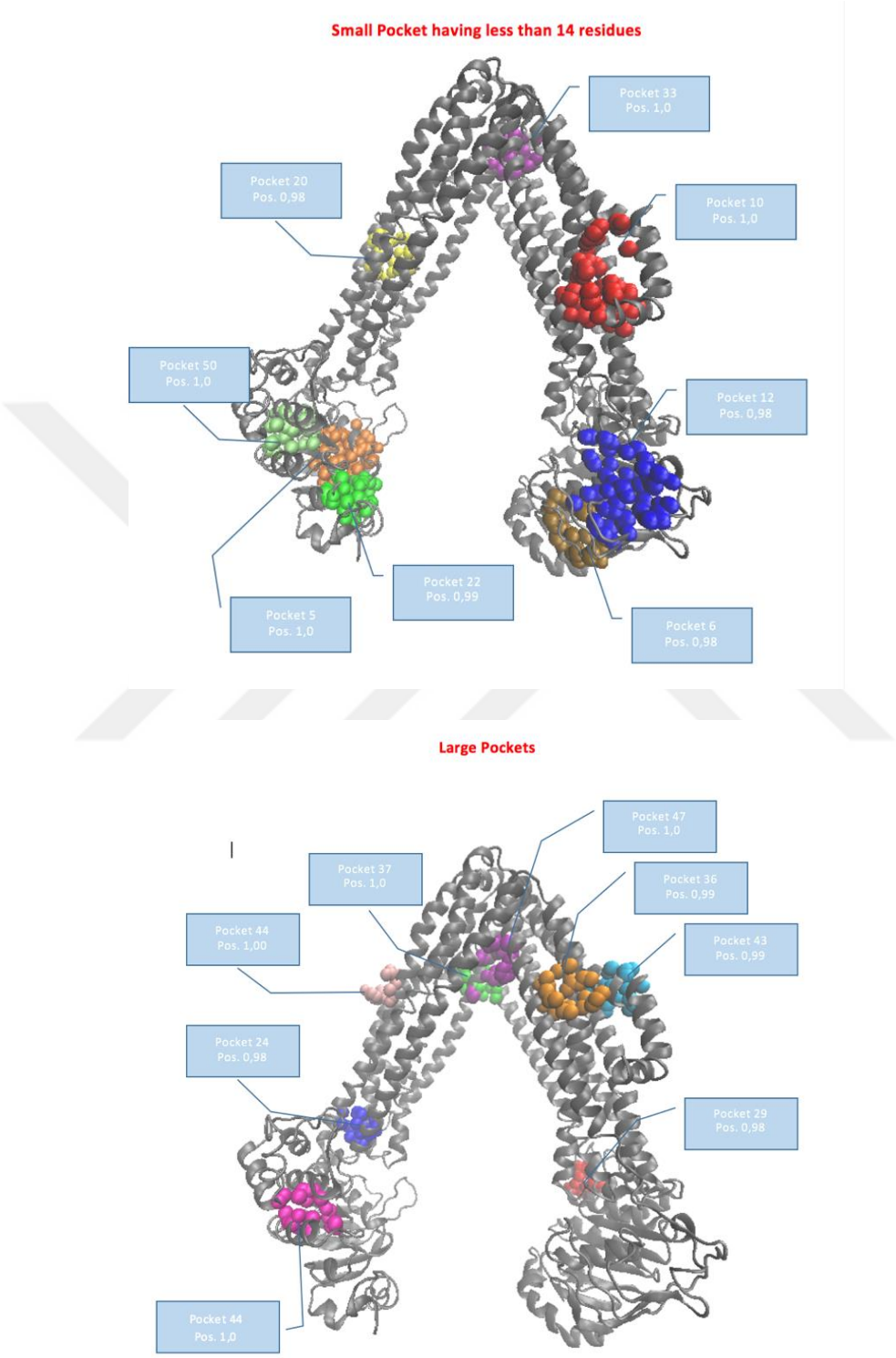

Figure 3.6. A representative image showing small and large druggable regions of BmrA based on the PockDrug results.

3.2.2. Chemotheca Library

Based on drug pocket regions of BmrA pump, AutoDock studies were conducted targeting three binding regions as the cavity, the right NBD and the left NBD, to find potential inhibitors of the BmrA efflux pump protein.

3.2.2.1. First Strategy Evaluation

Results obtained from cavity, and right and left NBD subunits, were evaluated together using the first assessment strategy. Drug-likeness of a total of 100 ligands having the lowest binding energy from all three regions, was evaluated with the DruLiTo program [74].

DruLiTo is an open source virtual screening tool. Its calculation is based on various drug-likeness rules such as Lipinski, MDDR, Veber, Ghose, BBB, CMC-50 and Quantitative Estimate of Drug-likeness (QED).

Table 3.6 The drug-likeness properties of first 100 ligands within Chemotheca Library.

Ligand	Lipisinki	Ghose	CMC-50	Veber	MDDR	BBB	uwQED	WQED
CM10	YES	YES	YES	YES	NO	YES	YES	YES
CM108	YES	YES	YES	YES	NO	YES	YES	YES
CM111	YES	YES	YES	YES	NO	YES	YES	YES
CM128	YES	YES	YES	YES	NO	YES	YES	YES
CM130	YES	YES	YES	YES	NO	YES	YES	YES
CM14	YES	YES	YES	YES	NO	YES	YES	YES
CM140	YES	YES	YES	YES	NO	YES	YES	YES
CM155	YES	YES	YES	YES	NO	YES	YES	YES
CM16	YES	YES	YES	YES	NO	YES	YES	YES
CM160	YES	YES	YES	YES	NO	YES	YES	YES
CM167	YES	YES	YES	YES	NO	YES	YES	YES
CM169	YES	YES	YES	YES	NO	YES	YES	YES
CM22	YES	YES	YES	YES	NO	YES	YES	YES
CM40	YES	YES	YES	YES	NO	YES	YES	YES
CM44	YES	YES	YES	YES	NO	YES	YES	YES
CM718	YES	YES	YES	YES	NO	YES	YES	YES
CM85	YES	YES	YES	YES	NO	YES	YES	YES
CM89	YES	YES	YES	YES	NO	YES	YES	YES

Table 3.6 The drug-likeness properties of first 100 ligands within Chemotheca Library (Continued).

Ligand	Lipisinki	Ghose	CMC-50	Veber	MDDR-Like	BBB	uwQED	WQED
CM1	YES	YES	YES	YES	NO	YES	YES	YES
CM31	YES	YES	YES	YES	NO	YES	YES	YES
CM113	YES	YES	YES	YES	NO	YES	YES	YES
CM92	YES	YES	YES	YES	NO	YES	YES	YES
CM3	YES	YES	YES	YES	NO	YES	YES	YES
CM35	YES	YES	YES	YES	NO	YES	YES	YES
CM46	YES	YES	YES	YES	NO	YES	YES	YES
CM199	YES	YES	YES	YES	NO	YES	YES	YES
CM2	YES	YES	YES	YES	NO	YES	YES	YES
CM4	YES	YES	YES	YES	NO	YES	YES	YES
CM154	YES	YES	YES	YES	NO	YES	YES	YES
CM115	YES	YES	YES	YES	NO	YES	YES	YES
CM174	YES	YES	YES	YES	NO	YES	YES	YES
CM19	YES	YES	YES	YES	NO	YES	YES	YES
CM54	YES	YES	YES	YES	NO	YES	YES	YES
CM172	YES	YES	YES	YES	NO	YES	YES	YES
CM259	YES	YES	YES	YES	NO	YES	YES	YES
CM94	YES	YES	YES	YES	NO	YES	YES	YES
CM177	YES	YES	YES	YES	NO	YES	YES	YES
CM29	YES	YES	YES	YES	NO	YES	YES	YES
CM159	YES	YES	YES	YES	NO	YES	YES	YES

According to DruLiTo results, there were no ligands that obeyed all rules within the first 100 inhibitor candidates when they were evaluated according to their drug-likeness properties, as given in Table 3.6. Among these, 39 ligands which obeyed all the rules except for the MDDR-like rule were chosen for further analysis. Interactions between these ligands and BmrA protein were investigated by the Discovery Studio version 1.5 program [75].

Interaction of the ligand with the ATP binding region of BmrA would prevent ATP hydrolysis and hence the activity of BmrA pump would be blocked. The ATP binding residues of BmrA are given in Table 3.7 and the ATP binding sequences are shown in the structure in Figure 3.7.

Table 3.7 ATP Binding Sequences in BmrA.

Name	Sequence
Signature Sequence	A: L479, S480, G481, G484, Q483 / B: L1068, S1069, G1070, G1071, Q1072
Walker A or P-loop	A: G374, P375, S376, G377, G378, G379, K380, T381, T382, L383, F384, K385, L386 B: G963, P964, S965, G966, G967, G968, K969, T970, T971, L972, F973, K974, L975

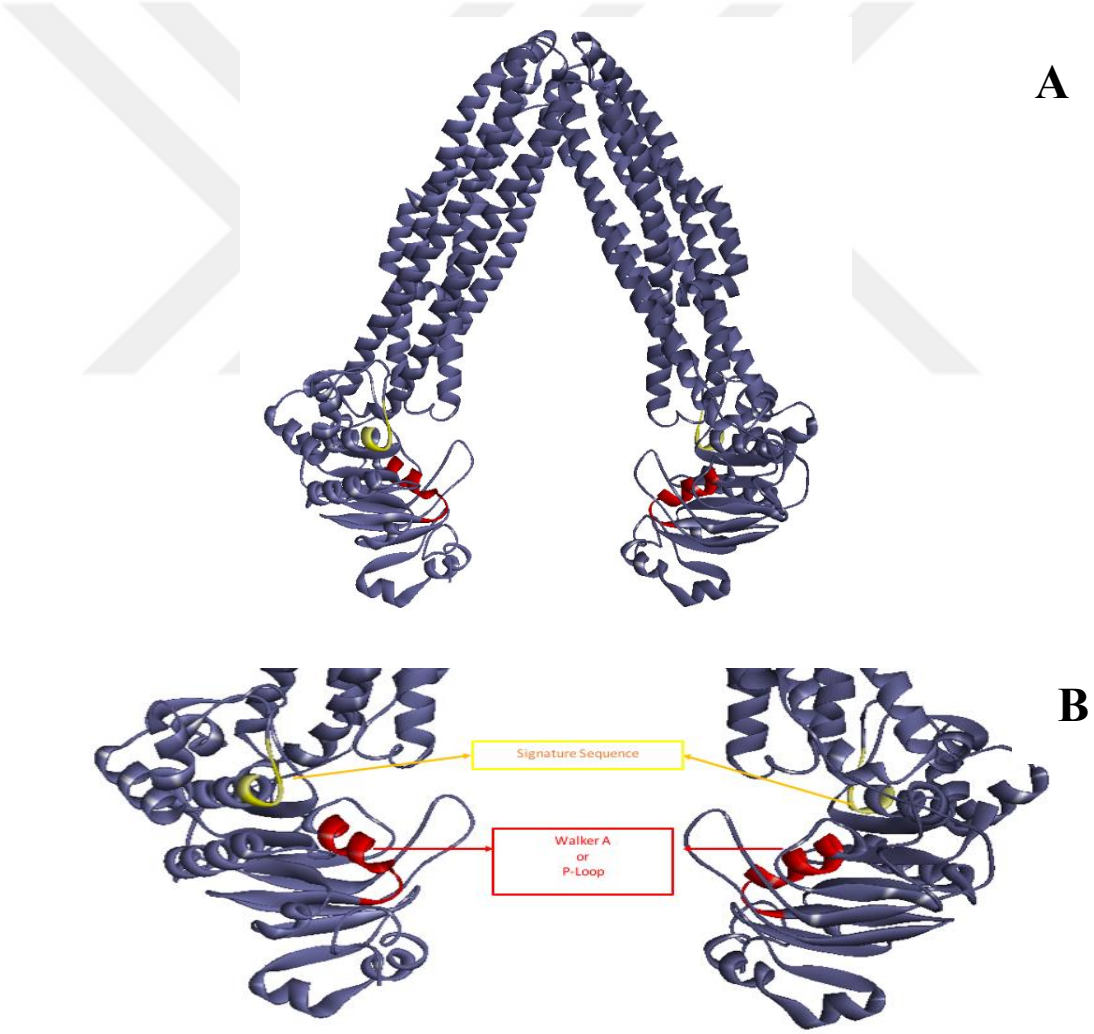

Figure 3.7 ATP binding sequences of the BmrA efflux pump; A) Complete structure, B) Right and Left NBD subunits showing ATP binding regions.

Analysis of the interacting residues showed that none of the ligands within the 39 candidates interacted with the ATP binding residues of BmrA. The representations of the interacting residues for the 39 ligands are given in Appendix 2 – Table I.

CM199 and CM174 that were found to bind the edge of the NBD, could be regarded as potential inhibitors since there was a similar binding interaction between P-gp and its inhibitor NB592, (Ward et al., 2013). The details of this binding are given in Figure 3.8 and Table 3.8.

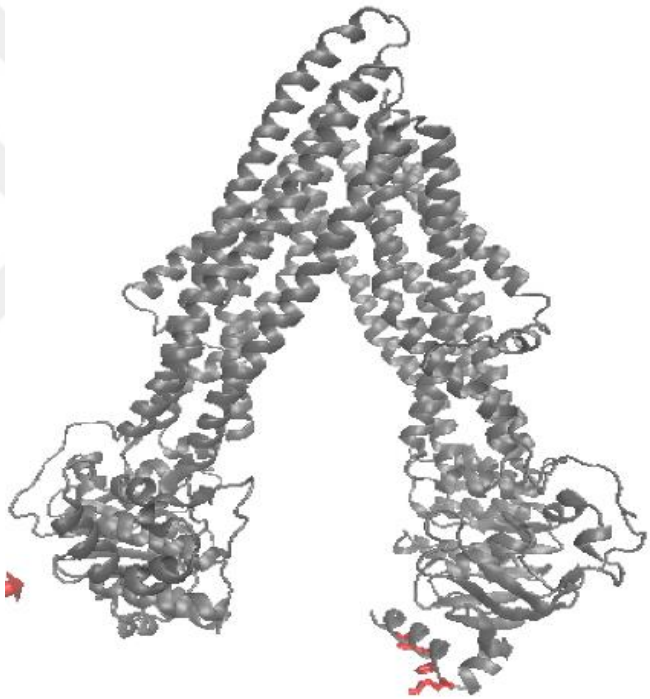

Figure 3.8 Representation of NB592 bound to p-gp (Ward et al., 2013)

Table 3.8 Residues of BmrA interacting with CM199 and CM174.

Ligand Name	Binding Energy (Kcal/mol)	Interacting Residues
CM199	-9.8	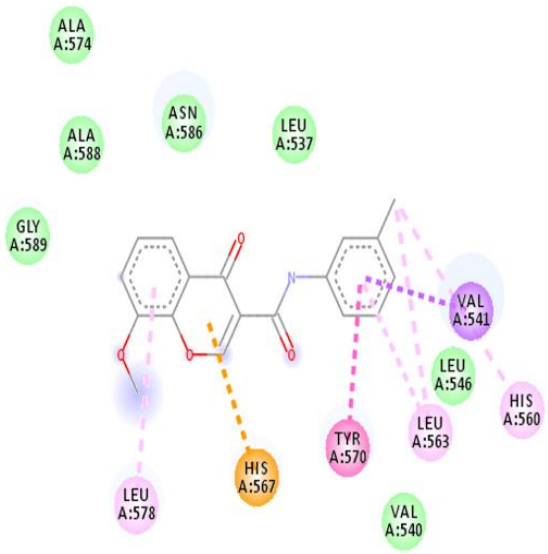 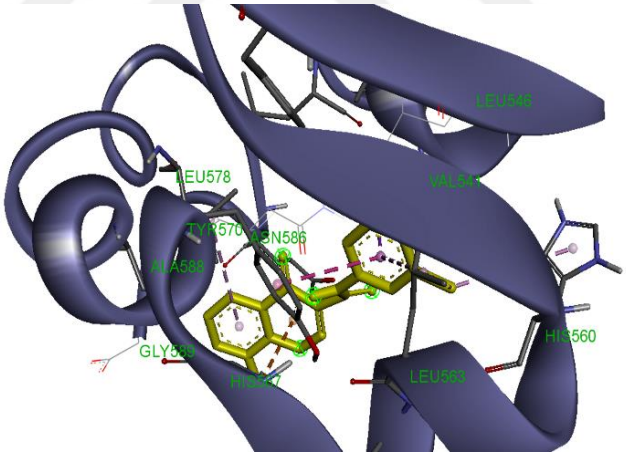

Table 3.8 Residues of BmrA interacting with CM199 and CM174 (Continued).

Ligand Name	Binding Energy (Kcal/mol)	Interacting Residues
CM174	-9.7	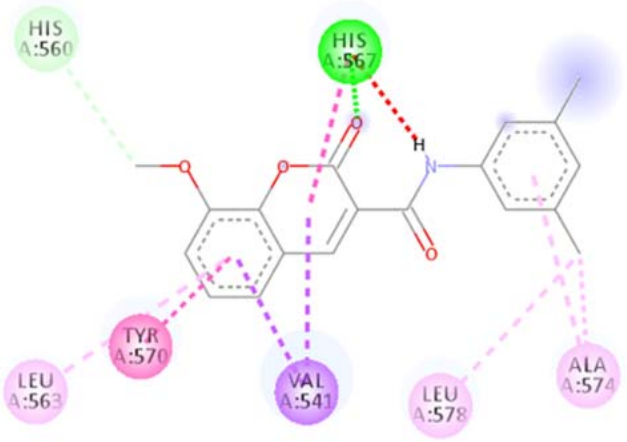 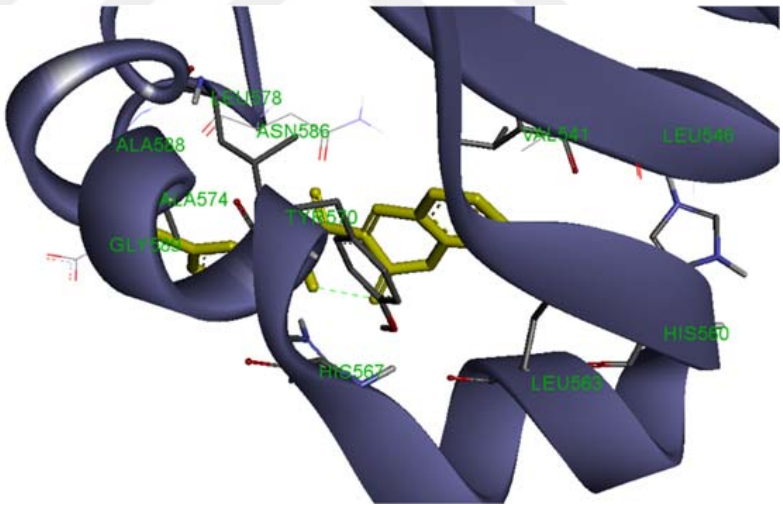

Since there were no ligands that obeyed all rules of DruLiTo within the top 100 ligands aligned based on their binding energies, the complete Chemotheca library was screened to find ligands that obeyed all seven rules of DruLiTo. This was possible since Chemotheca is a small library. A total 34 ligands were found to obey all the rules and the interactions of these ligands with BmrA were analyzed by Discovery Studio program. Five ligands structures were not suitable for viewing with the program.

Among the 34 ligands, only CM290 possessed residues interacting with BmrA. Results showed that CM290 interacted directly with the K385 residue of the ATP binding region and was in close vicinity of F384 and T381 residues of the ATP binding region (Table 3.9). All analysis results are given in Appendix 2 Table II.

Table 3.9 Residues of BmrA interacting with CM290 (Red: The residue is directly interacting with the ligand, Blue: The residue is not directly interacting with the ligand but is close to the ligand).

Ligand Name	Binding Energy (Kcal/mol)	Interacting Residues
CM290	-8,7	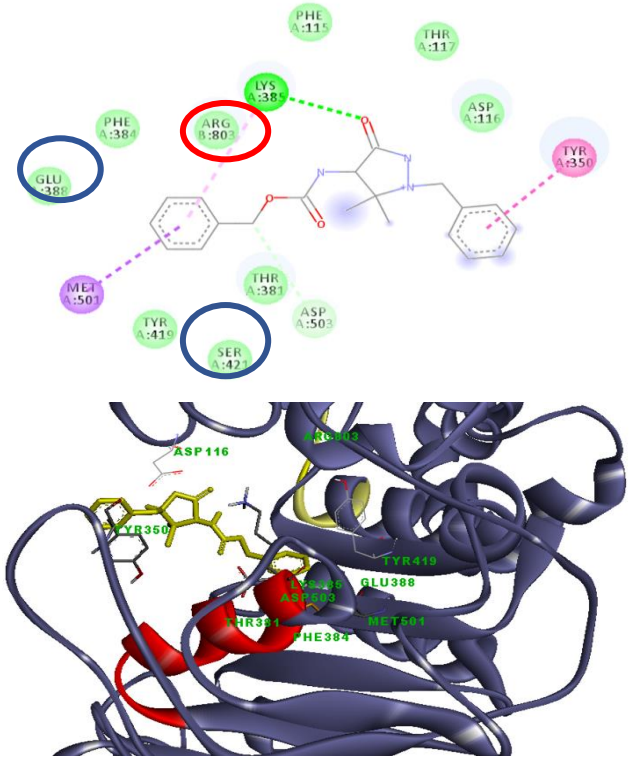

3.2.2.2. Second Strategy Evaluation

Chemotheca virtual screening results were also evaluated by the second strategy. Second strategy took into consideration two criteria, which were the binding free energy and the binding free energy difference between the two NBD subunits. The first criteria was to have a binding free energy equal to or less than -9 kcal/mol. This value was selected based on the results obtained with virtual screening using roemerine, boldine and bulbocapnine (section 3.2.1.) Since the binder roemerine gave the highest value of -8.2 kcal/mol for binding free energy, -9 kcal/mol was regarded to be a reasonable cut-off value. The second criteria for the selection was the value of the binding energy difference between the two NBD subunits. This was taken as equal to or less than 0.5. The idea behind the second criteria was that if a molecule can bind and inhibit both NBDs that it could be a better inhibitor preventing total ATP binding.

According to the criteria of the second strategy, 2 ligands obeying all rules but the MDDR-like rule and 1 ligand obeying all rules but BBB likeness, were selected (Tables 3.10 and 3.11).

Table 3.10 The binding free energy of the ligands selected from the Chemotheca library based on the second strategy

Ligand Name	Left Avg	Right Avg	Difference	Cavity Avg
CM263	-8.8	-9.22	0.42	-9.34
CM299	-8.94	-9.24	0.3	-8.34
CM51	-8.6	-9.00	0.4	-8.22

Table 3.11 DruLiTo assessment of the ligands which were selected based on the second strategy.

Ligand	Lipisinki	Ghose	CMC-50	Veber	MDDR	BBB	uwQED	WQED
CM263	YES	YES	YES	YES	NO	YES	YES	YES
CM299	YES	YES	YES	YES	YES	NO	YES	YES
CM51	YES	YES	YES	YES	NO	YES	YES	YES

Only CM263 and CM299 possessing residues interacting with BmrA were observed. CM263 interacted directly with T381 and A385 of the ATP binding region and was close to T382 and F384 residues of the ATP binding region. CM299 interacted directly with T970 and K974 of the ATP binding region and was close to T971 of the ATP binding region. Interaction representations are shown in Table 3.12. All studies' results are given in Appendix 2 Table III.

Table 3.12 Residues of BmrA interacting with CM263 and 299 (Red: The residue is directly interacted with the ligand, Blue: The residue is not directly interacted with the ligand but is close to the ligand).

Ligand Name	Binding Energy (Kcal/mol)	Interacting Residues
CM263 (Right)	-9.22	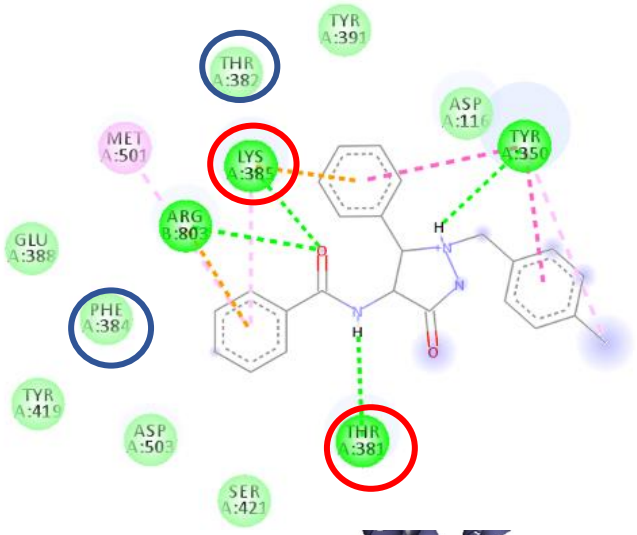
		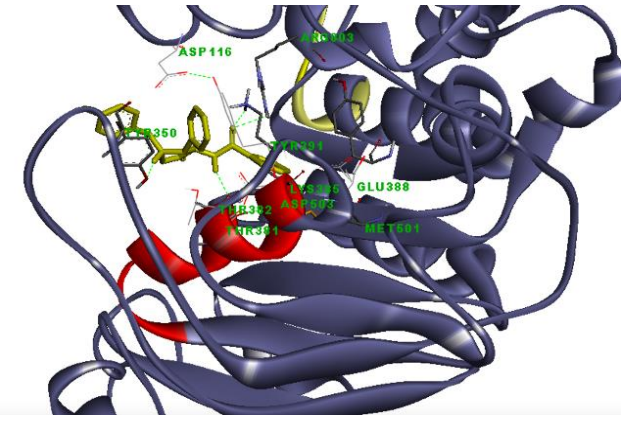
		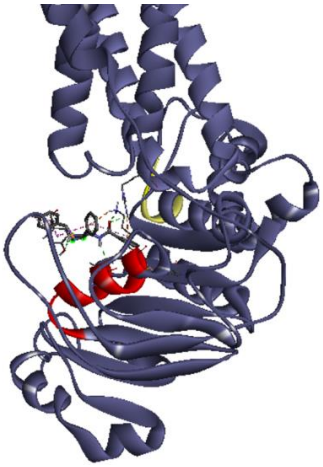

Table 3.12 Residues of BmrA interacting with CM263 and 299 (continued).

Ligand Name	Binding Energy (Kcal/mol)	Interacting Residues
CM299 (Left)	-8.94	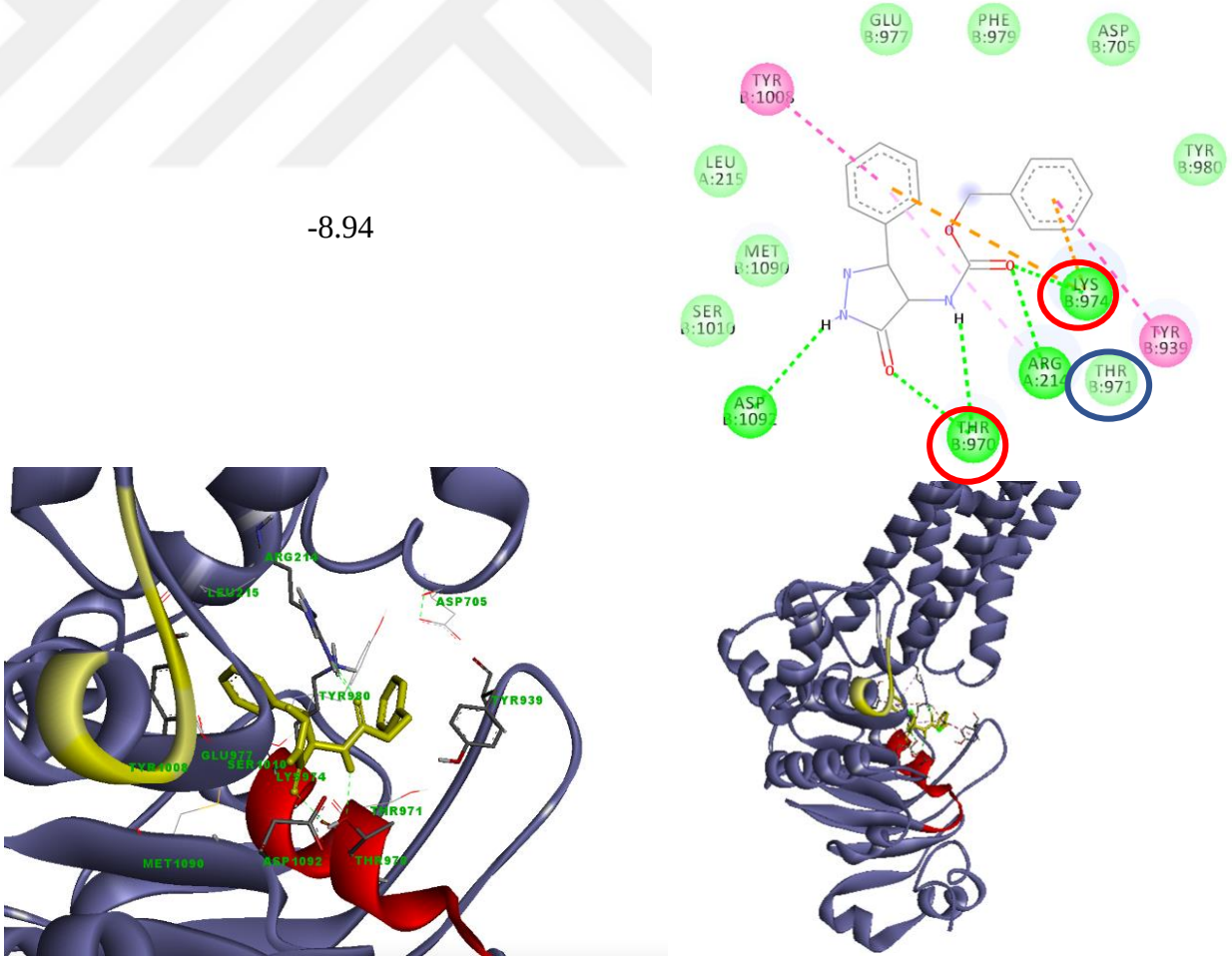

3.2.3. Chimiothèque Nationale Library

Chimiothèque Nationale Library consists of a total of 70,780 ligands but 3,780 of these are not suitable to be a drug since they have molecular weights higher 500 kDa (one of Lipisinki's rules). Therefore 67,000 ligands were evaluated for virtual screening. The two strategies, which were applied in the virtual screening of ligands of the Chemotheca library, were also implemented to this library to obtain potential inhibitors.

3.2.3.1. Evaluation of the Chimiothèque Nationale Library with the First Strategy

Free energies obtained with ligands binding to the cavity, the right NBD and the left NBD were evaluated together. Since the library has huge number of ligands, the first 1,000 ligands having the lowest binding energy from all calculations were selected. Then these ligands' drug-likeness properties were investigated by DruLiTo for their drug likeness.

Within the first 1,000 ligands, only 3 ligands (CN52946, CN53203, CN52560) obeying all the rules and 5 ligands (CN51357, CN52148, CN53019, CN50498, CN52716) obeying all rules but the MDDR-like rule were selected. The 3 ligands obeying all rules were found to interact with ATP binding sites of BmrA. The results were given in Table 3.13. CN52946 interacted directly with T970 and K974 of the ATP binding region and was close to S965 and G966 of the ATP binding region. CN53203 interacted directly with S965, G966, T970 and K974 of the ATP binding region and was close to G967 of the ATP binding region. CN2560 interacted directly with G1071 of the ATP binding region and was close to S1069 and G1070 of the ATP binding region. All results are shown in Appendix 3 Table IV.

Only 3 of other 5 ligands obeying 6 rules of DruLiTo were found to interact with the BmrA ATP binding sites and the results were given Table 3.14.

Table 3.13 Residues of BmrA interacting with CN52946, CN53203 and CN52560 (Red: The residue is directly interacting with the ligand, Blue: The residue is not directly interacting with the ligand but is close to the ligand).

Ligand Name	Binding Energy (Kcal/mol)	Interacting Residues
CN52946	-9.3	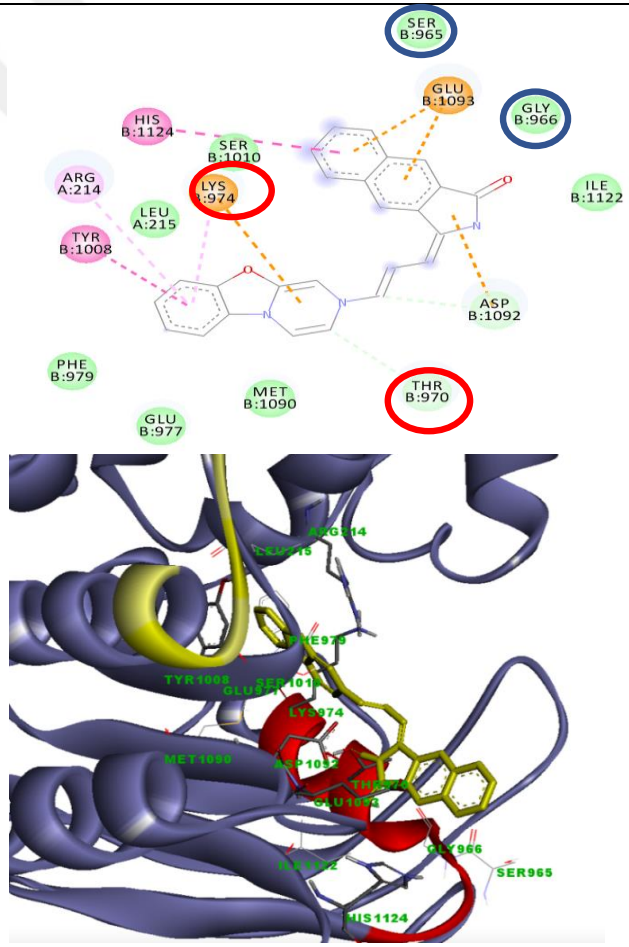

Table 3.13 Residues of BmrA interacting with CN52946, CN53203 and CN52560 (Red: The residue is directly interacting with the ligand, Blue: The residue is not directly interacting with the ligand but is close to the ligand) (continued).

Ligand Name	Binding Energy (Kcal/mol)	Interacting Residues
CN53203	-8.3	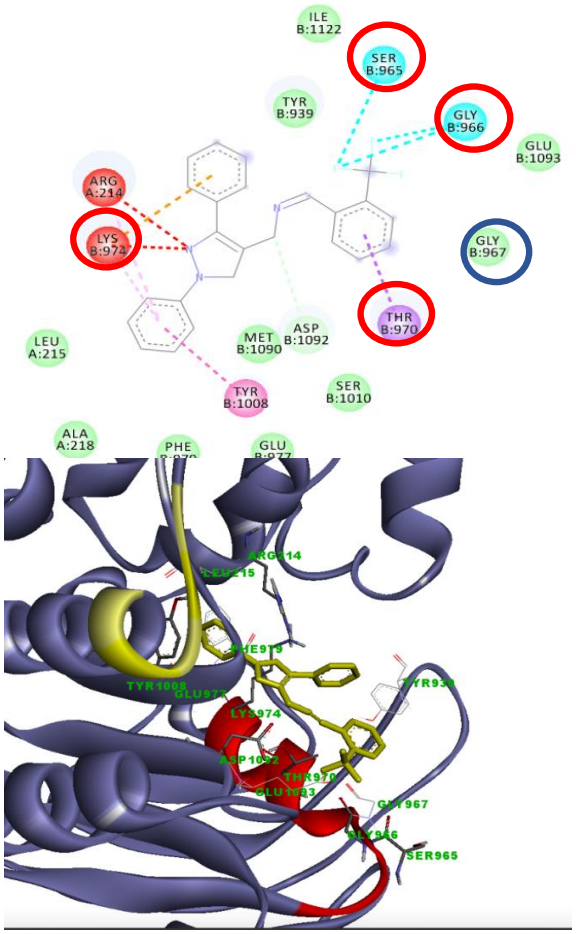

Table 3.13 Residues of BmrA interacting with CN52946, CN53203 and CN52560 (Red: The residue is directly interacting with the ligand, Blue: The residue is not directly interacting with the ligand but is close to the ligand) (continued).

Ligand Name	Binding Energy (Kcal/mol)	Interacting Residues
CN52560	-9.54	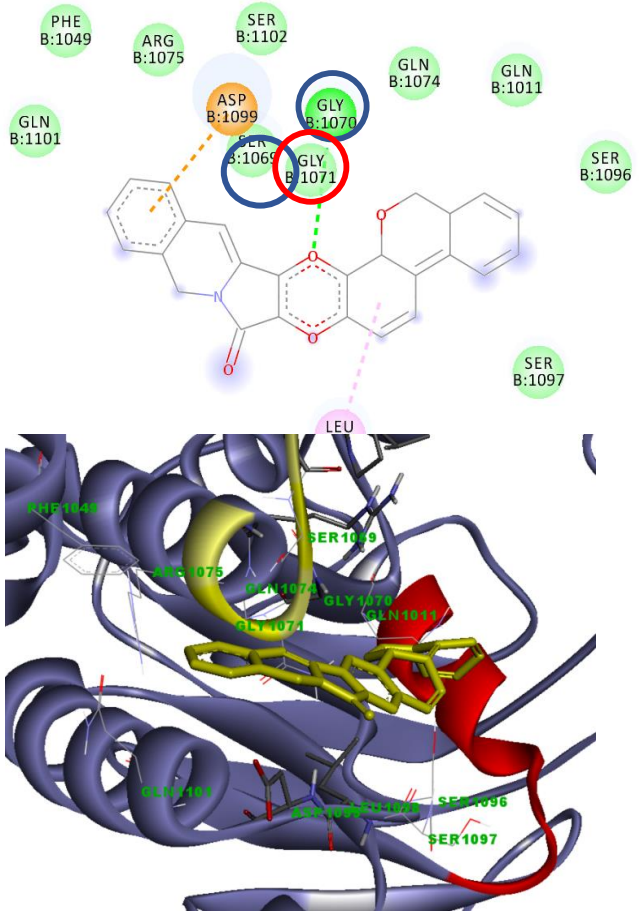

Table 3.14 Residues of BmrA interacting with CN51357, CN52148, CN53019 and CN52716 (Red: The residue is directly interacting with the ligand, Blue: The residue is not directly interacting with the ligand but is close to the ligand).

Ligand Name	Binding Energy (Kcal/mol)	Interacting Residues
CN51357	-9.72	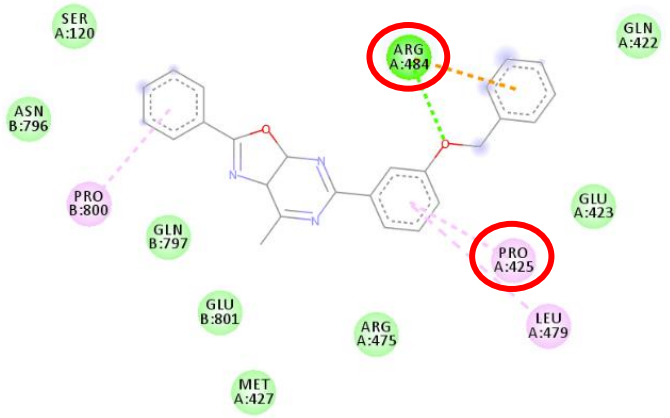 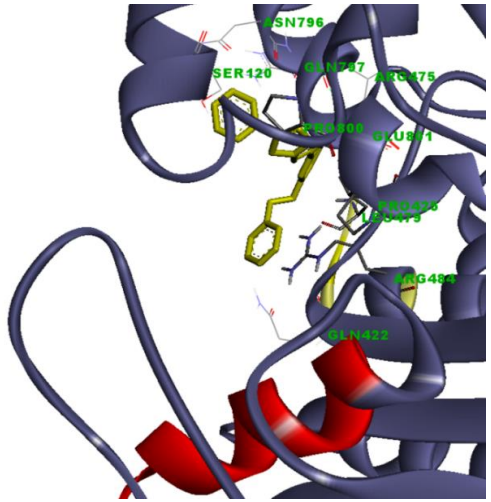

Table 3.14 Residues of BmrA interacting with CN51357, CN52148, CN53019 and CN52716 (Red: The residue is directly interacting with the ligand, Blue: The residue is not directly interacting with the ligand but is close to the ligand).

Ligand Name	Binding Energy (Kcal/mol)	Interacting Residues
		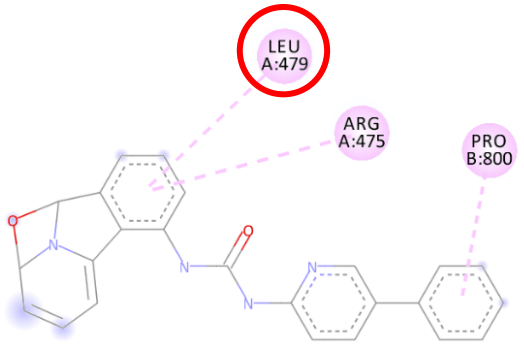
CN52148	-11.16	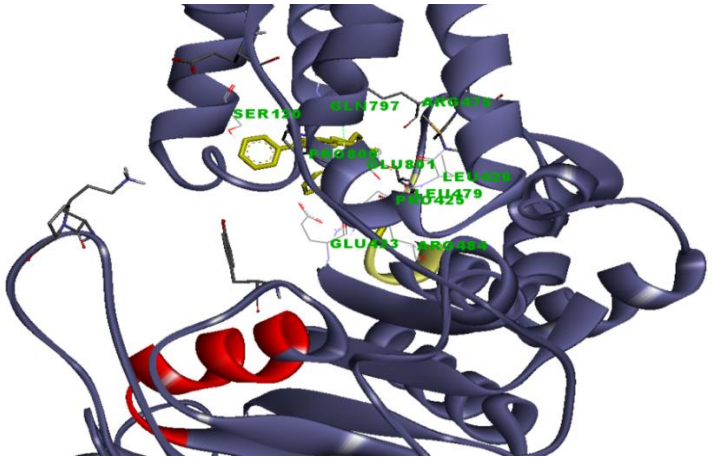

Table 3.14 Residues of BmrA interacting with CN51357, CN52148, CN53019 and CN52716 (Red: The residue is directly interacting with the ligand, Blue: The residue is not directly interacting with the ligand but is close to the ligand).

Ligand Name	Binding Energy (Kcal/mol)	Interacting Residues
CN52148	-9.14	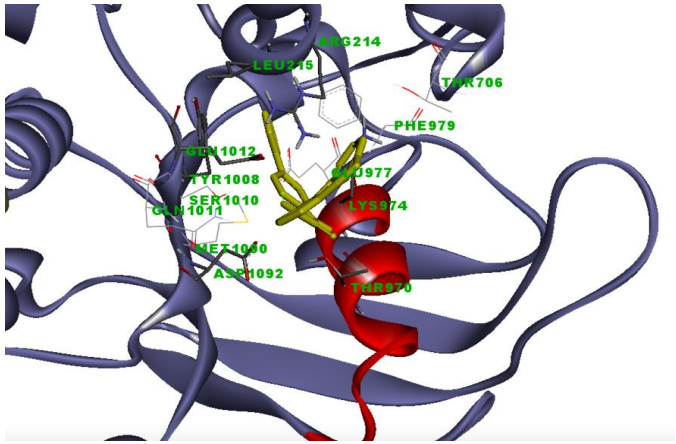

Table 3.14 Residues of BmrA interacting with CN51357, CN52148, CN53019 and CN52716 (Red: The residue is directly interacting with the ligand, Blue: The residue is not directly interacting with the ligand but is close to the ligand).

Ligand Name	Binding Energy (Kcal/mol)	Interacting Residues
CN53019	-9.86	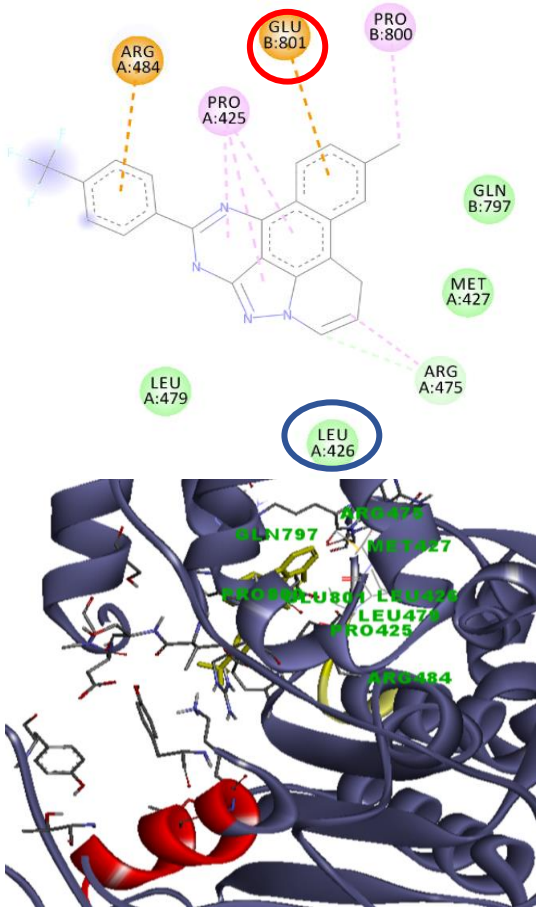

Table 3.14 Ligands of Chimiothèque Nationale Library obeying all rules but the MDDR-like of DruLiTo within the top 1,000 ligands (continued).

Ligand Name	Binding Energy (Kcal/mol)	Interacting Residues
CN52716	-11.06	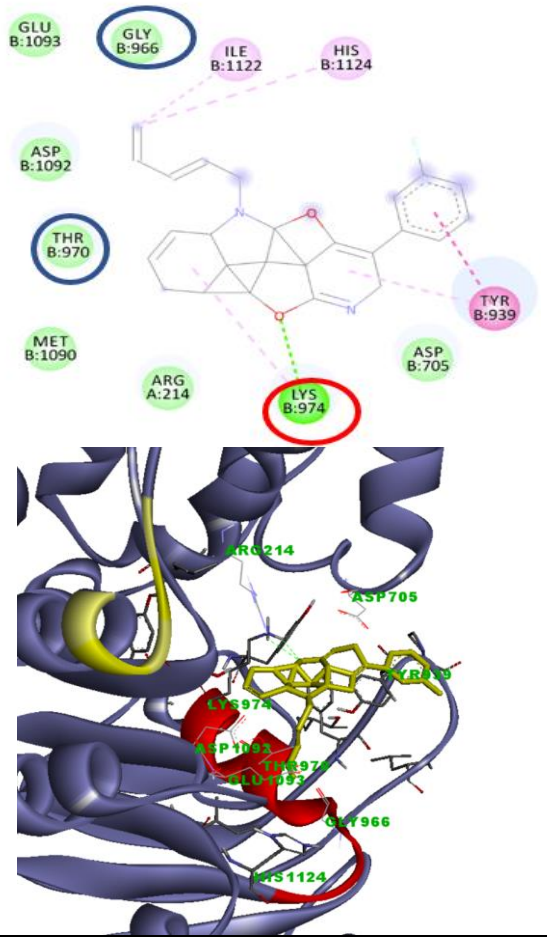

As seen in Table 3.14, CN51357 interacted directly with L479 and G484 of the ATP binding region of the right NBD and with K974 of the ATP binding region of the left NBD, and was close to T970 and T971 of the ATP binding region. CN52148 interacted directly with L479 of the ATP binding region of the right NBD and with T970 and K974 of the ATP binding region of the left NBD. CN53019 interacted directly with G484 of the ATP binding region of the right NBD and with T970 and K974 of the ATP binding region of the left NBD. It was also close to L479, G666 and G667 of the ATP binding region. CN52716 interacted directly with K974 and was close to T970 and G966. These interacting residues are given in Table 3.14. All results are shown in Appendix 3 Table V.

Thus, 7 ligands (CN52946, CN53203, CN52560, CN52148, CN51357, CN53019, CN52716) were selected as potential BmrA inhibitor candidates from the Chimiothèque Nationale Library when the first strategy was applied.

3.2.3.2. Evaluation of the Chimiothèque Nationale Library with the Second Strategy

Chimiothèque Nationale Library results were also evaluated by the second strategy. The threshold for maximum binding free energy was set at -9 kcal/mol (as explained in Section 3.2.2.2). The second criteria of binding energy difference was set to less than or equal to 0.04. Binding energy difference was lower for this library because Chimiothèque Nationale library was 100 times larger than the Chemotheca library. Furthermore, the results of this strategy was divided into three part based on ligands whose binding energy differences were 0 kcal/mol (Section 3.2.3.2.1), between 0 – 0.02 kcal/mol (Section 3.2.3.2.2) and between 0.02-0.04 kcal/mol (Section 3.2.3.2.3).

By first strategy, 7 ligands were selected due to their interaction with the ATP binding sites. By second strategy, 26 ligands were visualized and 20 of them were decided due to binding ATP binding sites. Thus, totally 27 ligands were selected as potential BmrA inhibitor candidates for further studies as seen in Table 3.15.

Table 3.15 Overall assessment the of Chimiothèque Nationale library virtual screening

Strategy	Binding Differences Kcal/mol	Numbers of Ligands visualized	All Rules	Without MDDR-like	Number of Ligands interacted with ATP Binding region	Ligands' Names
1st	-	9	3	6	7	CN52946 CN53203 CN52560 CN51357 CN52148 CN53019 CN52716 CN52562 CN53026
	0.02 – 0.04	7	4	3	6	CN53196 CN50557 CN43843 CN54231 CN54268 CM53648
2nd	0 – 0.02	11	4	7	9	CM51349 CN54733 CN52909 CN52713 CN54281 CN53219 CN52559 CN53592
	0	8	2	6	5	CN52150 CN51977 CN53545 CN48004

3.2.3.2.1. Ligands with a binding energy difference of 0 kcal/mol for the two NBDs

Based on this criteria, 2 ligands (CN53952, CN54578) obeying all rules and 6 ligands (CN52510, CN55373, CN50901, CN51977, CN53545, CN48004) obeying all rules but the MDDR-like rule were found by DruLiTo. These ligands' interacting residues were investigated with Discovery Studio program. The binding free energies and the drug-likeness properties are shown in Tables 3.16 and 3.17, respectively.

Table 3.16 Binding free energies of the ligands with a binding energy difference of 0 kcal/mol for the two NBDs, based on second strategy.

Ligand Name	Left Avg	Right Avg	Difference
CN53952	-8.18	-8.18	0
CN54578	-7.94	-7.94	0
CN52150	-9.5	-9.5	0
CN55373	-8.9	-8.9	0
CN50901	-8.6	-8.6	0
CN51977	-8.3	-8.3	0
CN53545	-8.14	-8.14	0
CN48004	-8.1	-8.1	0

Table 3.17 DruLiTo assessment of the ligands with a binding energy difference of 0 kcal/mol for the two NBDs, based on the second strategy.

Ligand	Lipisinki	Ghose	CMC-50	Veber	MDDR	BBB	uwQED	WQED
CN53952	YES	YES	YES	YES	YES	YES	YES	YES
CN54578	YES	YES	YES	YES	YES	YES	YES	YES
CN52150	YES	YES	YES	YES	NO	YES	YES	YES
CN55373	YES	YES	YES	YES	NO	YES	YES	YES
CN50901	YES	YES	YES	YES	NO	YES	YES	YES
CN51977	YES	YES	YES	YES	NO	YES	YES	YES
CN53545	YES	YES	YES	YES	NO	YES	YES	YES
CN48004	YES	YES	YES	YES	NO	YES	YES	YES

The examination of the results have shown that CN53592 interacted with K974 and T970, and was close to G967. CN52150 interacted with T970 and K974, was close to G966, G967, and S965. CN51977 interacted with K974 and was close to G967. In addition, CN53545 interacted with K974 and CN48004 interacted with L1068.

All interactions' representations are shown in Table 3.18. All results of the ligands with a binding energy difference of 0 kcal/mol for the two NBDs, is given Appendix 3 Table VI and Table VII.

Table 3.18 Residues of BmrA interacting with CN53952, CN52150, CN51977, CN53545 and CN48004 (Red: The residue is directly interacted with the ligand, Blue: The residue is not directly interacted with the ligand).

Ligand Name	Binding Energy (Kcal/mol)	Interacting Residues
CN53952	-8.18	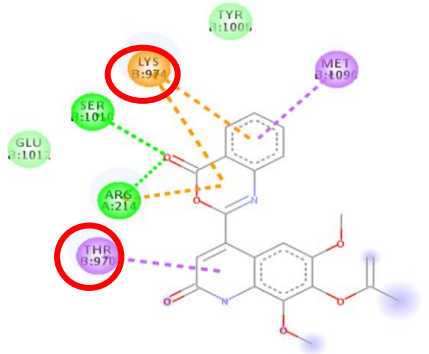 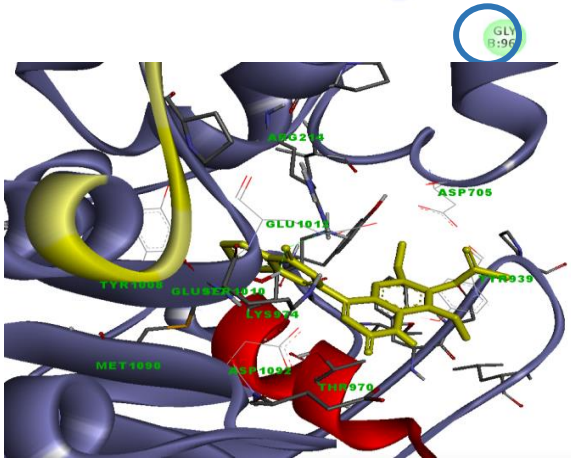

Table 3.18 Residues of BmrA interacting with CN53952, CN52150, CN51977, CN53545 and CN48004 (Red: The residue is directly interacted with the ligand, Blue: The residue is not directly interacted with the ligand but is closely to the ligand) (continued).

Ligand Name	Binding Energy (Kcal/mol)	Interacting Residues
CN52150	-9.5	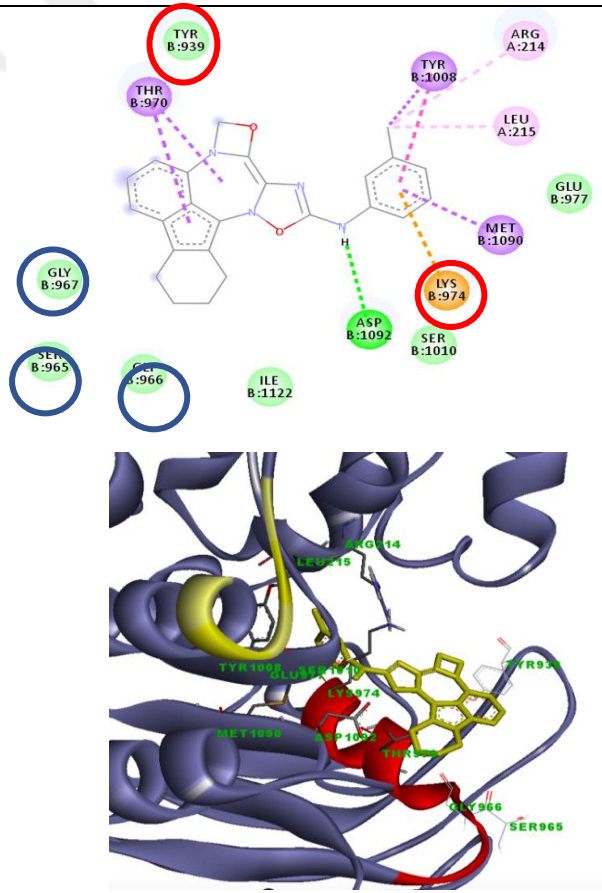

Table 3.18 Residues of BmrA interacting with CN53952, CN52150, CN51977, CN53545 and CN48004 (Red: The residue is directly interacted with the ligand, Blue: The residue is not directly interacted with the ligand but is closely to the ligand) (continued).

Ligand Name	Binding Energy (Kcal/mol)	Interacting Residues
CN51977	-8.3	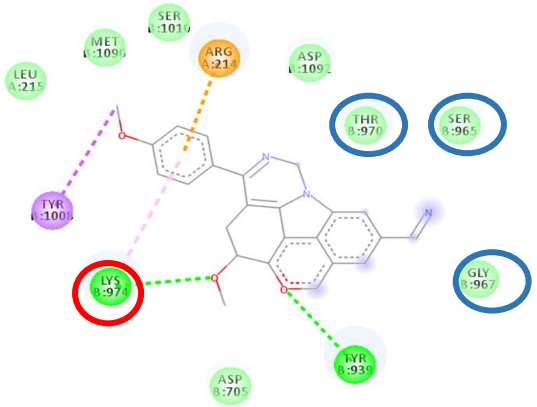 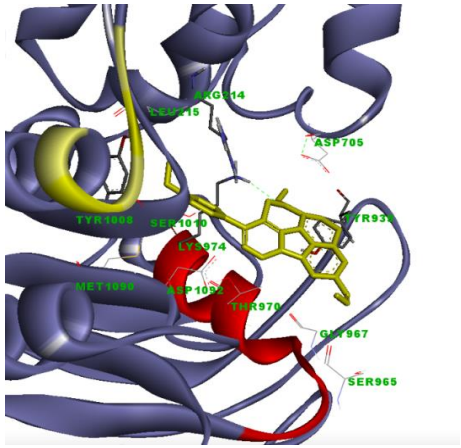

Table 3.18 Residues of BmrA interacting with CN53952, CN52150, CN51977, CN53545 and CN48004 (Red: The residue is directly interacted with the ligand, Blue: The residue is not directly interacted with the ligand but is closely to the ligand) (continued).

Ligand Name	Binding Energy (Kcal/mol)	Interacting Residues
CN53545	-8.14	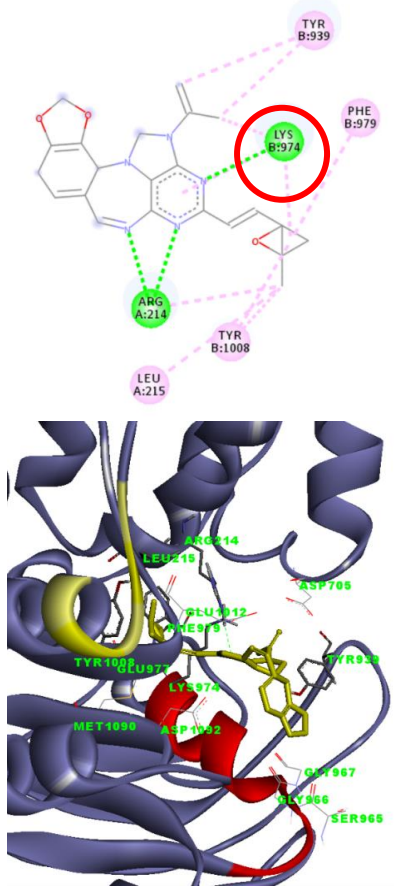

Table 3.18 Residues of BmrA interacting with CN53952, CN52150, CN51977, CN53545 and CN48004 (Red: The residue is directly interacted with the ligand, Blue: The residue is not directly interacted with the ligand but is closely to the ligand) (continued).

Ligand Name	Binding Energy (Kcal/mol)	Interacting Residues
CN48004	-8.1	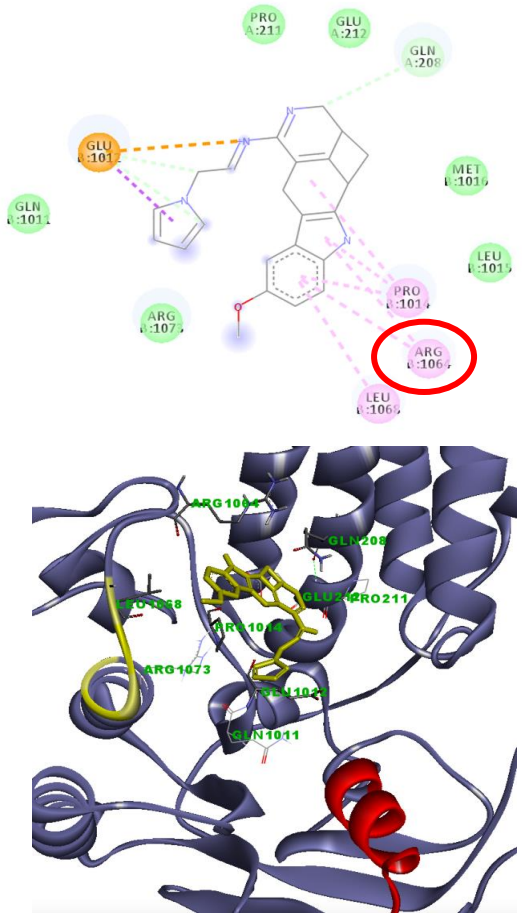

In this group of ligands, 5 ligands showed interaction with the ATP binding sites of BmrA and were selected as potential inhibitor candidates. One (CN53592) of these obeyed all rules and the other four (CN52150, CN51977, CN53545, CN48004) obeyed all rules but the MDDR-like rule of the DruLiTo drug-likeness evaluation.

3.2.3.2.2. Ligands with a binding energy difference between 0 – 0.02 kcal/mol for the two NBDs

In this group, 4 ligands (CN54268, CN52559, CN53648, CN53428) obeying all rules and 7 ligands (CN51349, CN54733, CN55511, CN52909, CN52713, CN54281, CN53219) obeying all the rules but the MDDR-like rule were found. Interactions between these ligands and BmrA efflux pump were investigated by Discovery Studio program. The binding energies and their drug-likeness properties are given in Tables 3.19 and 3.20, respectively.

Table 3.19 Binding free energies of the ligands with a binding energy difference between 0 – 0.02 kcal/mol for the two NBDs, based on second strategy.

Ligand Name	Left Avg	Right Avg	Difference
CN54268	-9.2	-9.22	0.02
CN52559	-8.84	-8.86	0.02
CN53648	-8.68	-8.7	0.02
CN53428	-8.48	-8.5	0.02
CN51349	-9.5	-9.48	0.02
CN54733	-9.32	-9.3	0.02
CN55511	-9.14	-9.16	0.02
CN52909	-8.9	-8.92	0.02
CN52713	-8.4	-8.42	0.02
CN54281	-8.28	-8.3	0.02
CN53219	-7.86	-7.88	0.02

Table 3.20 DruLiTo assessment of the ligands with a binding energy difference between 0 – 0.02 kcal/mol for the two NBDs, based on the second strategy.

Ligand	Lipisinki	Ghose	CMC-50	Veber	MDDR	BBB	uwQED	WQED
CN54268	YES	YES	YES	YES	YES	YES	YES	YES
CN52559	YES	YES	YES	YES	YES	YES	YES	YES
CN53648	YES	YES	YES	YES	YES	YES	YES	YES
CN53428	YES	YES	YES	YES	YES	YES	YES	YES
CN51349	YES	YES	YES	YES	NO	YES	YES	YES
CN54733	YES	YES	YES	YES	NO	YES	YES	YES
CN55511	YES	YES	YES	YES	NO	YES	YES	YES
CN52909	YES	YES	YES	YES	NO	YES	YES	YES
CN52713	YES	YES	YES	YES	NO	YES	YES	YES
CN54281	YES	YES	YES	YES	NO	YES	YES	YES
CN53219	YES	YES	YES	YES	NO	YES	YES	YES

The analysis of the ligands for their interactions has shown that most ligands interacted with the ATP binding sites of the BmrA pump. CN54268 interacted with K385 and K874 and was close to T381, T382, F384, G966, G967, and T970. CM53648 interacted directly with K385 of the ATP binding region and was close to T381, T382, and F384 of the ATP binding region. CN52559 was only close to L1068 but did not have any other interaction with BmrA. The interactions of all these ligands with the ATP binding sites are given in Table 3.21.

CM51349 interacted directly with L1068. CN52909 interacted directly with G484, L479 and L1068. CN54733 interacted directly with T381 and was close to T382 and K385. CN52713 interacted directly with S376, G377 and K385 and was close to T381, T382 and G378. CN54281 interacted with S376, T381, K385, T970 and K974, was close to G377, T382 and T971. CN53219 was close to L479 and G484 but did not have any other interaction with BmrA. The representations of the interacting residues are shown in Table 3.22. The representations of all the interacting residues are given in Appendix 3, Tables VIII and IX.

Table 3.21 Residues of BmrA interacting with CN54268, CN52559 and CN53648 (Red: The residue is directly interacted with the ligand, Blue: The residue is not directly interacted with the ligand but is closely to the ligand).

Ligand Name	Interacting Residues
CN54268	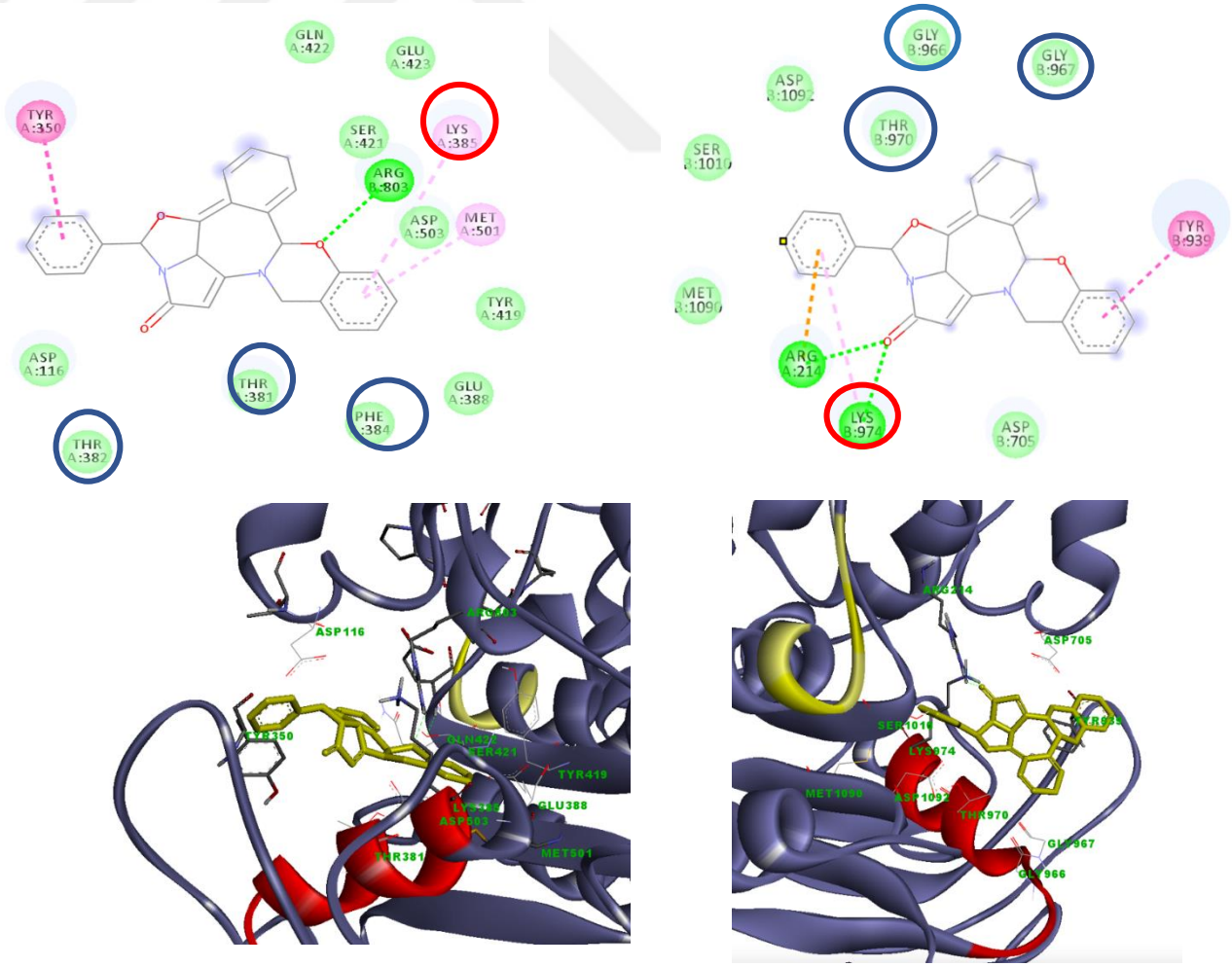

Table 3.21 Residues of BmrA interacting with CN54268, CN52559 and CN53648 (Red: The residue is directly interacted with the ligand, Blue: The residue is not directly interacted with the ligand but is closely to the ligand) (continued).

Ligand Name	Interacting Residues
CN53648	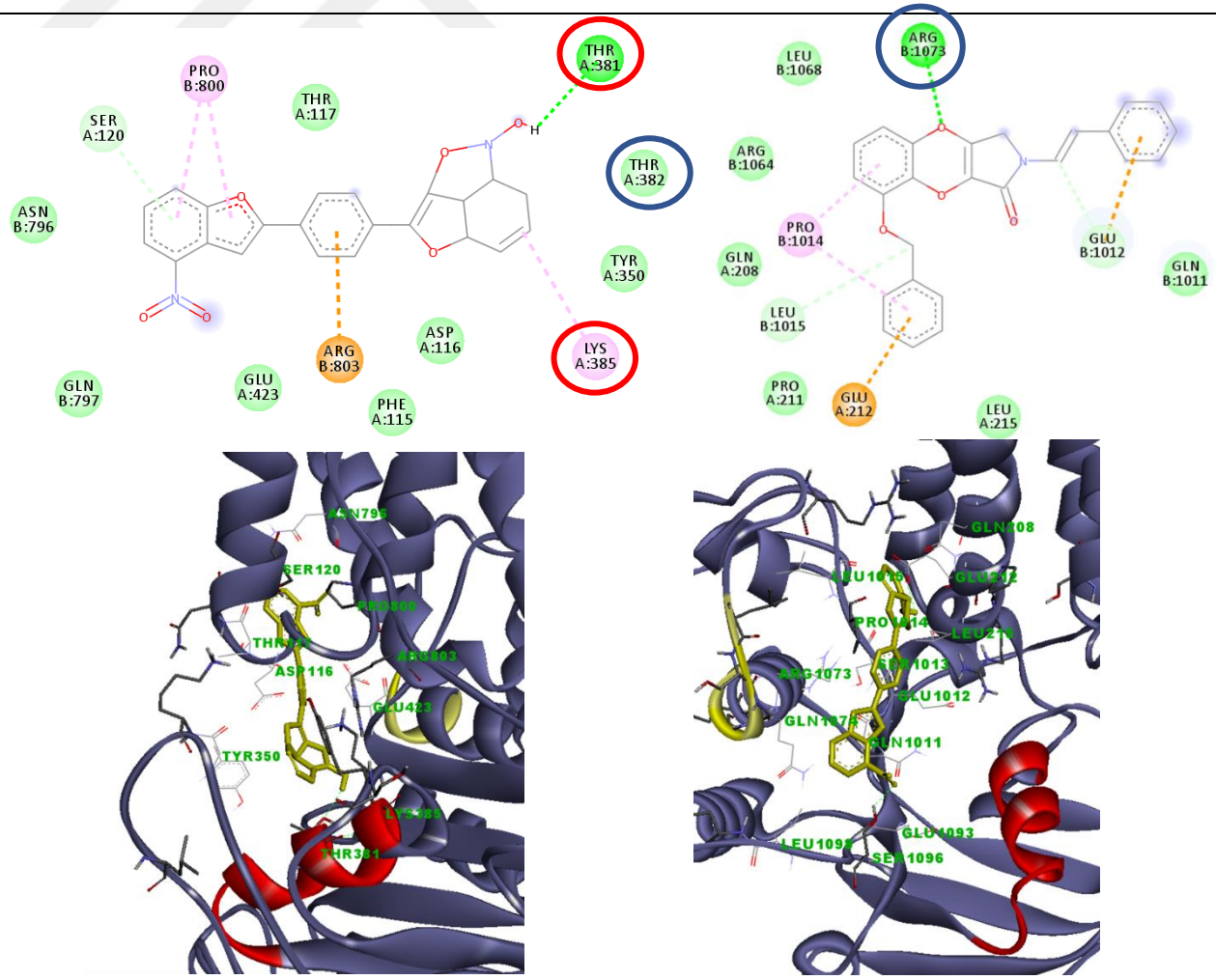

Table 3.21 Residues of BmrA interacting with CN54268, CN52559 and CN53648 (Red: The residue is directly interacted with the ligand, Blue: The residue is not directly interacted with the ligand but is closely to the ligand) (continued).

Ligand Name	Interacting Residues
CN52559	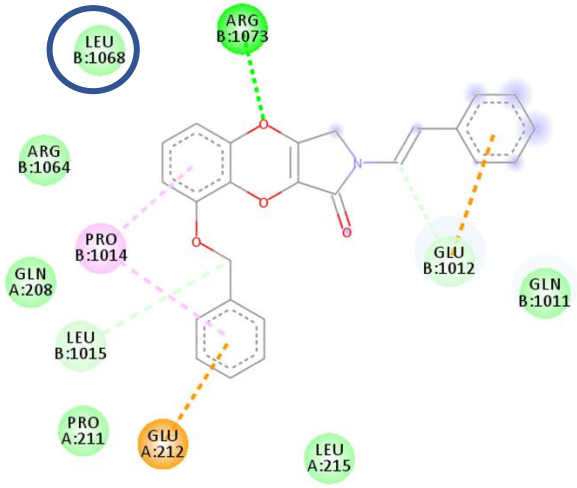 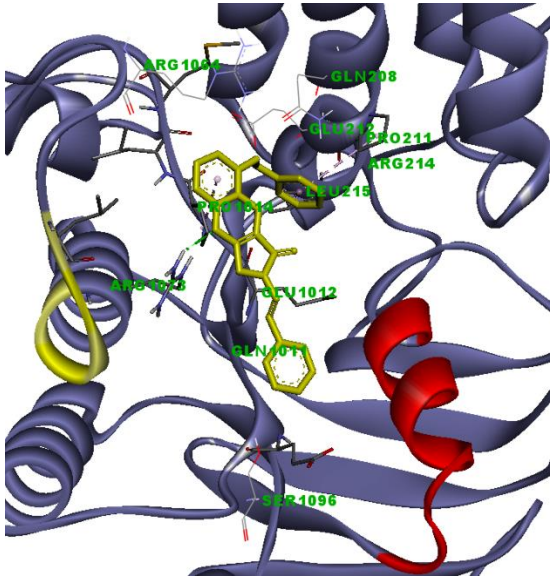

Table 3.22 Residues of BmrA interacting with CN51349, CN52909, CN54733, CN54281, CN52713 and CN53219 (Red: The residue is directly interacted with the ligand, Blue: The residue is not directly interacted with the ligand but is closely to the ligand).

Ligand Name	Interacting Residues	
CN51349	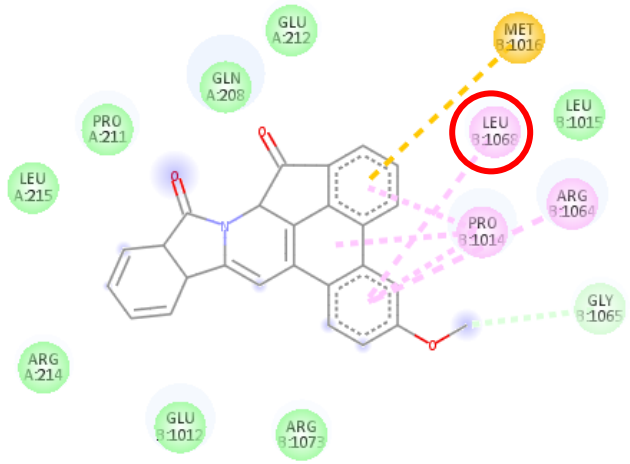	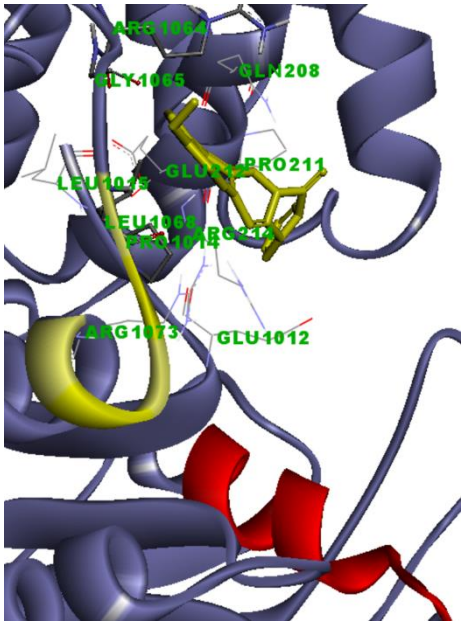

Table 3.22 Residues of BmrA interacting with CN51349, CN52909, CN54733, CN54281, CN52713 and CN53219 (Red: The residue is directly interacted with the ligand, Blue: The residue is not directly interacted with the ligand but is closely to the ligand) (continued).

Ligand Name	Interacting Residues
CN52909	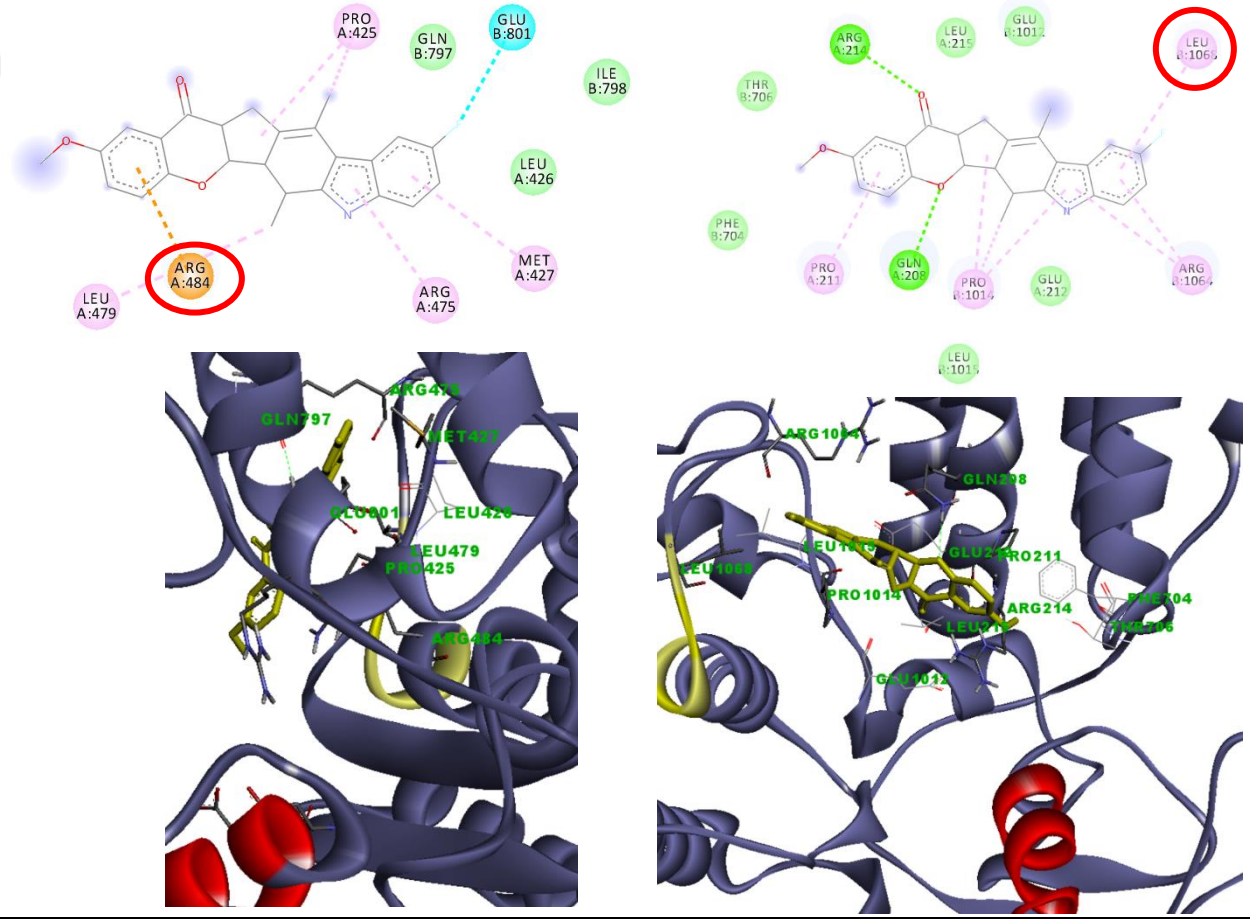

Table 3.22 Residues of BmrA interacting with CN51349, CN52909, CN54733, CN54281, CN52713 and CN53219 (Red: The residue is directly interacted with the ligand, Blue: The residue is not directly interacted with the ligand but is closely to the ligand) (continued).

Ligand Name	Interacting Residues
CN54733	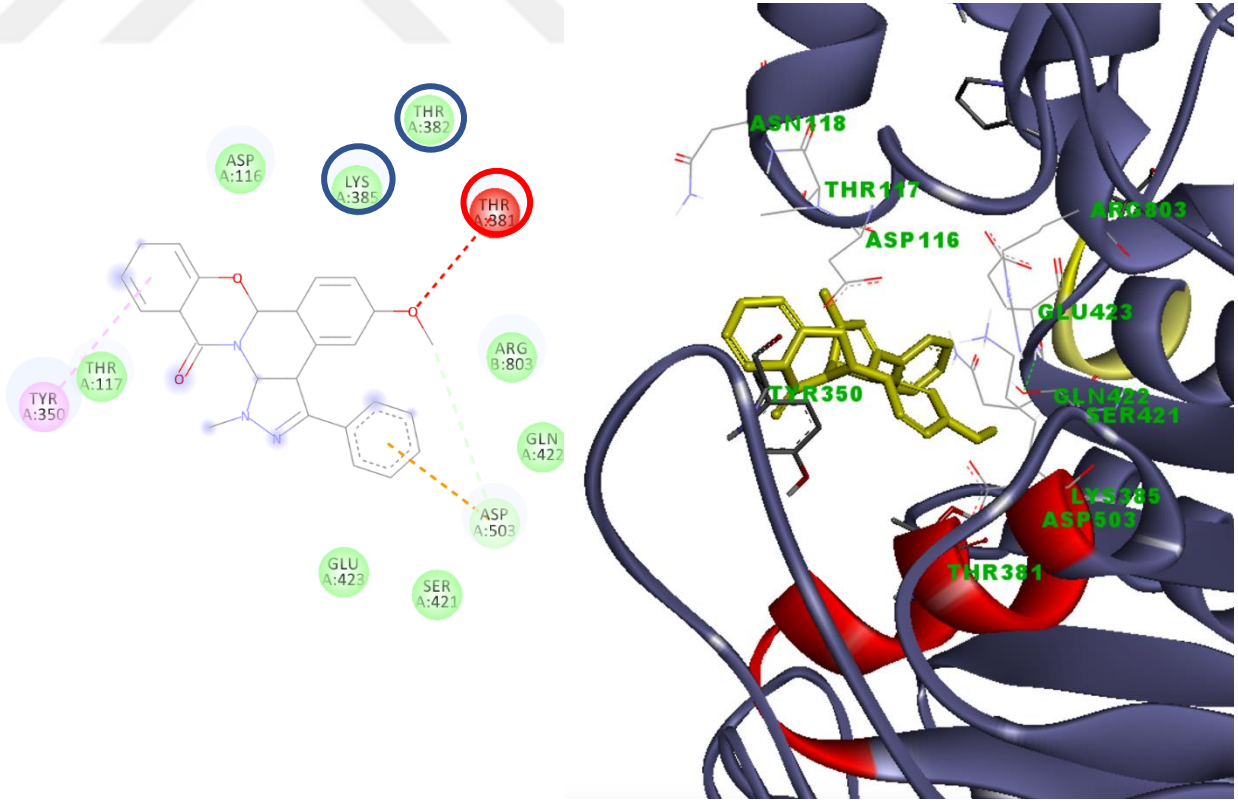

Table 3.22 Residues of BmrA interacting with CN51349, CN52909, CN54733, CN54281, CN52713 and CN53219 (Red: The residue is directly interacted with the ligand, Blue: The residue is not directly interacted with the ligand but is closely to the ligand) (continued).

Ligand Name	Interacting Residues	
CN54281	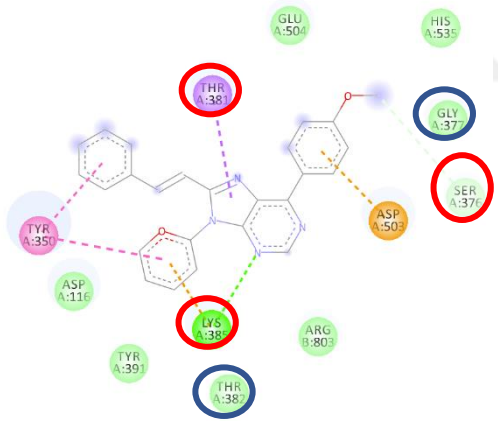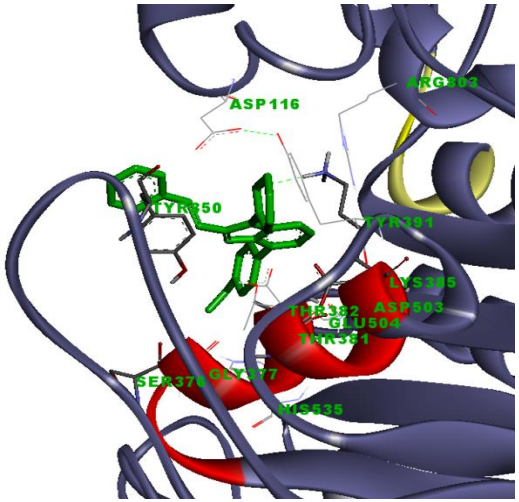	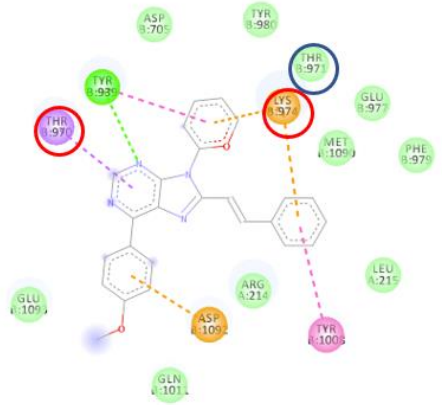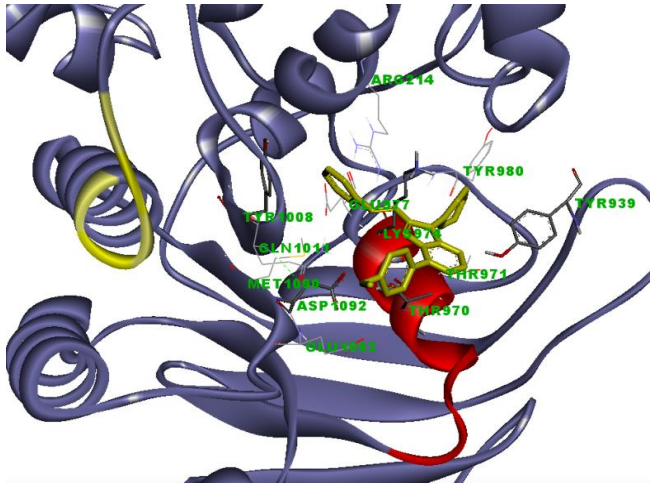

Table 3.22 Residues of BmrA interacting with CN51349, CN52909, CN54733, CN54281, CN52713 and CN53219 (Red: The residue is directly interacted with the ligand, Blue: The residue is not directly interacted with the ligand but is closely to the ligand) (continued).

Ligand Name	Interacting Residues
CN52713	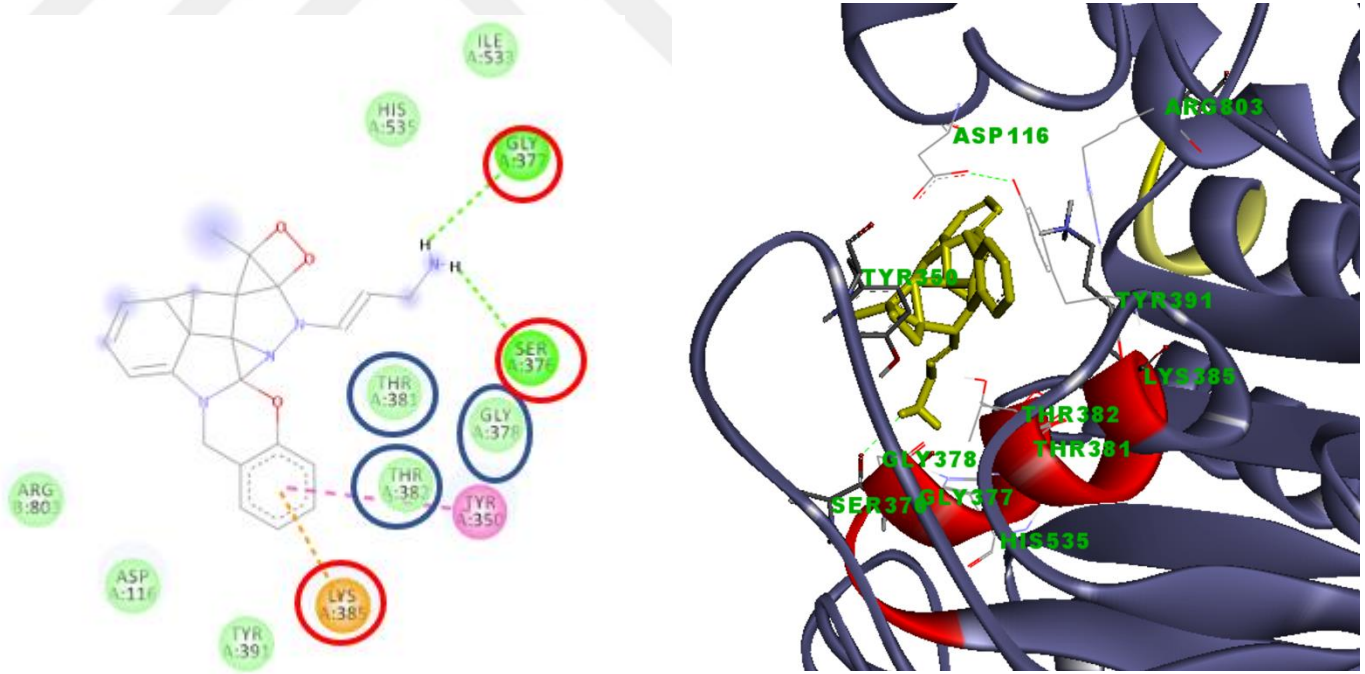

Table 3.22 Residues of BmrA interacting with CN51349, CN52909, CN54733, CN54281, CN52713 and CN53219 (Red: The residue is directly interacted with the ligand, Blue: The residue is not directly interacted with the ligand but is closely to the ligand) (continued).

Ligand Name	Interacting Residues
CN53219	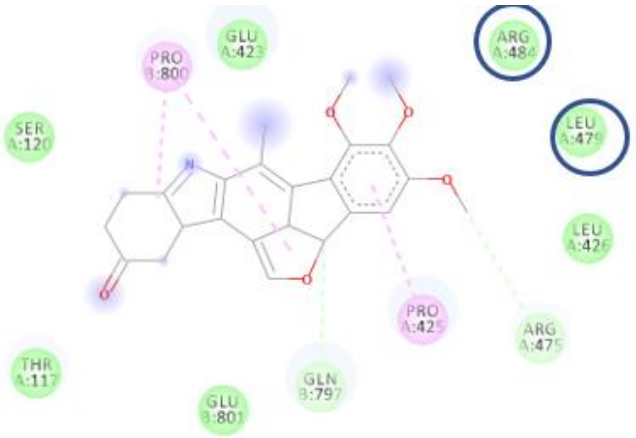 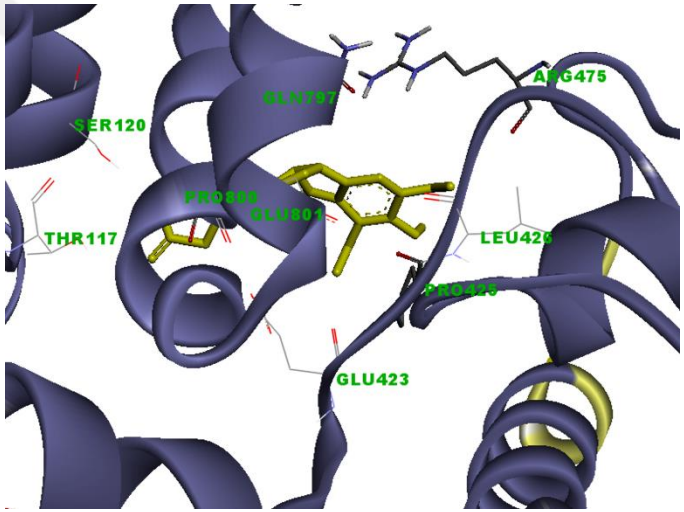

The results obtained in this group have shown that, eleven ligands possibly interacted with the residues of the ATP binding sites of BmrA. Analysis have shown that only 9 of these had interacting residues in the ATP binding site interaction. These were selected as potential inhibitor candidates. Three ligands (CN54268, CN52559, CN53648) obeyed all rules and 6 ligands (CN51349, CN54733, CN52909, CN52713, CN54281, CN53219) obeyed all rules but the MDDR-like rule.

3.2.3.2.3. Ligands with a binding energy difference between 0.02 – 0.04 kcal/mol for the two NBDs

In this group, ligands with a binding energy difference between 0.02 – 0.04 kcal/mol for the two NBDs were investigated. Four ligands (CN52562, CN53026, CN53196, CN50557) obeying all rules and 3 ligands (CN52318, CN43483, CN54231) obeying all the rules but the MDDR-like rule were found. The binding energy and drug-likeness information of the ligands are given in Tables 3.23 and 3.24, respectively.

Table 3.23 Binding free energies of the ligands with a binding energy difference between 0.02 – 0.04 kcal/mol for the two NBDs, based on second strategy.

Ligand Name	Left Avg	Right Avg	Difference
CN52562	-9.14	-9.1	0.04
CN53026	-8.52	-8.56	0.04
CN53196	-8.12	-8.16	0.04
CN50557	-8.06	-8.1	0.04
CN52318	-8.52	-8.56	0.04
CN43843	-8.5	-8.54	0.04
CN54231	-8.04	-8.08	0.04

Table 3.24 DruLiTo assessment of the ligands with a binding energy difference between 0.02 – 0.04 kcal/mol for the two NBDs, based on the second strategy.

Ligand	Lipisinki	Ghose	CMC-50	Veber	MDDR	BBB	uwQED	WQED
CN52562	YES	YES	YES	YES	YES	YES	YES	YES
CN53026	YES	YES	YES	YES	YES	YES	YES	YES
CN53196	YES	YES	YES	YES	YES	YES	YES	YES
CN50557	YES	YES	YES	YES	YES	YES	YES	YES
CN52318	YES	YES	YES	YES	NO	YES	YES	YES
CN43843	YES	YES	YES	YES	NO	YES	YES	YES
CN54231	YES	YES	YES	YES	NO	YES	YES	YES

Results have shown that CN52562 interacted with K974 and was close to F973 and T970. CN53026 interacted with T381, F384, K385 and K974 and was close to G377, K380, G966, T970 and T971. CN53196 interacted with K385 and was close to T381, T382, L1068, S1069 and G1070. CN50557 was close to K974, G966, G967 and T970. In addition, CN43843 interacted with T970, T971 and K974 and CN54231 was close to L1068 (Tables 3.25 and 3.26) The interactions of all the ligands are given in Appendix 3 Tables X and XI.

Table 3.25 Residues of BmrA interacting with CN52562, CN53026, CN53196 and CN50557 (Red: The residue is directly interacted with the ligand, Blue: The residue is not directly interacted with the ligand but is closely to the ligand).

Ligand Name	Interacting Residues
CN52562	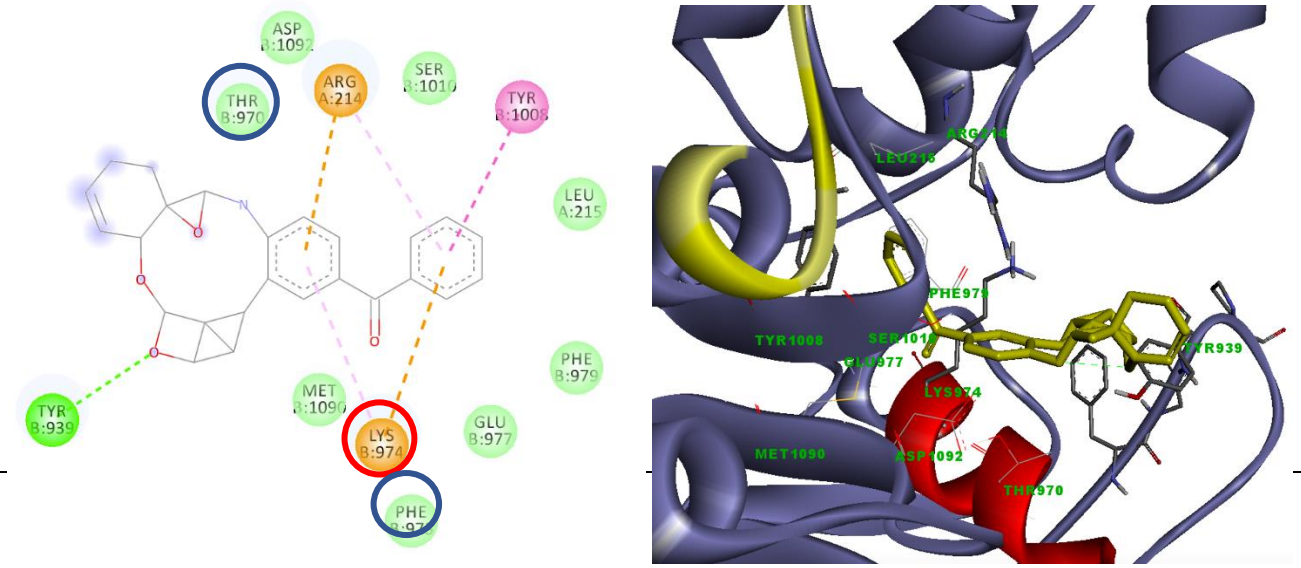

Table 3.25 Residues of BmrA interacting with CN52562, CN53026, CN53196 and CN50557 (Red: The residue is directly interacted with the ligand, Blue: The residue is not directly interacted with the ligand but is closely to the ligand) (continued).

Ligand Name	Interacting Residues
CN53026	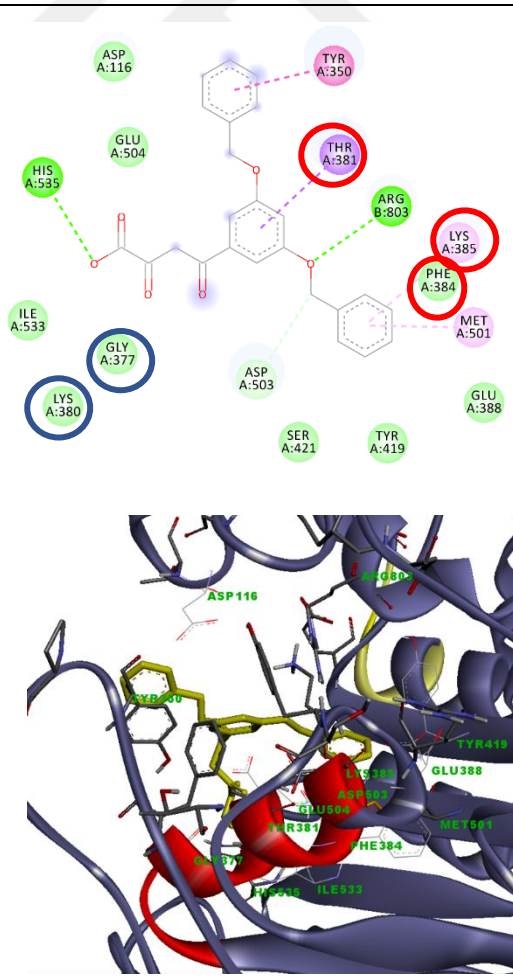

Table 3.25 Residues of BmrA interacting with CN52562, CN53026, CN53196 and CN50557 (Red: The residue is directly interacted with the ligand, Blue: The residue is not directly interacted with the ligand but is closely to the ligand) (continued).

Ligand Name	Interacting Residues
CN53196	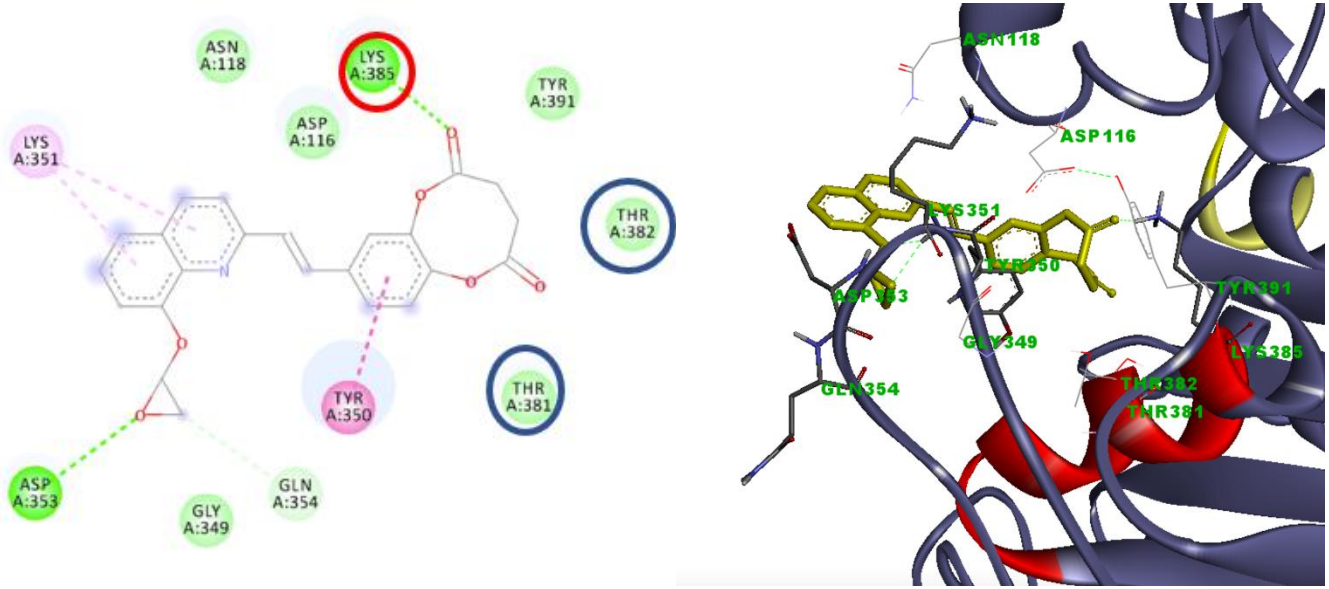

Table 3.25 Residues of BmrA interacting with CN52562, CN53026, CN53196 and CN50557 (Red: The residue is directly interacted with the ligand, Blue: The residue is not directly interacted with the ligand but is closely to the ligand) (continued).

Ligand Name	Interacting Residues
CN50557	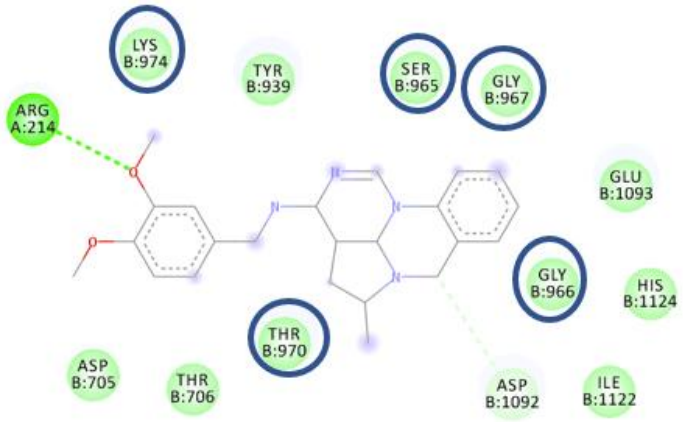 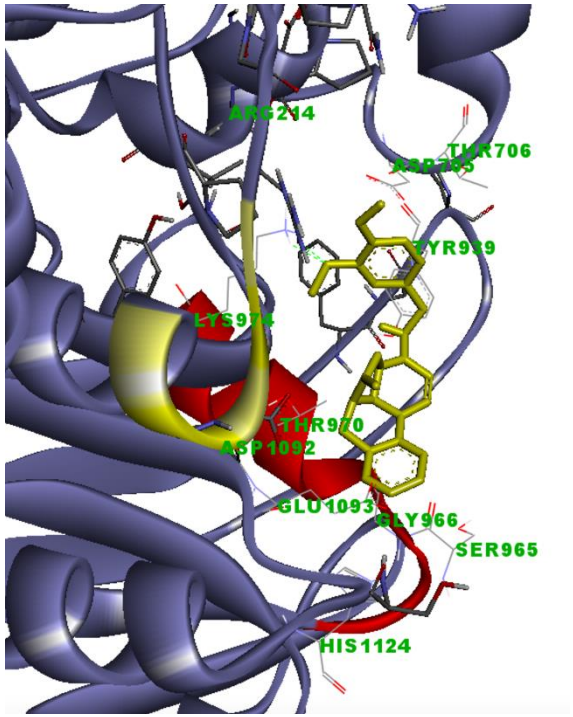

Table 3.26 Residues of BmrA interacting with CN43843 and CN54231 (Red: The residue is directly interacted with the ligand, Blue: The residue is not directly interacted with the ligand but is closely to the ligand).

Ligand Name	Interacting Residues	
CN43843	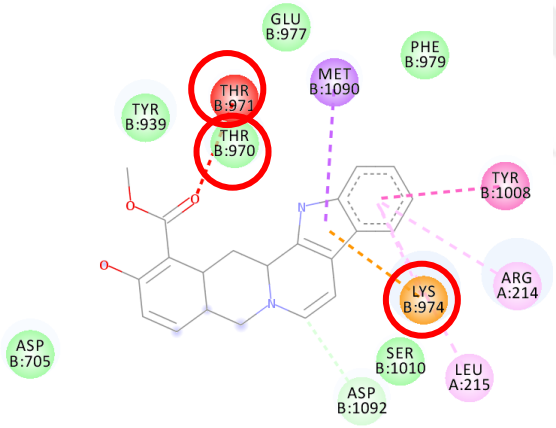	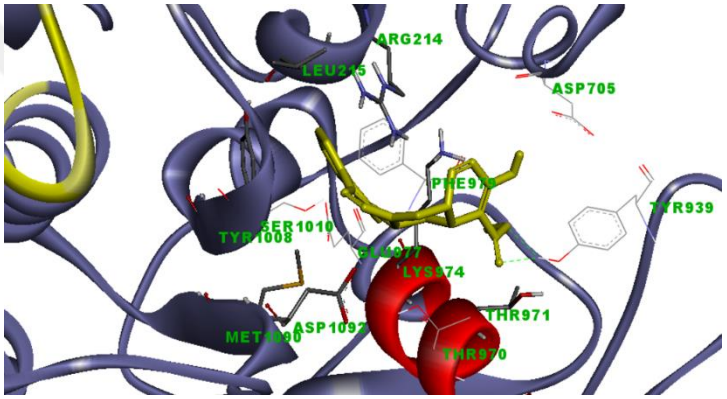
CN54231	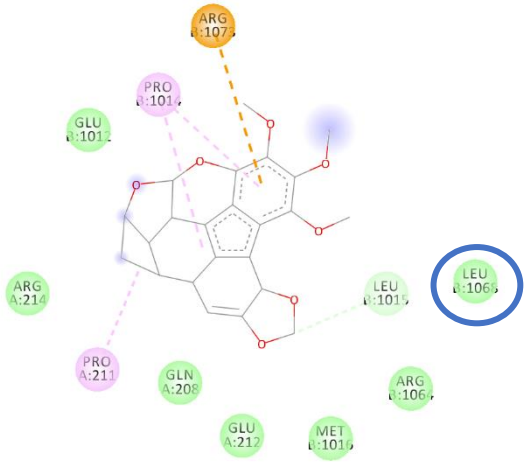	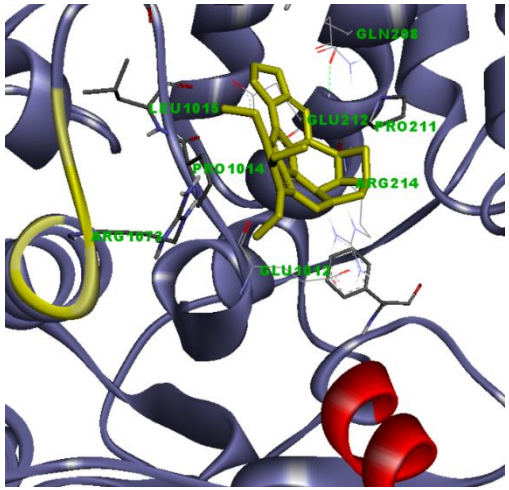

Within this group of ligands with a binding energy difference between 0.02 – 0.04 kcal/mol for the two NBDs, seven ligands were investigated for their interactions. Six ligands interacted with the BmrA ATP binding sites. Four ligands (CN52562, CN53026, CN53196, CN50557) were selected as potential inhibitor ligands obeying all rules and two ligands (CN43483, CN54231) obeyed only 6 rules based on DruLiTo assessment.

3.2.4. Libraries Evaluation

A total of 32 ligands were determined as potential inhibitors for further studies. The residues interacting with the ligands and the residues close to the ligands are summarized in Table 3.27. Many residues are common. Thus, these residues frequently found at the binding interphase could represent the targets of BmrA for inhibition. Thus, new molecules targeting these residues could be designed as new inhibitors of BmrA.

Table 3.27. It is shown that the residues interacting and/or close to ATP binding sites of the ligands selected from virtual screening.

Library	Ligand Name	Drug-likeness	Interacted Residue	Closer Residue
Chemotheca	CM19	Without MDDR	-	Edge of NBD
	CM174	Without MDDR	-	Edge of NBD
	CM290	Without MDDR	K385	T381, F384
	CM263	Without MDDR	T381, K385	T382, F384
	CM299	Without BBB	T970, K974	T971
Chimiothèque Nationale	CN52946	All	T970, K974	S965, G966
	CN53203	All	S965, G966, T970, K974	G967
	CN52560	All	G1071	S1069, G1070
	CN52148	Without MDDR	L479	-
	CN51357	Without MDDR	L479, G484, K974	T970, T971
	CN52148	Without MDDR	L479, T970, K974	-
	CN53019	Without MDDR	G484, T970, K974	L479, G966, G967
	CN52716	Without MDDR	K974	G966, T970
	CN53592	Without MDDR	T970, K974	G967
	CN52150	Without MDDR	T970, K974	S965, G966, G967
	CN51977	Without MDDR	K974	G967
	CN53545	Without MDDR	K974	-
Chimiothèque Nationale	CN48004	Without MDDR	L1068	-
	CN54268	Without MDDR	K385, K874	T381, T382, F384, G966, G967, T970

	CN52559	Without MDDR	-	L1068
	CN53648	Without MDDR	K385	T381, T382, F384
	CN51349	Without MDDR	L1068	-
	CN54733	Without MDDR	T381	T382, K385
	CN52909	Without MDDR	G484, L479, L1068	-
	CN52713	Without MDDR	S376, G377, K385	T381, T382, G378
	CN54281	Without MDDR	S376, T381, K385, T970, K974	G377, T382, G971
	CN53219	Without MDDR	-	L479, G484
	CN52562	Without MDDR	K974	T970, F973
	CN53026	Without MDDR	T381, F384, K385, K974	G377, K380, G966, T970, T971
	CN53196	Without MDDR	K385	T381, T382, L1068, S1069, G1070
	CN50557	Without MDDR	K974	G966, G967, T970
	CN43843	Without MDDR	T970, T971, K974	-
	CN54231	Without MDDR	-	L1068

CHAPTER 4 - CONCLUSION

In conclusion, virtual screening studies were performed in order to find new inhibitor candidates against BmrA multidrug efflux pump for contribution of human infection disease treatments. For virtual screening studies, firstly BmrA efflux pump structure was homology modelled based on *E. coli* MsbA structure with full coordinates (kindly provided by Geoffrey Chang) and *S. aureus* SAV1866 (PDB: 2HYD) templates by using Modeller program. It was shown that new model has higher quality than the BmrA structure modelled in 2009 [85]. After the homology modelling studies, virtual screening was performed for 2 libraries and 32 ligands were selected as potential inhibitors from the libraries. In addition, by evaluating the ATP binding sites' interacting residues, they are seen quite similar within the potential inhibitor ligands. This result shows that all results are consistent, and these residues could be target region for BmrA multidrug efflux pump inhibition.

Nevertheless, all selected ligands activity should be proven with experimental data. In further studies, this computational study will be verified with the optimized experiment examination.

REFERENCES

[1] Saga, T., Yamaguchi, K. (2009) History of antimicrobial agents and resistant bacteria. Japan Medical Association Journal, 52(2), 103-108.

[2] Durand, G. A., Raoult, D., Dubourg, G. (2018) Antibiotic discovery: History, methods and perspectives. International Journal of Antimicrobial Agents, 53(4), 371-382.

[3] Pećanac, M., Janjić, Z., Komarčević, A., Pajić, M., Dobanovački, D., Mišković-Skeledžija, S. (2013) Burns treatment in ancient times. Medicinski Pregled, 66(5-6), 263-267.

[4] Lewis, K. (2013) Platforms for antibiotic discovery. Nature Reviews Drug discovery, 12(5), 371.

[5] Fleming, A., Chain, E., Florey, H. (1945) Sir Alexander Fleming-Nobel Lecture: Penicillin. The Nobel Prize (1945) 83-93, http://www. nobelprize. org/nobel_prizes/medicine/laureates/1945/fleming-lecture. html. (11.12.1945)

[6] Abraham, E. P., Chain, E. (1940) An enzyme from bacteria able to destroy penicillin. Nature International Journal of Science, 146(3713), 837.

[7] Demain, A. L. (2009) Antibiotics: natural products essential to human health. Medicinal Research Reviews, 29(6), 821-842.

[8] Lewis, K. (2013) Platforms for antibiotic discovery. Nature Reviews Drug Discovery, 12(5), 371.

[9] Schatz, A., Bugle, E., Waksman, S. A. (1944) Streptomycin, a Substance Exhibiting Antibiotic Activity Against Gram-Positive and Gram-Negative Bacteria. Proceedings of the Society for Experimental Biology and Medicine, 55(1), 66-69.

[10] Blaskovich, M. A., Butler, M. S., Cooper, M. A. (2017) Polishing the tarnished silver bullet: the quest for new antibiotics. Essays in Biochemistry, 61(1), 103-114.

[11] Wise, R., Hart, T., Cars, O. (1998) Antimicrobial resistance is a major threat to public health. British Medical Journal, 317, 609-610.

[12] K Bhardwaj, A., Mohanty, P. (2012) Bacterial efflux pumps involved in multidrug resistance and their inhibitors: rejuvinating the antimicrobial chemotherapy. Recent Patents on Anti-Infective Drug Discovery, 7(1), 73-89.

[13] Bolla, J. R. (2014) Bacterial multidrug efflux pumps: structure, function and regulation. PhD Thesis, Iowa State University, Ames, Iowa, USA, 1-2.

[14] Du, D., Wang-Kan, X., Neuberger, A., van Veen, H. W., Pos, K. M., Piddock, L. J., Luisi, B. F. (2018) Multidrug efflux pumps: structure, function and regulation. Nature Reviews Microbiology, 16(9), 523.

[15] Martinez, J. L., Sánchez, M. B., Martínez-Solano, L., Hernandez, A., Garmendia, L., Fajardo, A., Alvarez-Ortega, C. (2009) Functional role of bacterial multidrug efflux pumps in microbial natural ecosystems. Federation of European Microbiological Societies Microbiology Reviews, 33(2), 430-449.

[16] Jardetzky, O. (1966) Simple allosteric model for membrane pumps. Nature International Journal of Science, 211(5052), 969.

[17] Li X.Z., Elkinds C.A., Zgurskaya H.I. (2016) Efflux-Mediated Antimicrobial Resistance in Bacteria: Mechanisms, Regulation and Clinical Implications, 1st Edition, Springer International Publishing, Switzerland.

[18] Rees, D. C., Johnson, E., Lewinson, O. (2009) ABC transporters: the power to change. Nature Reviews Molecular Cell Biology, 10(3), 218.

[19] Ramaswamy, V. K., Cacciotto, P., Malloci, G., Vargiu, A. V., Ruggerone, P. (2017) Computational modelling of efflux pumps and their inhibitors. Essays in Biochemistry, 61(1), 141-156.

[20] Higgins, C. F., Linton, K. J. (2004) The ATP switch model for ABC transporters. Nature Structural & Molecular Biology, 11(10), 918.

[21] Ernst, R., Kueppers, P., Stindt, J., Kuchler, K., Schmitt, L. (2010) Multidrug efflux pumps: Substrate selection in ATP-binding cassette multidrug efflux pumps–first come,

first served?. The Federation of European Microbiological Societies Journal, 277(3), 540-549.

[22] Van Der Does, C., Tampe, R. (2004) How do ABC transporters drive transport?. Biological Chemistry, 385(10), 927-933.

[23] Du, D., Wang-Kan, X., Neuberger, A., van Veen, H. W., Pos, K. M., Piddock, L. J., Luisi, B. F. (2018) Multidrug efflux pumps: structure, function and regulation. Nature Reviews Microbiology, 16(9), 523.

[24] Orelle, C., Dalmas, O., Gros, P., Di Pietro, A., Jault, J. M. (2003) The conserved glutamate residue adjacent to the Walker-B motif is the catalytic base for ATP hydrolysis in the ATP-binding cassette transporter BmrA. Journal of Biological Chemistry, 278(47), 47002-47008.

[25] Steinfels, E., Orelle, C., Fantino, J. R., Dalmas, O., Rigaud, J. L., Denizot, F., Pietro A. D., Jault, J. M. (2004) Characterization of YvcC (BmrA), a multidrug ABC transporter constitutively expressed in Bacillus subtilis. Biochemistry, 43(23), 7491-7502.

[26] Mus-Veteau, I. (2016) Heterologous Expression of Membrane Proteins: Methods and Protocols, 2nd Edition, Humana Press, New York, USA.

[27] Dawson, R. J., Locher, K. P. (2006) Structure of a bacterial multidrug ABC transporter. Nature, 443(7108), 180.

[28] Ward, A., Reyes, C. L., Yu, J., Roth, C. B., Chang, G. (2007) Flexibility in the ABC transporter MsbA: Alternating access with a twist. Proceedings of The National Academy of Sciences, 104(48), 19005-19010.

[29] Do Cao, M. A., Crouzy, S., Kim, M., Becchi, M., Cafiso, D. S., Pietro, A. D., Jault, J. M. (2009) Probing the conformation of the resting state of a bacterial multidrug ABC transporter, BmrA, by a site-directed spin labeling approach. Protein Science, 18(7), 1507-1520.

[30] Kunert, B., Gardiennet, C., Lacabanne, D., Calles-Garcia, D., Falson, P., Jault, J. M., Meier B.H., Penin F., Böckmann, A. (2014) Efficient and stable reconstitution of the ABC transporter BmrA for solid-state NMR studies. Frontiers in Molecular Biosciences, 1, 5.

[31] Calabrese, A. N., Radford, S. E. (2018). Mass spectrometry-enabled structural biology of membrane proteins. Methods, 147, 187-205.

[32] Ravaud, S., Do Cao, M. A., Jidenko, M., Ebel, C., Le Maire, M., Jault, J. M., Pietro A.D., Haser, R., Aghajari, N. (2006) The ABC transporter BmrA from Bacillus subtilis is a functional dimer when in a detergent-solubilized state. Biochemical Journal, 395(2), 345-353.

[33] Meng, X. Y., Zhang, H. X., Mezei, M., Cui, M. (2011) Molecular docking: a powerful approach for structure-based drug discovery. Current Computer-Aided Drug Design, 7(2), 146-157.

[34] Roche, D., Brackenridge, D., McGuffin, L. (2015) Proteins and their interacting partners: An introduction to protein–ligand binding site prediction methods. International Journal of Molecular Sciences, 16(12), 29829-29842.

[35] Fu, Y., Zhao, J., Chen, Z. (2018) Insights into the Molecular Mechanisms of Protein-Ligand Interactions by Molecular Docking and Molecular Dynamics Simulation: A Case of Oligopeptide Binding Protein. Computational and Mathematical Methods in Medicine, 2018, 1-12.

[36] Salmaso, V., Moro, S. (2018) Bridging molecular docking to molecular dynamics in exploring ligand-protein recognition process: an overview. Frontiers in Pharmacology, 9 (923), 1-16.

[37] Ferreira, L., dos Santos, R., Oliva, G., Andricopulo, A. (2015) Molecular docking and structure-based drug design strategies. Molecules, 20(7), 13384-13421.

[38] Kukol, A. (2008) Molecular Modeling of Proteins, 1st Edition, Humana Press, New York, USA.

[39] Guedes, I. A., Pereira, F. S., Dardenne, L. E. (2018) Empirical scoring functions for structure-based virtual screening: applications, critical aspects, and challenges. Frontiers in Pharmacology, 9, 1089.

[40] Yang, C. Y., Wang, R., Wang, S. (2006) M-score: a knowledge-based potential scoring function accounting for protein atom mobility. Journal of Medicinal Chemistry, 49(20), 5903-5911.

[41] Huang, S. Y., Grinter, S. Z., Zou, X. (2010) Scoring functions and their evaluation methods for protein–ligand docking: recent advances and future directions. Physical Chemistry Chemical Physics, 12(40), 12899-12908.

[42] Wang, R., Lu, Y., Wang, S. (2003) Comparative evaluation of 11 scoring functions for molecular docking. Journal of Medicinal Chemistry, 46(12), 2287-2303.

[43] Pason, L. P., Sotriffer, C. A. (2016) Empirical Scoring Functions for Affinity Prediction of Protein-ligand Complexes. Molecular Informatics, 35(11-12), 541-548.

[44] De Magalhães, C. S., Almeida, D. M., Barbosa, H. J. C., Dardenne, L. E. (2014) A dynamic niching genetic algorithm strategy for docking highly flexible ligands. Information Sciences, 289, 206-224.

[45] Debroise, T., Shakhnovich, E. I., Chéron, N. (2017) A hybrid knowledge-based and empirical scoring function for protein–ligand interaction: SMoG2016. Journal of Chemical Information and Modeling, 57(3), 584-593.

[46] Baek, M., Shin, W. H., Chung, H. W., Seok, C. (2017) GalaxyDock BP2 score: a hybrid scoring function for accurate protein–ligand docking. Journal of Computer-Aided Molecular Design, 31(7), 653-666.

[47] Goodsell, D. S., Olson, A. J. (1990) Automated docking of substrates to proteins by simulated annealing. Proteins: Structure, Function, and Bioinformatics, 8(3), 195-202.

[48] Morris, G. M., Goodsell, D. S., Halliday, R. S., Huey, R., Hart, W. E., Belew, R. K., Olson, A. J. (1998) Automated docking using a Lamarckian genetic algorithm and an

empirical binding free energy function. Journal of Computational Chemistry, 19(14), 1639-1662.

[49] Trott, O., Olson, A. J. (2010) AutoDock Vina: improving the speed and accuracy of docking with a new scoring function, efficient optimization, and multithreading. Journal of Computational Chemistry, 31(2), 455-461.

[50] Morris, G. M., Huey, R., Lindstrom, W., Sanner, M. F., Belew, R. K., Goodsell, D. S., Olson, A. J. (2009) AutoDock4 and AutoDockTools4: Automated docking with selective receptor flexibility. Journal of Computational Chemistry, 30(16), 2785-2791.

[51] Goodsell, D. S., Morris, G. M., Olson, A. J. (1996) Automated docking of flexible ligands: applications of AutoDock. Journal of Molecular Recognition, 9(1), 1-5.

[52] Gibbs, J. W. (1873) A Method of Geometrical Representation of the Thermodynamic Properties by Means of Surfaces. Transactions of Connecticut Academy of Arts and Sciences, 382-404.

[53] Böhm, H. J., Schneider, G. (2003) Protein-ligand interactions from molecular recognition to drug design, 1st Edition, Wiley-VCH GmbH, Weinheim, Germany.

[54] Waterhouse, A., Bertoni, M., Bienert, S., Studer, G., Tauriello, G., Gumienny, R., Heer, F.T., de Beer, T.A.P., Rempfer, C., Bordoli, L., Lepore, R. Scwede, T. (2018) SWISS-MODEL: homology modelling of protein structures and complexes. Nucleic Acids Research, 46(web server issue), 296-303.

[55] Aszódi, A., Taylor, W. R. (1996) Homology modelling by distance geometry. Folding and Design, 1(5), 325-334.

[56] Lesk, A. M., Chothia, C. (1980) How different amino acid sequences determine similar protein structures: the structure and evolutionary dynamics of the globins. Journal of Molecular Biology, 136(3), 225-270.

[57] Chothia, C., Lesk, A. M. (1986) The relation between the divergence of sequence and structure in proteins. European Molecular Biology Organization Journal, *5*(4), 823-826.

[58] Wieman, H., Anderssen, E., Drablos, F. (2004) Homology-based modelling of targets for rational drug design. Mini Reviews in Medicinal Chemistry, *4*(7), 793-804.

[59] Arnold, K., Bordoli, L., Kopp, J., Schwede, T. (2006) The SWISS-MODEL workspace: a web-based environment for protein structure homology modelling. Bioinformatics, *22*(2), 195-201.

[60] Saxena, A., Sangwan, R. S., Mishra, S. (2013) Fundamentals of homology modeling steps and comparison among important bioinformatics tools: An overview. Science International, *1*(7), 237-252.

[61] Vyas, V. K., Ukawala, R. D., Ghate, M., Chintha, C. (2012) Homology modeling a fast tool for drug discovery: current perspectives. Indian Journal of Pharmaceutical Sciences, 74(1), 1.

[62] Kunst, F., Ogasawara, N., Moszer, I., Albertini, A. M., Alloni, G. O., Azevedo, V., ... & Borriss, R. (1997) The complete genome sequence of the gram-positive bacterium Bacillus subtilis. Nature, *390*(6657), 249.

[63] Dawson, R. J., Locher, K. P. (2006) Structure of a bacterial multidrug ABC transporter. Nature, 443(7108), 180.

[64] Ortuso, F., Bagetta, D., Maruca, A., Talarico, C., Bolognesi, M. L., Haider, N., Borges, F., Bryant, S., Langer, T., Senderowitz, H., Alcaro, S. (2018) The Mu. Ta. Lig. Chemotheca: a community-populated molecular database for multi-target ligands identification and compound-repurposing. Frontiers in chemistry, 6, 130, http://chemotheca.unicz.it/index.php. (10.01.2018).

[65] Mahuteau-Betzer, F. (2015) Chimiothèque Nationale Avancées et perspectives. Médecine/Sciences, 31(4), 417-422, http://chimiotheque-nationale.cn.cnrs.fr/?-Acces-utilisateurs- , (23.04.2018).

[66] Webb, B., Sali, A. (2016) Comparative Protein Structure Modeling Using Modeller. Current Protocols in Bioinformatics, 54, 5.6.1-5.6.37.

[67] Laskowski, R. A., MacArthur, M. W., Moss, D. S., & Thornton, J. M. (1993) PROCHECK: a program to check the stereochemical quality of protein structures. Journal of Applied Crystallography, 26(2), 283-291.

[68] RCSB Protein Data Bank, http://www.rcsb.org/ (24.04.2018).

[69] DSX^{ONLINE} Scoring Functions for Protein-Ligand Complexes, (http://pc1664.pharmazie.uni-marburg.de/drugscore/ (19.05.2018)

[70] Fan, H., Schneidman-Duhovny, D., Irwin, J. J., Dong, G., Shoichet, B. K., & Sali, A. (2011) Statistical potential for modeling and ranking of protein–ligand interactions. Journal of Chemical Information and Modeling, 51(12), 3078-3092.

[71] Forli, S., Huey, R., Pique, M. E., Sanner, M. F., Goodsell, D. S., & Olson, A. J. (2016). Computational protein–ligand docking and virtual drug screening with the AutoDock suite. Nature protocols, 11(5), 905.

[72] AutoDockTools version 1.5.6., http://mgltools.scripps.edu/downloads (17.12.2017)

[73] Hussein, H. A., Borrel, A., Geneix, C., Petitjean, M., Regad, L., Camproux, A. C. (2015) PockDrug-Server: a new web server for predicting pocket druggability on holo and apo proteins. Nucleic Acids Research, 43(web server issue), 436-442.

[74] Drug Likeness Tool (DruLiTo), http://www.niper.gov.in/pi_dev_tools/DruLiToWeb/DruLiTo_Reference.html (13.02.2019

[75] Discovery Studio version 1.5, https://www.3dsbiovia.com/resource-center/downloads/updates/discovery-studio/dstudio15/dstudio15.html (13.02.2019)

[76] Do Cao, M. A., Crouzy, S., Kim, M., Becchi, M., Cafiso, D. S., Pietro, A. D., Jault, J. M. (2009) Probing the conformation of the resting state of a bacterial multidrug ABC

transporter, BmrA, by a site-directed spin labeling approach. Protein Science, 18(7), 1507-1520.

[77] Sippl, M. J. (1993). Recognition of errors in three-dimensional structures of proteins. Proteins: Structure, Function, and Bioinformatics, 17(4), 355-362, https://prosa.services.came.sbg.ac.at/prosa.php (5 Aralık 2017)

[78] Wiederstein, M., Sippl, M. J. (2007) ProSA-web: interactive web service for the recognition of errors in three-dimensional structures of proteins. Nucleic Acids Research, 35(suppl_2), 407-410.

[79] Verify3D Server Platform, http://servicesn.mbi.ucla.edu/Verify3D/ (12 Aralık 2017)

[80] Eisenberg, D., Lüthy, R., Bowie, J. U. (1997) VERIFY3D: Assessment of protein models with three-dimensional profiles. Methods in Enzymology, 277, 396-404.

[81] Ward, A., Reyes, C. L., Yu, J., Roth, C. B., & Chang, G. (2007) Flexibility in the ABC transporter MsbA: Alternating access with a twist. Proceedings of the National Academy of Sciences, 104(48), 19005-19010.

[82] Dawson, R. J., & Locher, K. P. (2006) Structure of a bacterial multidrug ABC transporter. Nature, 443(7108), 180.

[83] VMD version 1.9.3., https://www.ks.uiuc.edu/Research/vmd/vmd-1.9.3/ , 22 Kasım 2017.

[84] Avcı, F. G. (2018) Investigation of Aporphine Alkaloids for Their Antimicrobial Activities. PhD Thesis, Marmara University Institute of Pure and Applied Sciences, Istanbul, Turkey, 30-34.

[85] Do Cao, M. A., Crouzy, S., Kim, M., Becchi, M., Cafiso, D. S., Pietro, A. D., & Jault, J. M. 2009) Probing the conformation of the resting state of a bacterial multidrug ABC transporter, BmrA, by a site-directed spin labeling approach. Protein Science, 18(7), 1507-1520.

APPENDIX

APPENDIX 1. HOMOLOGY MODELLING AND VIRTUAL SCREENING SCRIPTS

build_profile.py 〉No Selection

```
from modeller import *

log.verbose()
env = environ()

#-- Prepare the input files

#-- Read in the sequence database
sdb = sequence_db(env)
sdb.read(seq_database_file='pdb_95.pir', seq_database_format='PIR',
         chains_list='ALL', minmax_db_seq_len=(30, 4000), clean_sequences=True)

#-- Write the sequence database in binary form
sdb.write(seq_database_file='pdb_95.bin', seq_database_format='BINARY',
          chains_list='ALL')

#-- Now, read in the binary database
sdb.read(seq_database_file='pdb_95.bin', seq_database_format='BINARY',
         chains_list='ALL')

#-- Read in the target sequence/alignment
aln = alignment(env)
aln.append(file='BmrA.ali', alignment_format='PIR', align_codes='ALL')

#-- Convert the input sequence/alignment into
#   profile format
prf = aln.to_profile()

#-- Scan sequence database to pick up homologous sequences
prf.build(sdb, matrix_offset=-450, rr_file='${LIB}/blosum62.sim.mat',
          gap_penalties_1d=(-500, -50), n_prof_iterations=1,
          check_profile=False, max_aln_evalue=0.01)

#-- Write out the profile in text format
prf.write(file='build_profile.prf', profile_format='TEXT')

#-- Convert the profile back to alignment format
aln = prf.to_alignment()

#-- Write out the alignment file
aln.write(file='build_profile.ali', alignment_format='PIR')
```

Figure I. Build_profile.py script.

align2d.py 〉No Selection

```
from modeller import *

env = environ()
aln = alignment(env)
mdl = model(env, file='ec_full_cor', model_segment=('FIRST:A','LAST:B'))
aln.append_model(mdl, align_codes='ec_full_cor', atom_files='ec_full_cor.pdb')
aln.append(file='BmrA.ali', align_codes='BmrA')
aln.align2d()
aln.write(file='BmrA-ec_full_cor.ali', alignment_format='PIR')
aln.write(file='BmrA-ec_full_cor.pap', alignment_format='PAP')
```

Figure II. Align2d.py script.

```
# Comparative modeling by the automodel class
#
# Demonstrates how to build multi-chain models, and symmetry restraints
#
from modeller import *
from modeller.automodel import *    # Load the automodel class

log.verbose()

# Override the 'special_restraints' and 'user_after_single_model' methods:
class MyModel(automodel):
    def special_restraints(self, aln):
        # Constrain the A and B chains to be identical (but only restrain
        # the C-alpha atoms, to reduce the number of interatomic distances
        # that need to be calculated):
        rsr = self.restraints
        at = self.atoms
        s1 = selection(self.chains['A']).only_atom_types('CA')
        s2 = selection(self.chains['B']).only_atom_types('CA')
        self.restraints.symmetry.append(symmetry(s1, s2, 1.0))
        rsr.add(secondary_structure.alpha(self.residue_range('2:A', '9:A')))
        rsr.add(secondary_structure.alpha(self.residue_range('13:A', '24:A')))
        rsr.add(secondary_structure.alpha(self.residue_range('28:A', '44:A')))
        rsr.add(secondary_structure.alpha(self.residue_range('52:A', '72:A')))
        rsr.add(secondary_structure.alpha(self.residue_range('74:A', '106:A')))
        rsr.add(secondary_structure.alpha(self.residue_range('109:A', '113:A')))
        rsr.add(secondary_structure.alpha(self.residue_range('117:A', '130:A')))
        rsr.add(secondary_structure.alpha(self.residue_range('132:A', '136:A')))
        rsr.add(secondary_structure.alpha(self.residue_range('142:A', '159:A')))
        rsr.add(secondary_structure.alpha(self.residue_range('164:A', '167:A')))
        rsr.add(secondary_structure.alpha(self.residue_range('170:A', '215:A')))
        rsr.add(secondary_structure.alpha(self.residue_range('219:A', '272:A')))
        rsr.add(secondary_structure.alpha(self.residue_range('277:A', '285:A')))
        rsr.add(secondary_structure.alpha(self.residue_range('287:A', '290:A')))
        rsr.add(secondary_structure.alpha(self.residue_range('293:A', '318:A')))
        rsr.add(secondary_structure.alpha(self.residue_range('380:A', '384:A')))
        rsr.add(secondary_structure.alpha(self.residue_range('410:A', '415:A')))
        rsr.add(secondary_structure.alpha(self.residue_range('431:A', '435:A')))
        rsr.add(secondary_structure.alpha(self.residue_range('444:A', '453:A')))
        rsr.add(secondary_structure.alpha(self.residue_range('457:A', '461:A')))
        rsr.add(secondary_structure.alpha(self.residue_range('480:A', '494:A')))
        rsr.add(secondary_structure.alpha(self.residue_range('510:A', '523:A')))
        rsr.add(secondary_structure.alpha(self.residue_range('559:A', '564:A')))
        rsr.add(secondary_structure.alpha(self.residue_range('568:A', '573:A')))
        rsr.add(secondary_structure.alpha(self.residue_range('591:B', '598:B')))
        rsr.add(secondary_structure.alpha(self.residue_range('602:B', '613:B')))
        rsr.add(secondary_structure.alpha(self.residue_range('617:B', '633:B')))
        rsr.add(secondary_structure.alpha(self.residue_range('641:B', '661:B')))
        rsr.add(secondary_structure.alpha(self.residue_range('663:B', '695:B')))
        rsr.add(secondary_structure.alpha(self.residue_range('698:B', '702:B')))
        rsr.add(secondary_structure.alpha(self.residue_range('706:B', '719:B')))
        rsr.add(secondary_structure.alpha(self.residue_range('721:B', '725:B')))
        rsr.add(secondary_structure.alpha(self.residue_range('731:B', '748:B')))
        rsr.add(secondary_structure.alpha(self.residue_range('753:B', '756:B')))
        rsr.add(secondary_structure.alpha(self.residue_range('759:B', '804:B')))
        rsr.add(secondary_structure.alpha(self.residue_range('808:B', '861:B')))
        rsr.add(secondary_structure.alpha(self.residue_range('866:B', '874:B')))
        rsr.add(secondary_structure.alpha(self.residue_range('876:B', '879:B')))
        rsr.add(secondary_structure.alpha(self.residue_range('882:B', '907:B')))
        rsr.add(secondary_structure.alpha(self.residue_range('969:B', '973:B')))
        rsr.add(secondary_structure.alpha(self.residue_range('999:B', '1004:B')))
        rsr.add(secondary_structure.alpha(self.residue_range('1020:B', '1024:B')))
        rsr.add(secondary_structure.alpha(self.residue_range('1033:B', '1042:B')))
        rsr.add(secondary_structure.alpha(self.residue_range('1046:B', '1050:B')))
        rsr.add(secondary_structure.alpha(self.residue_range('1069:B', '1083:B')))
        rsr.add(secondary_structure.alpha(self.residue_range('1099:B', '1112:B')))
        rsr.add(secondary_structure.alpha(self.residue_range('1148:B', '1153:B')))
        rsr.add(secondary_structure.alpha(self.residue_range('1157:B', '1162:B')))
        #       Two beta-strands:
        rsr.add(secondary_structure.strand(self.residue_range('340:A', '347:A')))
        rsr.add(secondary_structure.strand(self.residue_range('357:A', '364:A')))
        rsr.add(secondary_structure.strand(self.residue_range('369:A', '373:A')))
        rsr.add(secondary_structure.strand(self.residue_range('395:A', '400:A')))
        rsr.add(secondary_structure.strand(self.residue_range('417:A', '420:A')))
        rsr.add(secondary_structure.strand(self.residue_range('498:A', '502:A')))
        rsr.add(secondary_structure.strand(self.residue_range('528:A', '532:A')))
        rsr.add(secondary_structure.strand(self.residue_range('544:A', '549:A')))
        rsr.add(secondary_structure.strand(self.residue_range('552:A', '557:A')))
        rsr.add(secondary_structure.strand(self.residue_range('929:B', '936:B')))
        rsr.add(secondary_structure.strand(self.residue_range('946:B', '953:B')))
        rsr.add(secondary_structure.strand(self.residue_range('958:B', '962:B')))
        rsr.add(secondary_structure.strand(self.residue_range('984:B', '989:B')))
        rsr.add(secondary_structure.strand(self.residue_range('1006:B', '1009:B')))
        rsr.add(secondary_structure.strand(self.residue_range('1087:B', '1091:B')))
        rsr.add(secondary_structure.strand(self.residue_range('1117:B', '1121:B')))
        rsr.add(secondary_structure.strand(self.residue_range('1133:B', '1138:B')))
        rsr.add(secondary_structure.strand(self.residue_range('1141:B', '1146:B')))

```

Figure III. Model-multichain-sym.py script file.

```
89
90      def user_after_single_model(self):
91          # Report on symmetry violations greater than 1A after building
92          # each model:
93          self.restraints.symmetry.report(1.0)
94
95  env = environ()
96  # directories for input atom files
97  env.io.atom_files_directory = ['.', '../atom_files']
98
99  # Be sure to use 'MyModel' rather than 'automodel' here!
100 a = MyModel(env,
101             alnfile  = 'BmrA-ec_full_cor.ali' ,     # alignment filename
102             knowns   = 'ec_full_cor',              # codes of the templates
103             sequence = 'BmrA',              # code of the target
104             assess_methods=(assess.DOPE, assess.GA341))
105
106 a.starting_model= 1                 # index of the first model
107 a.ending_model  = 100                 # index of the last model
108 # (determines how many models to calculate)
109 # Very thorough VTFM optimization:
110 a.library_schedule = autosched.slow
111 a.max_var_iterations = 300
112
113 # Repeat the whole cycle 3 times and do not stop unless obj.func. > 1E6
114 a.repeat_optimization = 3
115 a.max_molpdf = 1e6
116 a.make()                            # do comparative homology modeling
```

Figure III. Model-multichain-sym.py script file (Continue).

evaluate_model.py 〉 No Selection

```
1  from modeller import *
2  from modeller.scripts import complete_pdb
3
4  log.verbose()    # request verbose output
5  env = environ()
6  env.libs.topology.read(file='$(LIB)/top_heav.lib') # read topology
7  env.libs.parameters.read(file='$(LIB)/par.lib') # read parameters
8
9  # read model file
10 mdl = complete_pdb(env, 'BmrA_044.pdb')
11
12 # Assess with DOPE:
13 s = selection(mdl)   # all atom selection
14 s.assess_dope(output='ENERGY_PROFILE NO_REPORT', file='BmrA.profile',
15              normalize_profile=True, smoothing_window=15)
```

Figure IV. Evaluate_model.py script file

```python
import os
import glob
import sys

outfile = sys.argv[1]
library_folder = sys.argv[2]
vina_exe = sys.argv[3]
receptor = sys.argv[4]
exhaust = sys.argv[5]
cpu = sys.argv[6]

ligand_list = glob.glob(library_folder+'/*.pdbqt')

f = open(outfile,'w')

for ligand in ligand_list:
    ligand = os.path.split(ligand)[-1]
    ligand_out = 'Results_cavity_25092018'+ligand.replace('.pdbqt','')+'_out.pdbqt'
    if os.path.exists(os.path.abspath(ligand_out)):
        print('skipping')
        continue

    ligand_log = 'Results_cavity_25092018/'+ligand.replace('.pdbqt','')+'_log.log'
    vina_command = vina_exe+' --receptor ' + receptor + \
            ' --ligand ' + os.path.abspath('Chemotheca/'+ligand) + \
            ' --center_x -105 --center_y -110 --center_z -135 ' + \
            '--size_x 50 --size_y 50 --size_z 50 ' + \
            '--out ' + os.path.abspath(ligand_out) + \
            ' --log ' + os.path.abspath(ligand_log) + \
            ' --exhaustiveness ' + exhaust + \
            ' --num_modes 100 --cpu ' + cpu + ' ;\n'
    f.write(vina_command)
f.close()
```

Figure V. The script which was used to generate the AutoDock command for each ligand in a library.

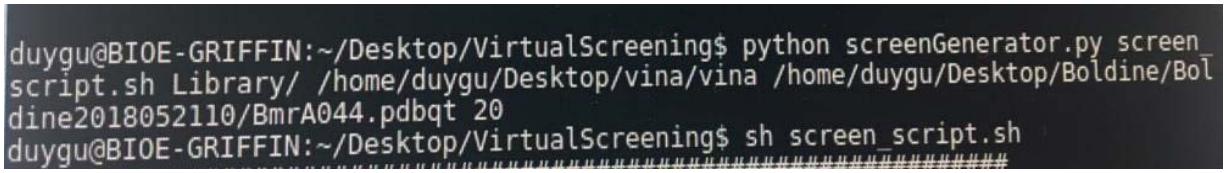

Figure VI. Command window script which was used to run the library script for virtual screening.

APPENDIX 2. Chemotheca Library Virtual Screening Results

Table I: Residues of BmrA interacting with 39 ligands selected from first top 100 ligands of Chemotheca library based on first strategy (These ligands obeyed all drug-likeness rules except for MDDR-like rule).

Ligand Name	Binding Energy (Kcal/mol)	Region	Interacting Residues
CM10	-10.4	Right	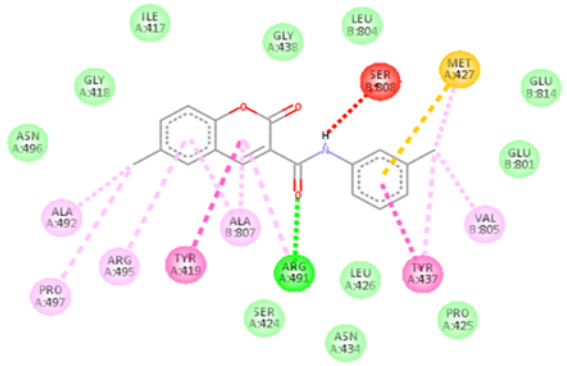
CM108	-10	Right	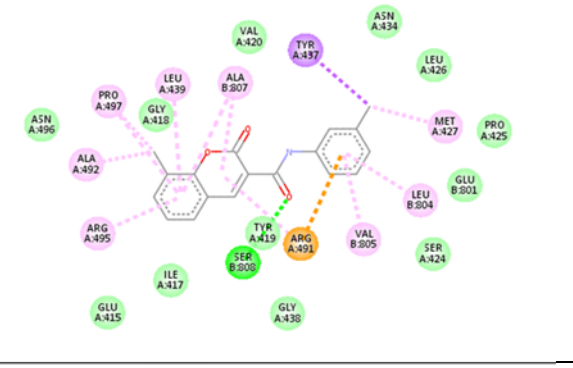
CM111	-10.2	Right	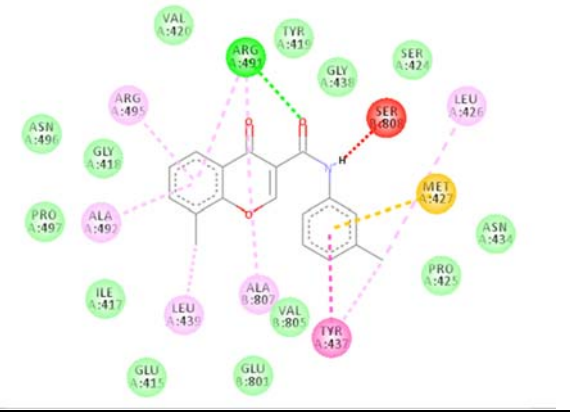

Table I: Residues of BmrA interacting with 39 ligands selected from first top 100 ligands of Chemotheca library based on first strategy (These ligands obeyed all drug-likeness rules except for MDDR-like rule) (Continue).

Ligand Name	Binding Energy (Kcal/mol)	Region	Interacting Residues
CM128	-10.12	Right	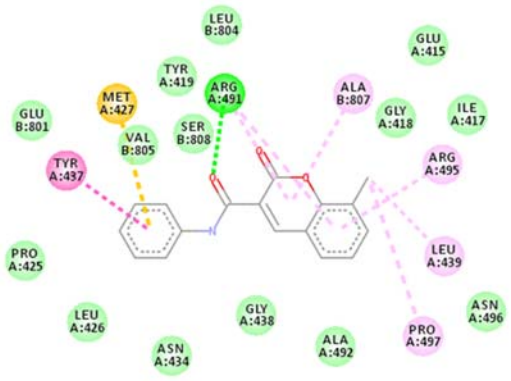
CM130	-10.2	Right	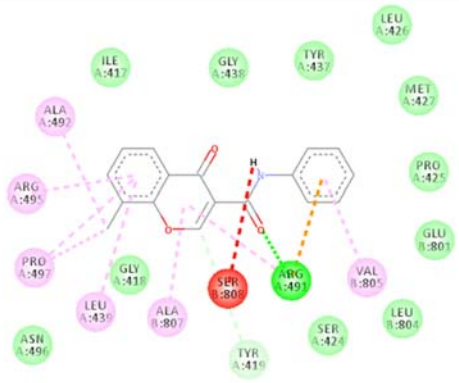
CM14	-10.08	Right	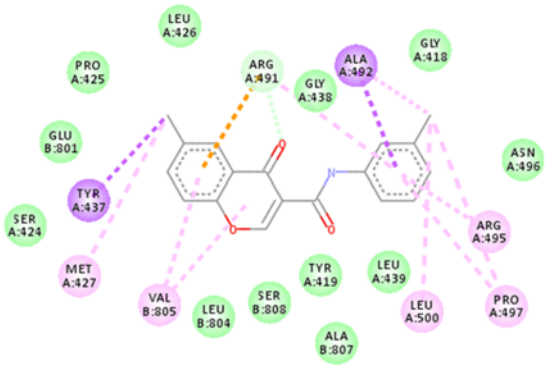

Table I: Residues of BmrA interacting with 39 ligands selected from first top 100 ligands of Chemotheca library based on first strategy (These ligands obeyed all drug-likeness rules except for MDDR-like rule) (Continue).

Ligand Name	Binding Energy (Kcal/mol)	Region	Interacting Residues
CM140	-10	Right	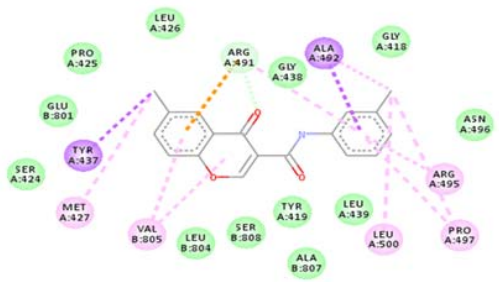
CM155	-10.12	Right	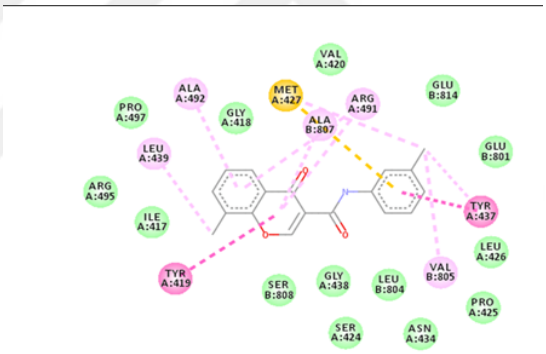
CM16	-10.4	Right	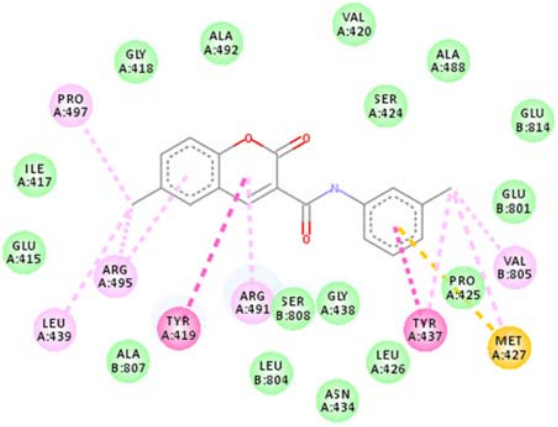

Table I: Residues of BmrA interacting with 39 ligands selected from first top 100 ligands of Chemotheca library based on first strategy (These ligands obeyed all drug-likeness rules except for MDDR-like rule) (Continue).

Ligand Name	Binding Energy (Kcal/mol)	Region	Interacting Residues
CM160	-10.2	Right	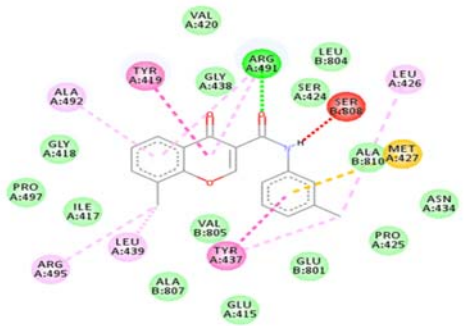
CM167	-10.26	Right	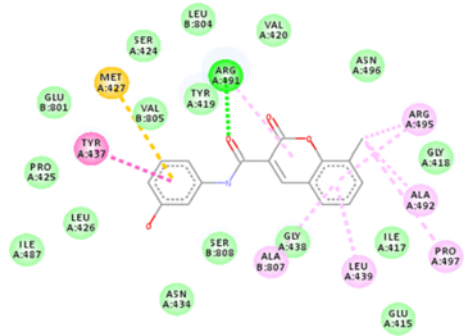
CM169	-10.2	Right	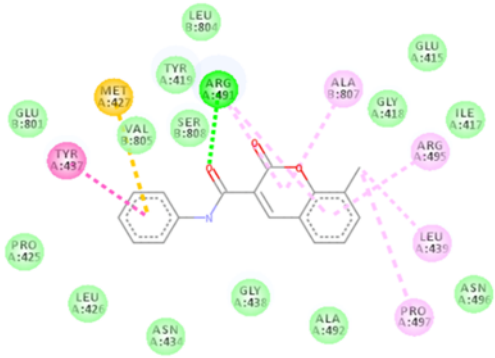

Table I: Residues of BmrA interacting with 39 ligands selected from first top 100 ligands of Chemotheca library based on first strategy (These ligands obeyed all drug-likeness rules except for MDDR-like rule) (Continue).

Ligand Name	Binding Energy (Kcal/mol)	Region	Interacting Residues
CM22	-10.6	Right	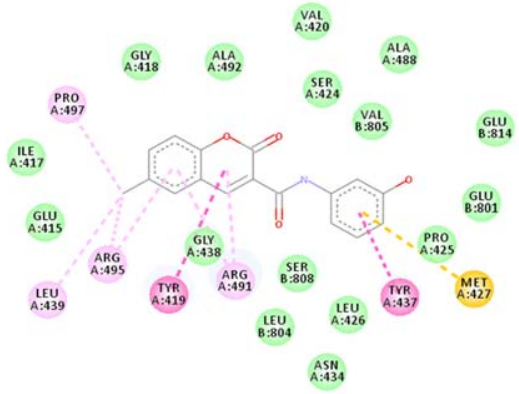
CM40	-10.32	Right	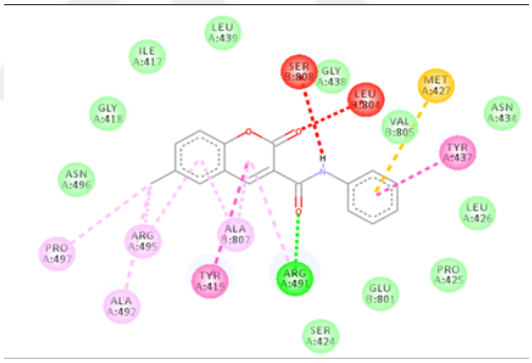
CM44	-10.36	Right	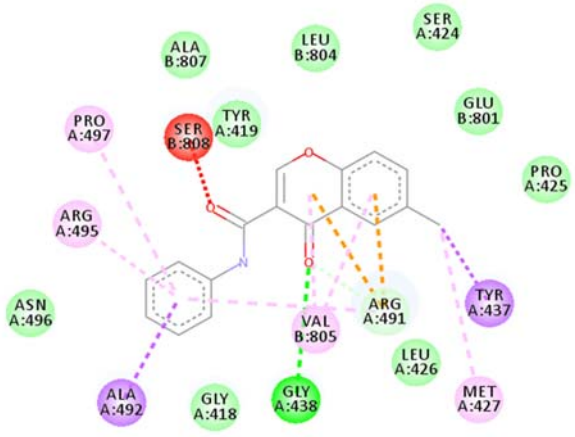

Table I: Residues of BmrA interacting with 39 ligands selected from first top 100 ligands of Chemotheca library based on first strategy (These ligands obeyed all drug-likeness rules except for MDDR-like rule) (Continue).

Ligand Name	Binding Energy (Kcal/mol)	Region	Interacting Residues
CM718	-10.1	Right	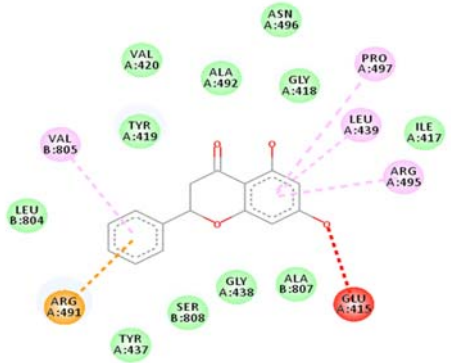
CM85	-10.42	Right	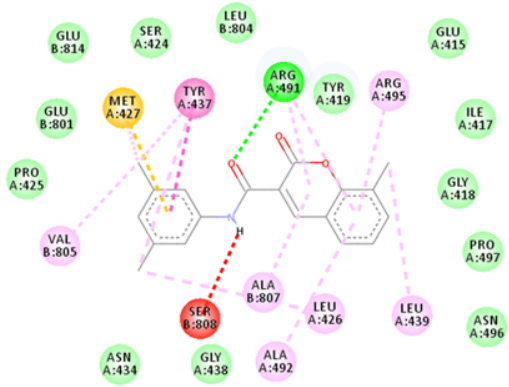
CM89	-10.2	Right	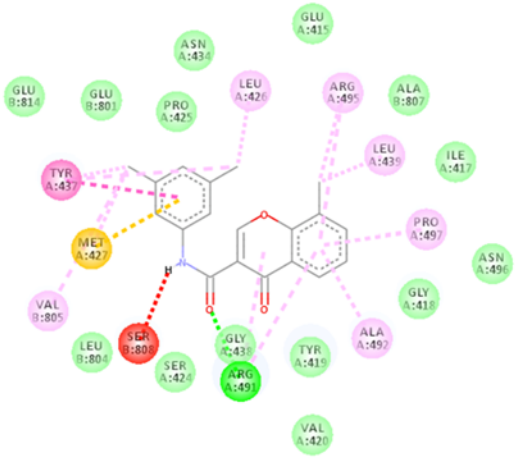

Table I: Residues of BmrA interacting with 39 ligands selected from first top 100 ligands of Chemotheca library based on first strategy (These ligands obeyed all drug-likeness rules except for MDDR-like rule) (Continue).

Ligand Name	Binding Energy (Kcal/mol)	Region	Interacting Residues
CM612	-9.98	Left	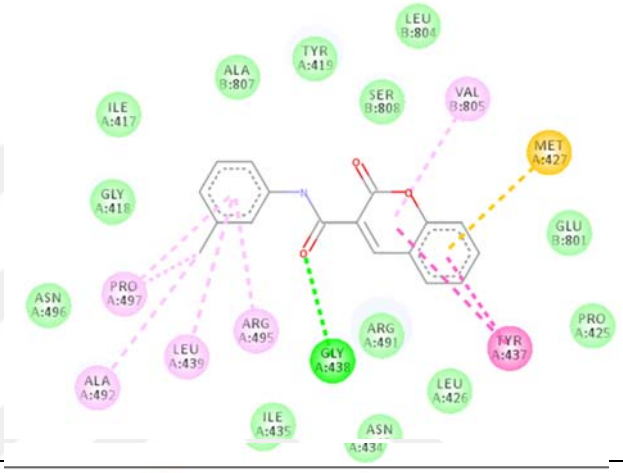
CM31	-9.98	Right	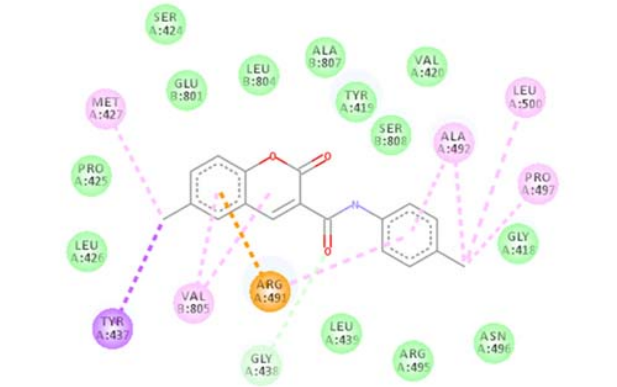
CM113	-9.94	Right	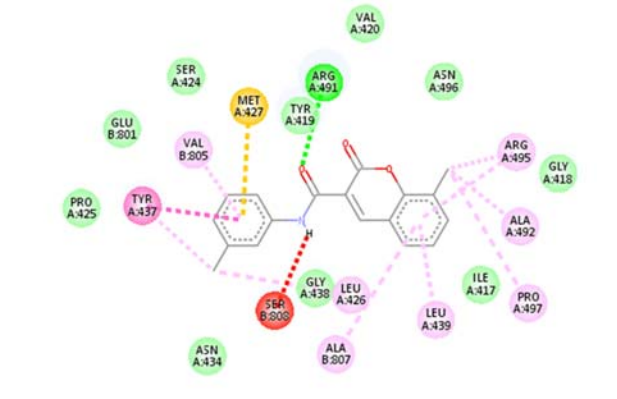

Table I: Residues of BmrA interacting with 39 ligands selected from first top 100 ligands of Chemotheca library based on first strategy (These ligands obeyed all drug-likeness rules except for MDDR-like rule) (Continue).

Ligand Name	Binding Energy (Kcal/mol)	Region	Interacting Residues
CM92	-9.9	Right	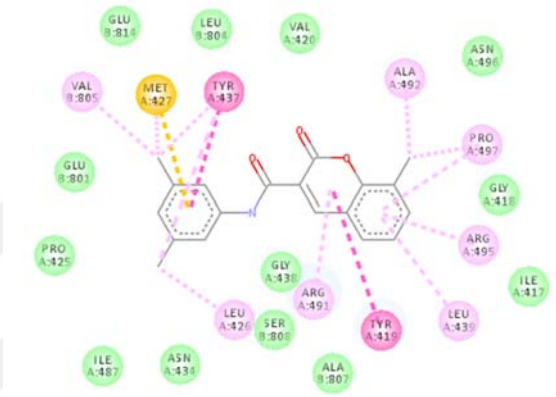
CM3	-9.84	Right	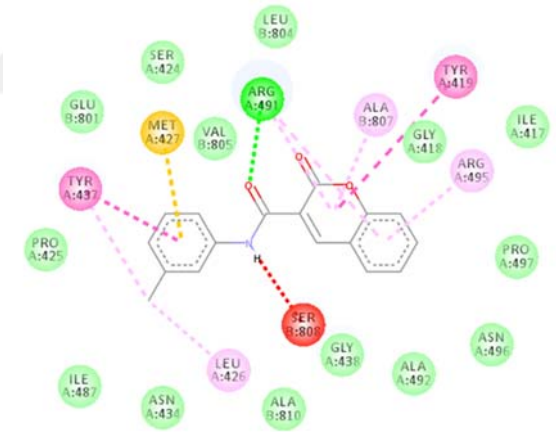
CM35	-9.84	Right	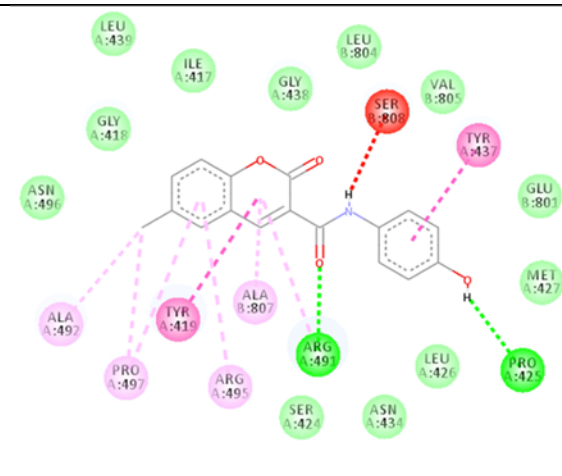

Table I: Residues of BmrA interacting with 39 ligands selected from first top 100 ligands of Chemotheca library based on first strategy (These ligands obeyed all drug-likeness rules except for MDDR-like rule) (Continue).

Ligand Name	Binding Energy (Kcal/mol)	Region	Interacting Residues
CM46	-9.82	Right	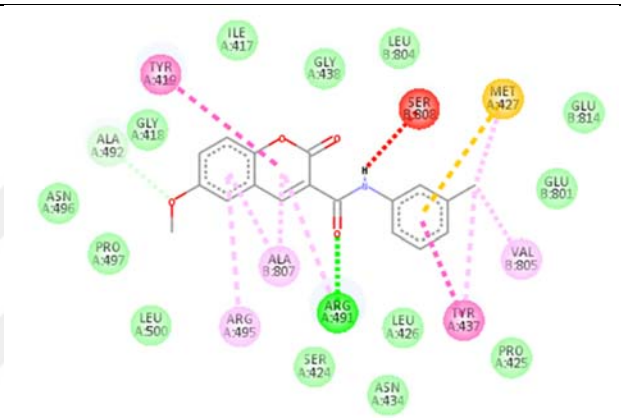
CM199	-9.8	Right	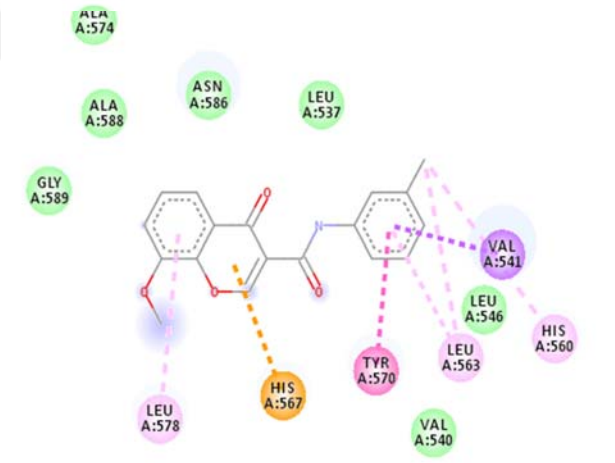
CM2	-9.8	Right	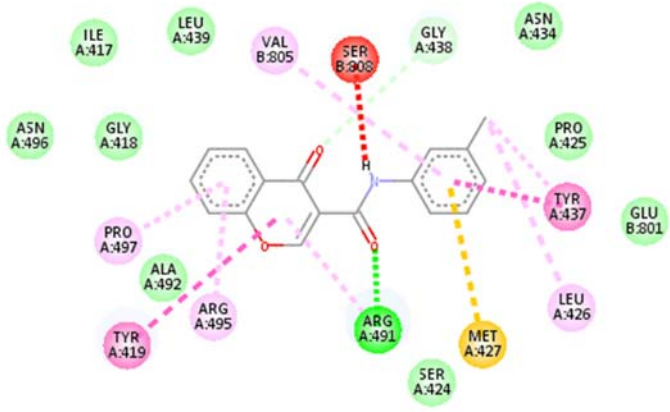

Table I: Residues of BmrA interacting with 39 ligands selected from first top 100 ligands of Chemotheca library based on first strategy (These ligands obeyed all drug-likeness rules except for MDDR-like rule) (Continue).

Ligand Name	Binding Energy (Kcal/mol)	Region	Interacting Residues
CM4	-9.8	Right	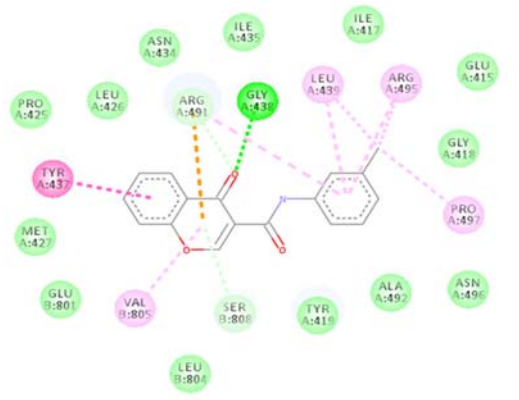
CM154	-9.72	Right	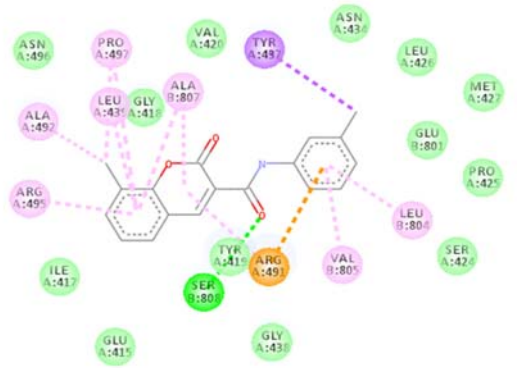
CM115	-9.7	Right	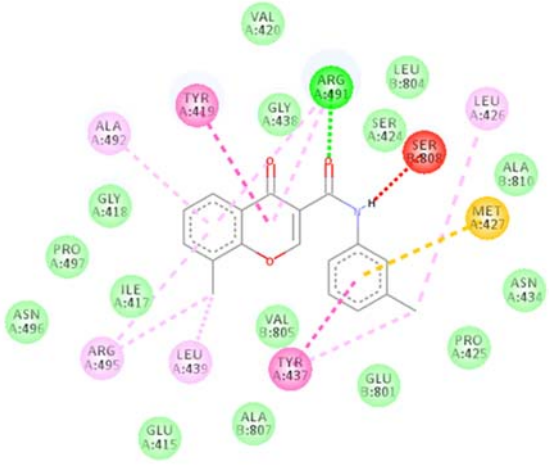

Table I: Residues of BmrA interacting with 39 ligands selected from first top 100 ligands of Chemotheca library based on first strategy (These ligands obeyed all drug-likeness rules except for MDDR-like rule) (Continue).

Ligand Name	Binding Energy (Kcal/mol)	Region	Interacting Residues
CM19	-9.7	Right	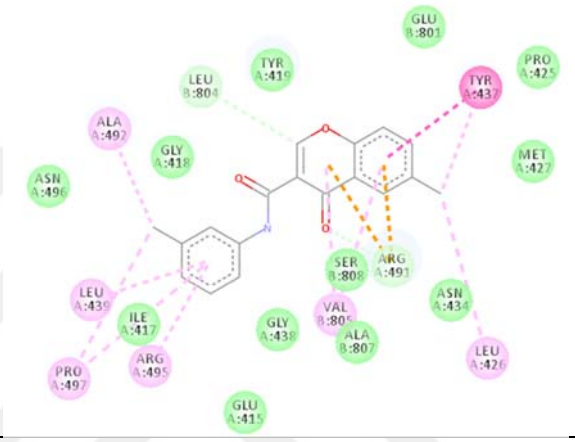
CM54	-9.68	Right	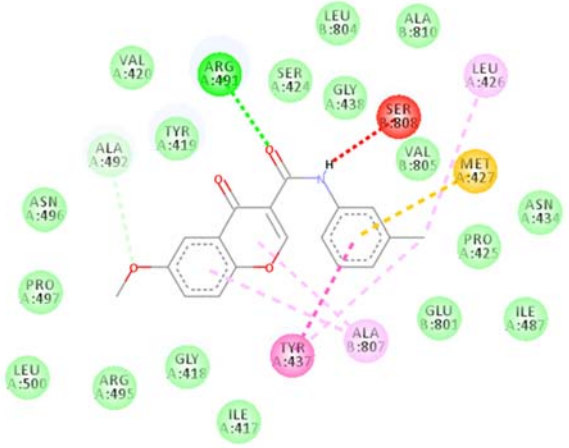

Table I: Residues of BmrA interacting with 39 ligands selected from first top 100 ligands of Chemotheca library based on first strategy (These ligands obeyed all drug-likeness rules except for MDDR-like rule) (Continue).

Ligand Name	Binding Energy (Kcal/mol)	Region	Interacting Residues
CM172	-9.66	Right	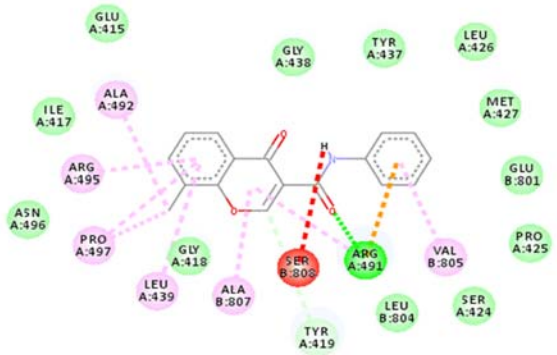
CM259	-9.66	Right	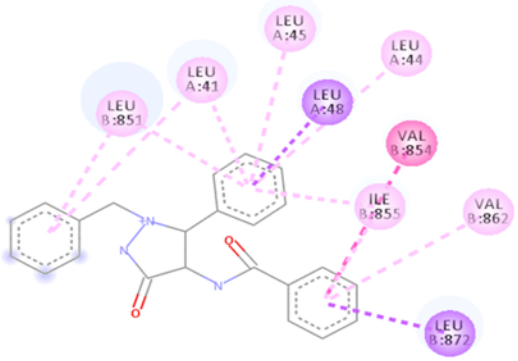
CM94	-9.62	Right	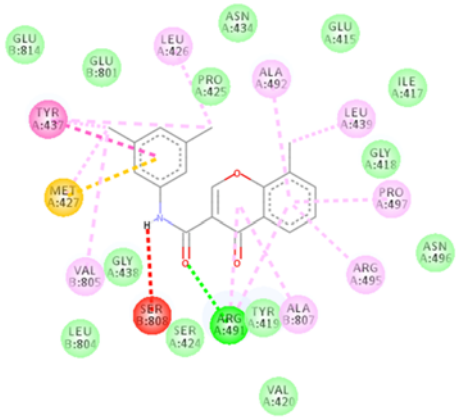

Table I: Residues of BmrA interacting with 39 ligands selected from first top 100 ligands of Chemotheca library based on first strategy (These ligands obeyed all drug-likeness rules except for MDDR-like rule) (Continue).

Ligand Name	Binding Energy (Kcal/mol)	Region	Interacting Residues
CM177	-9.6	Right	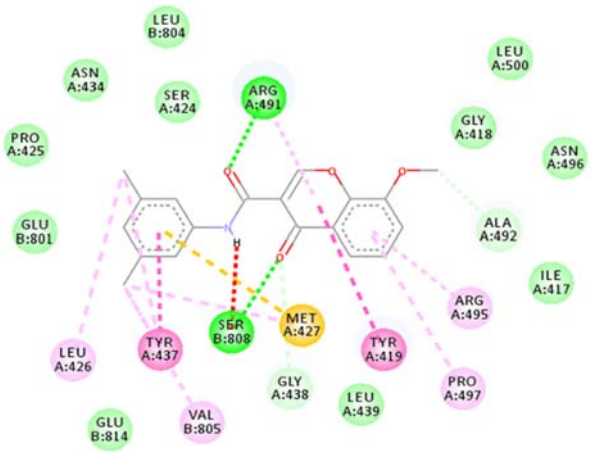
CM29	-9.58	Right	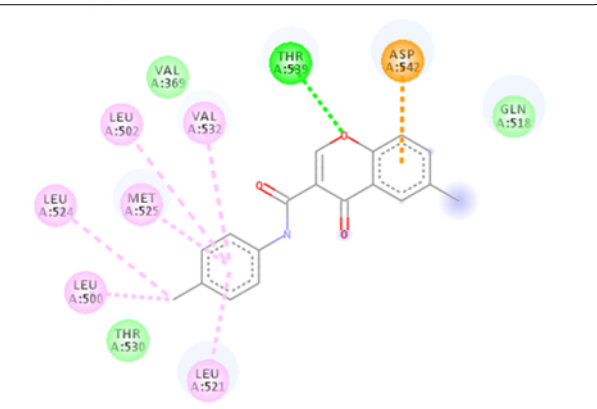
CM159	-9.48	Right	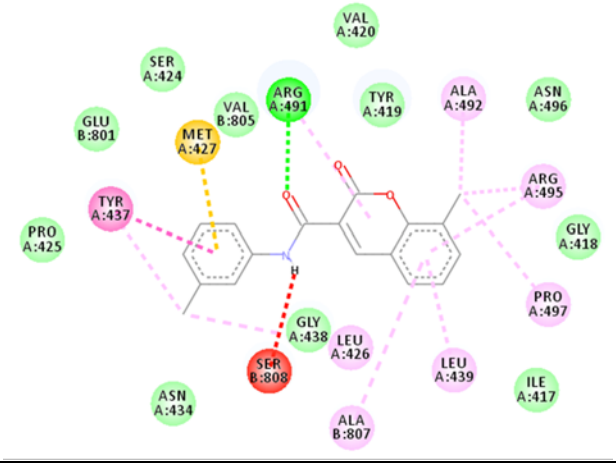

Table II: Residues of BmrA interacting with 34 Ligands from all Chemotheca library, obey all drug-likeness rules.

Ligand Name	Binding Energy (Kcal/mol)	Region	Interacting Residues
CM759	-9.28	Left	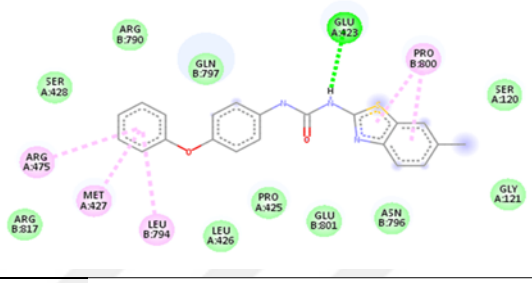
CM586	-9.2	Left	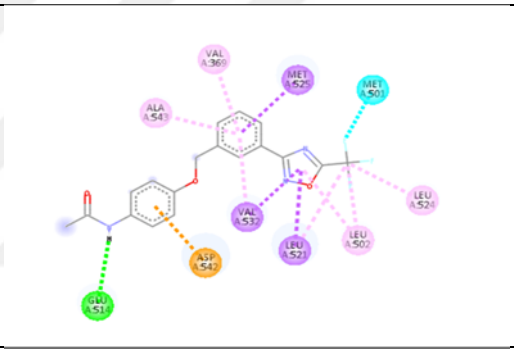
CM17	-9.12	Right	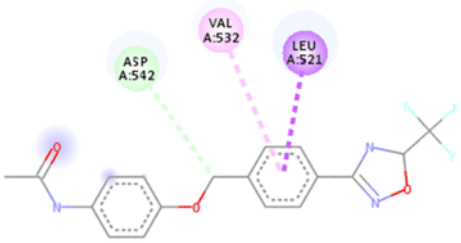
CM581	-9.08	Right	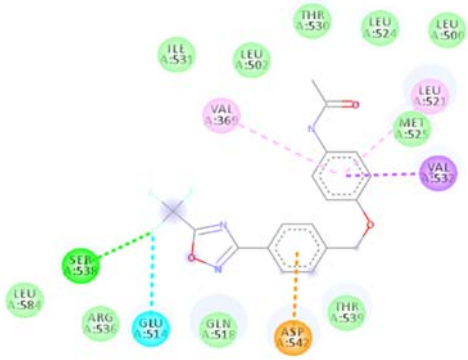

Table II: Residues of BmrA interacting with 34 Ligands from all Chemotheca library, obey all drug-likeness rules (Continue).

Ligand Name	Binding Energy (Kcal/mol)	Region	Interacting Residues
CM264	-9.06	Cavity	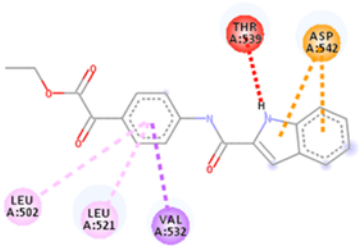
CM585	-9.06	Right	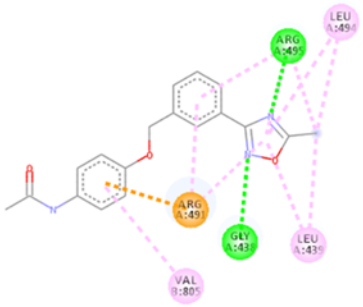
CM794	-8.86	Right	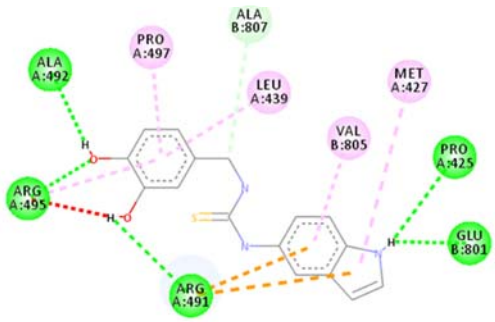
CM564	-8.82	Right	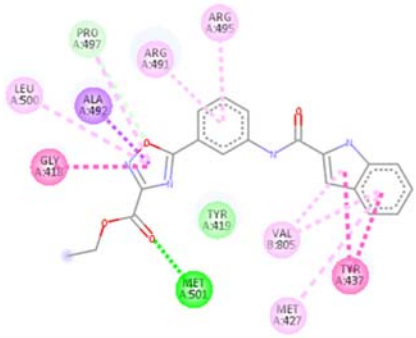

Table II: Residues of BmrA interacting with 34 Ligands from all Chemotheca library, obey all drug-likeness rules (Continue).

Ligand Name	Binding Energy (Kcal/mol)	Region	Interacting Residues
CM764	-8.76	Right	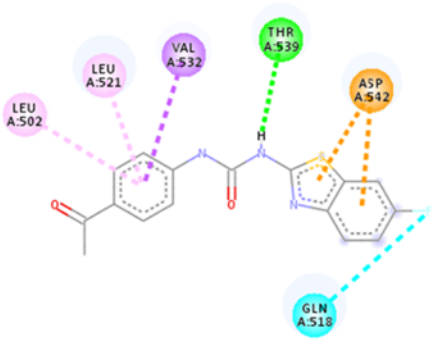
CM788	-8.76	Right	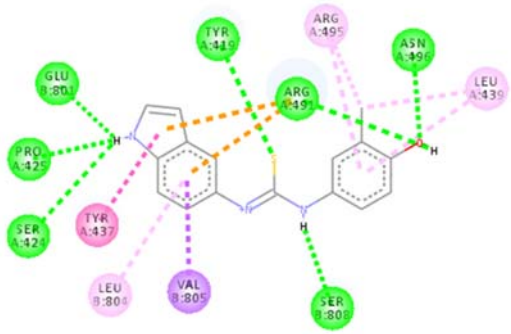
CM239	-8.74	Cavity	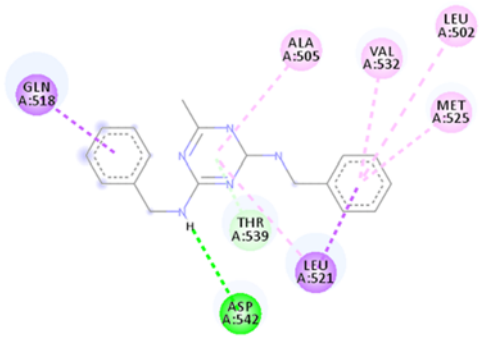

Table II: Residues of BmrA interacting with 34 Ligands from all Chemotheca library, obey all drug-likeness rules (Continue).

Ligand Name	Binding Energy (Kcal/mol)	Region	Interacting Residues
CM26	-8.7	Right	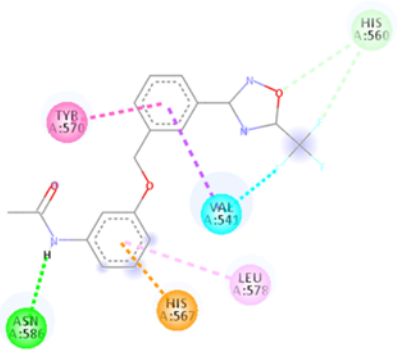
CM290	-8.7	Left	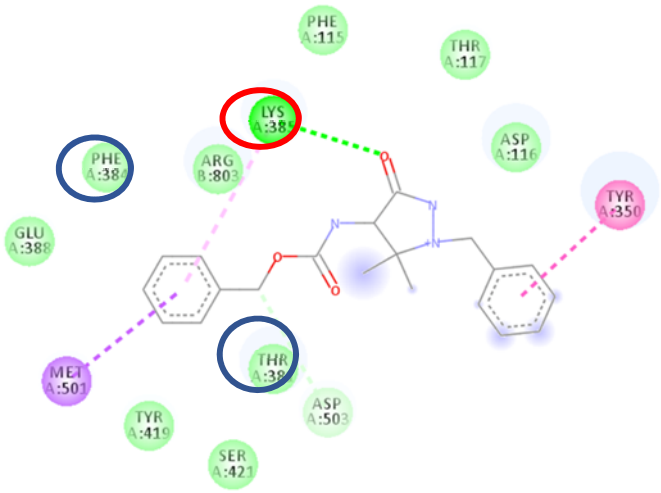
CM475	-8.58	Left	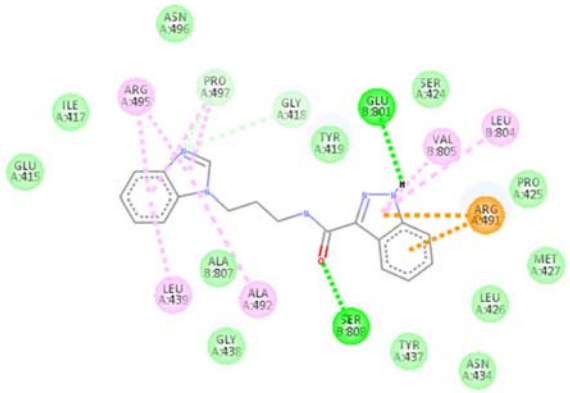

Table II: Residues of BmrA interacting with 34 Ligands from all Chemotheca library, obey all drug-likeness rules (Continue).

Ligand Name	Binding Energy (Kcal/mol)	Region	Interacting Residues
CM21	-8.54	Cavity	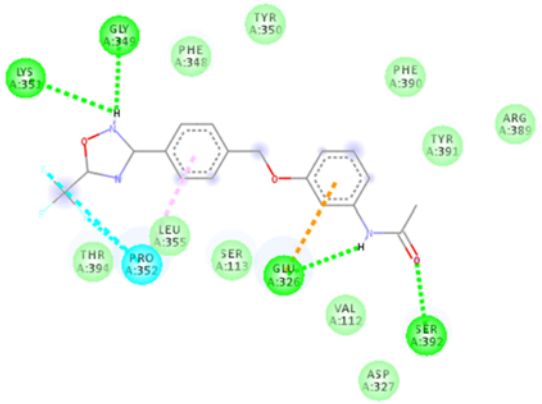
CM807	-8.5	Right	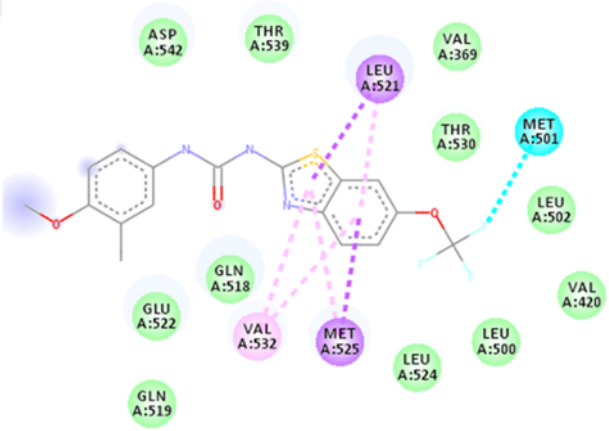
CM824	-8.44	Right	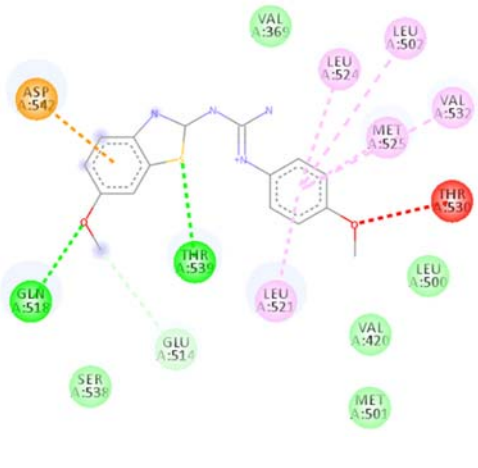

Table II: Residues of BmrA interacting with 34 Ligands from all Chemotheca library, obey all drug-likeness rules (Continue).

Ligand Name	Binding Energy (Kcal/mol)	Region	Interacting Residues
CM83	-8.38	Cavity	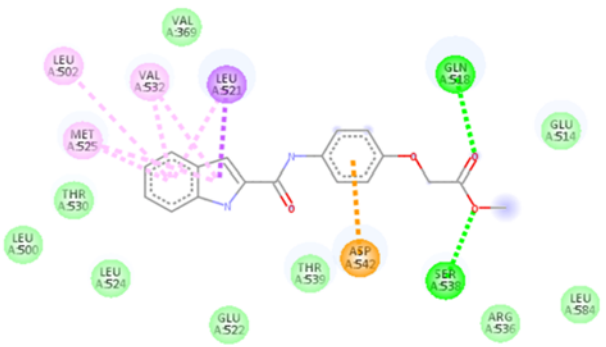
CM785	-8.36	Right	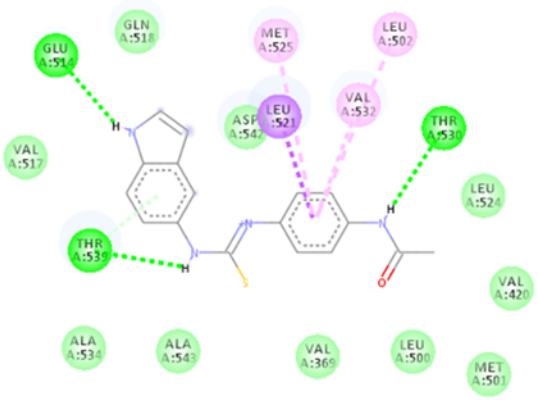
CM580	-8.32	Right	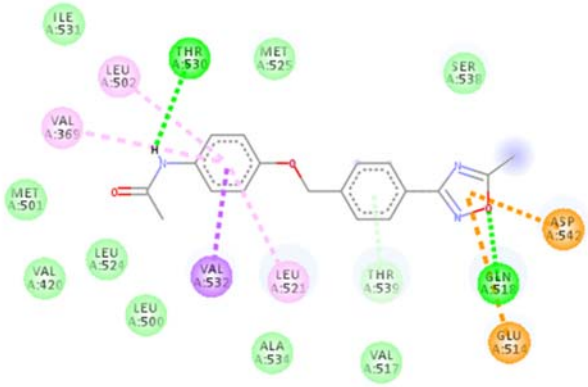

Table II: Residues of BmrA interacting with 34 Ligands from all Chemotheca library, obey all drug-likeness rules (Continue).

Ligand Name	Binding Energy (Kcal/mol)	Region	Interacting Residues
CM813	-8.26	Left	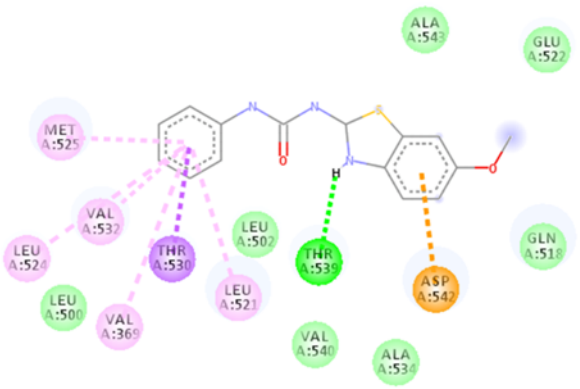
CM158	-8.18	Right	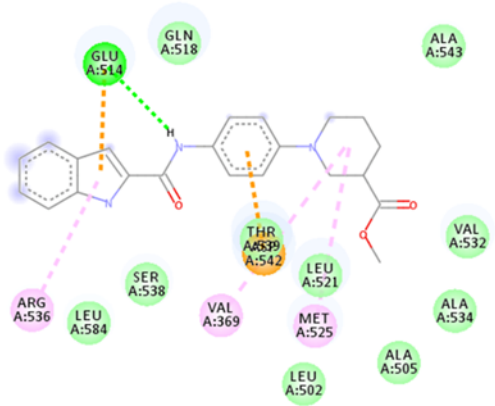
CM279	-8.12	Cavity	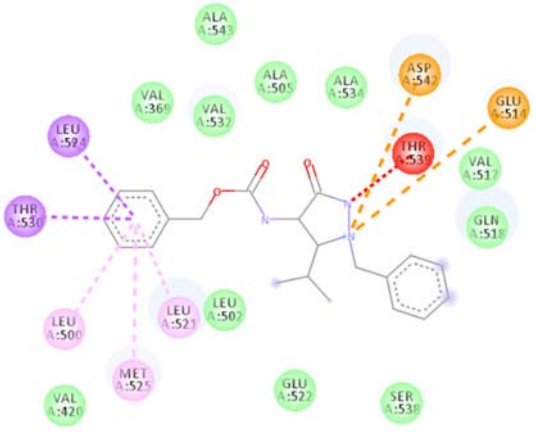

Table II: Residues of BmrA interacting with 34 Ligands from all Chemotheca library, obey all drug-likeness rules (Continue).

Ligand Name	Binding Energy (Kcal/mol)	Region	Interacting Residues
CM830	-8.12	Right	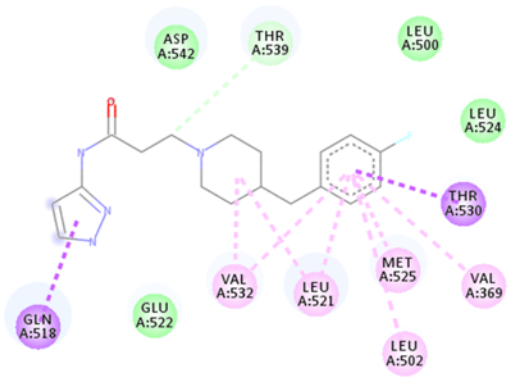
CM833	-7.98	Right	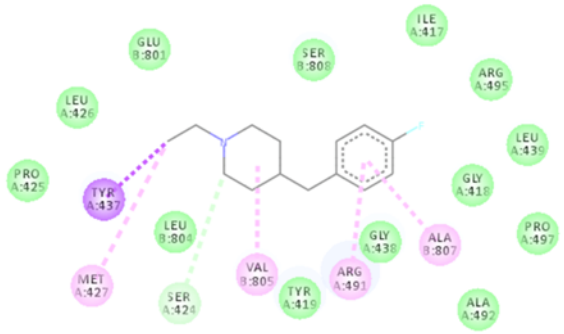
CM507	-7.94	Cavity	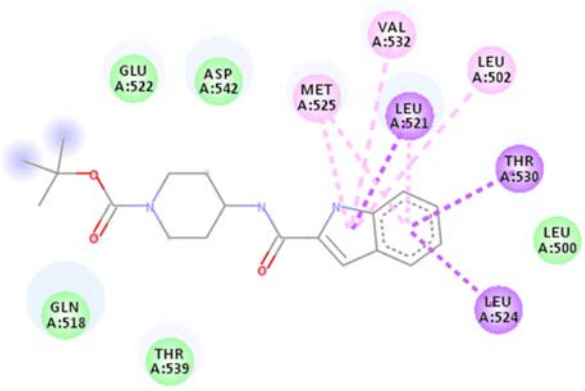

Table II: Residues of BmrA interacting with 34 Ligands from all Chemotheca library, obey all drug-likeness rules (Continue).

Ligand Name	Binding Energy (Kcal/mol)	Region	Interacting Residues
CM331	-7.84	Cavity	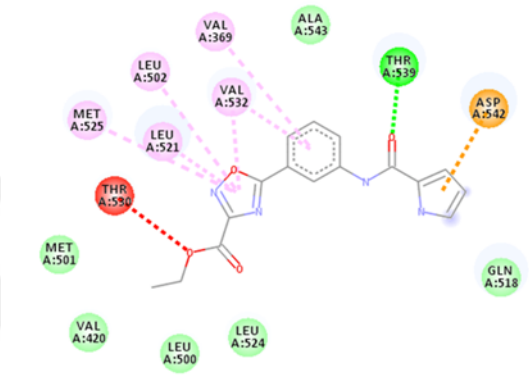
CM756	-7.76	Left	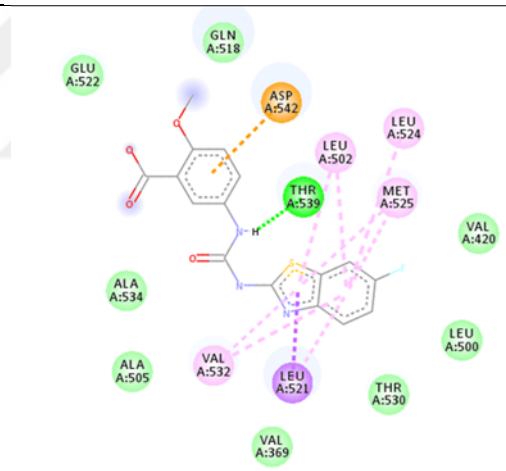
CM784	-7.74	Right	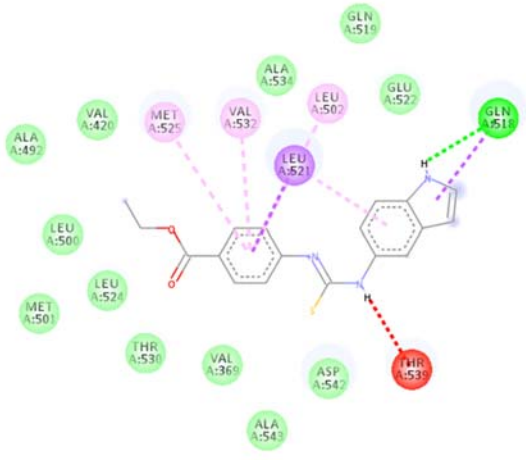

Table II: Residues of BmrA interacting with 34 Ligands from all Chemotheca library, obey all drug-likeness rules (Continue).

Ligand Name	Binding Energy (Kcal/mol)	Region	Interacting Residues
CM102	-7.72	Right	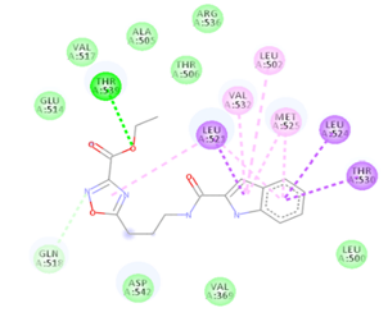
CM729	-7.7	Right	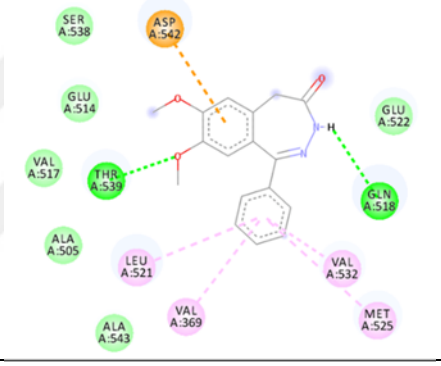
CM821	-7.62	Cavity	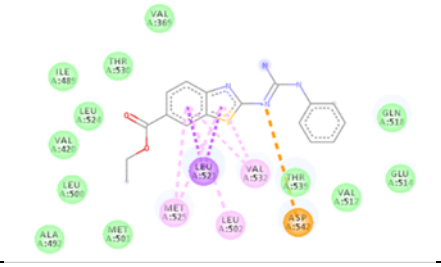
CM722	-7.24	Right	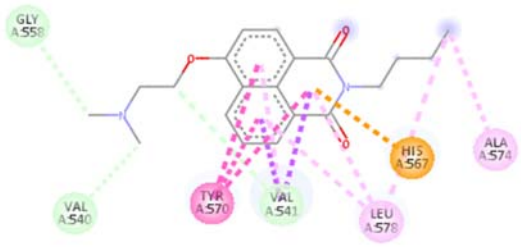

Table III: Residues of BmrA interacting with the ligands whose binding energy difference is 0.5 kcal/mol or less, selected based on the second strategy (These ligands obeyed only 6 rules).

Ligand Name	Binding Energy (Kcal/mol)	Region	Interacting Residues
CM263	-9.22	Right	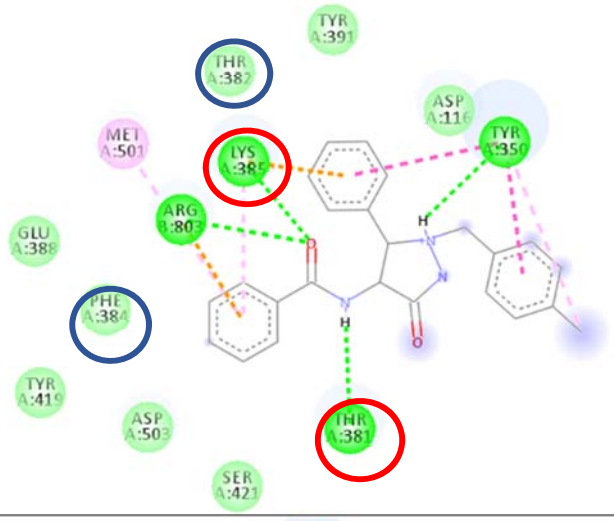
CM263	-8.8	Left	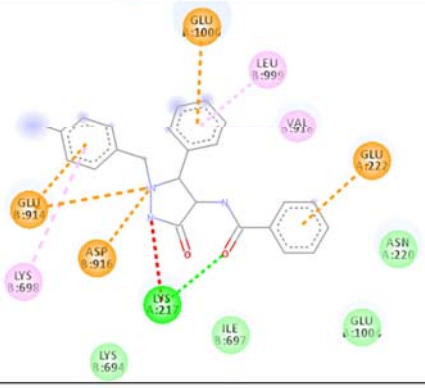
CM263	9.34	Cavity	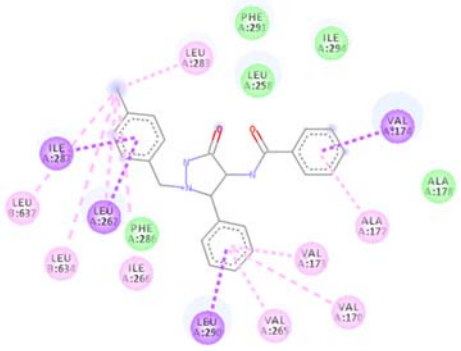

Table III: Residues of BmrA interacting with the ligands whose binding energy difference is 0.5 kcal/mol or less, selected based on the second strategy (These ligands obeyed only 6 rules) (Continue).

Ligand Name	Binding Energy (Kcal/mol)	Region	Interacting Residues
CM299	-9.24	Right	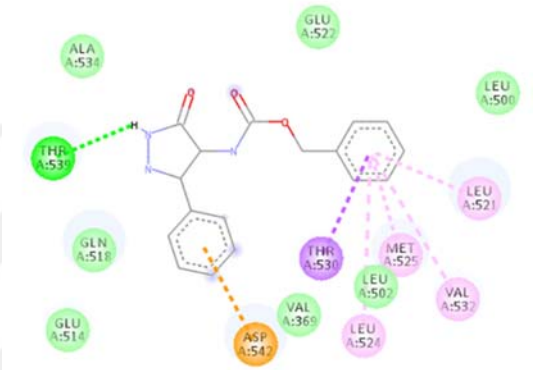
CM299	-8.94	Left	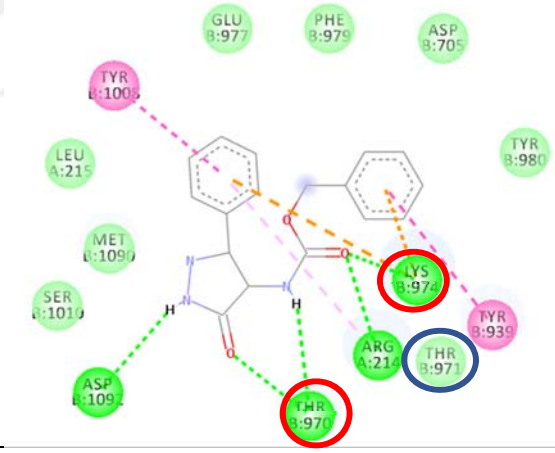
CM299	-8.34	Cavity	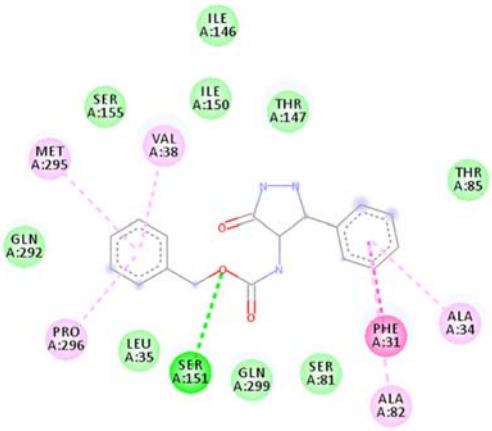

Table III: Residues of BmrA interacting with the ligands whose binding energy difference is 0.5 kcal/mol or less, selected based on the second strategy (These ligands obeyed only 6 rules) (Continue).

Ligand Name	Binding Energy (Kcal/mol)	Region	Interacting Residues
CM51	-9	Right	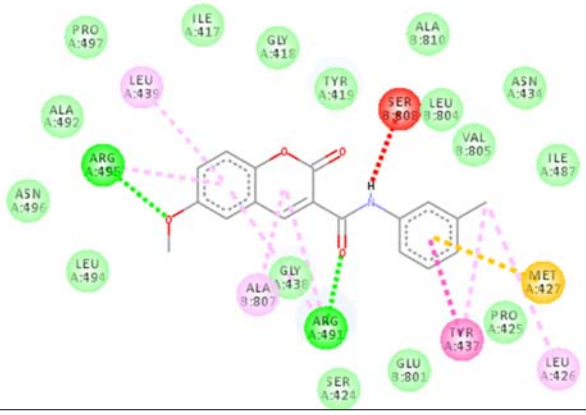
CM51	-8.6	Left	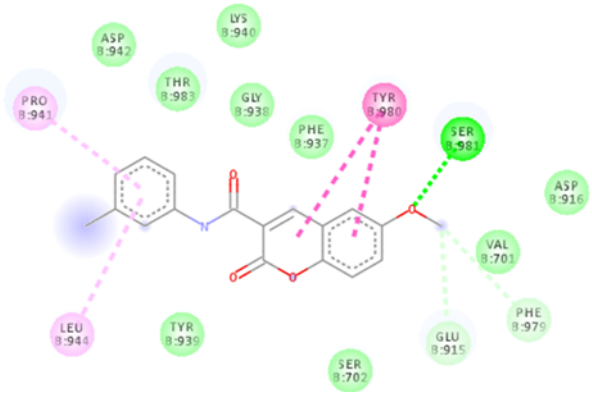
CM51	-8.22	Cavity	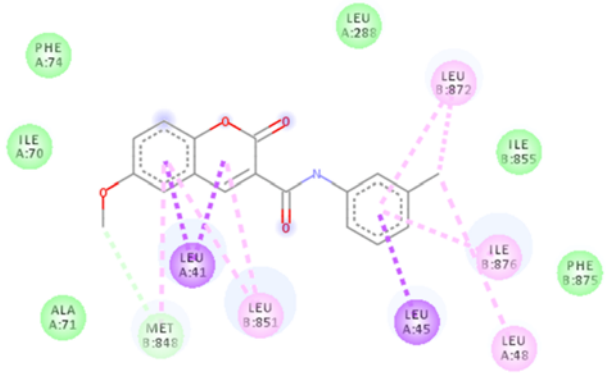

APPENDIX 3. Chimiothèque Nationale Library Virtual Screening Results

Table IV: Residues of BmrA interacting with 3 ligands selected from first top 1000 ligands of Chimiothèque Nationale Library based on first strategy. (These ligands obeyed all drug-likeness rules).

Ligand Name	Binding Energy (Kcal/mol)	Region	Interacting Residues
CN52946	-11.5	Cavity	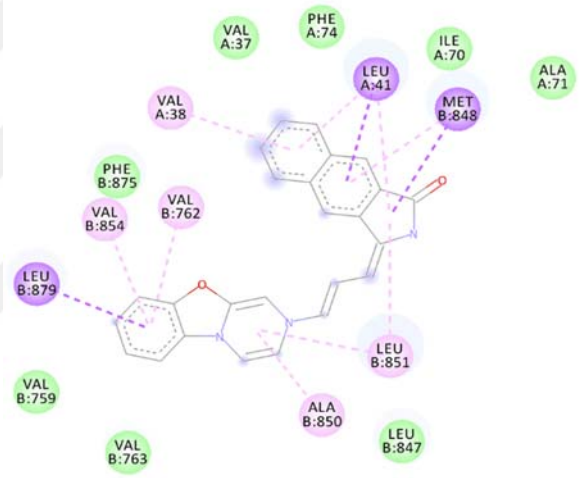
CN52946	-9.96	Right	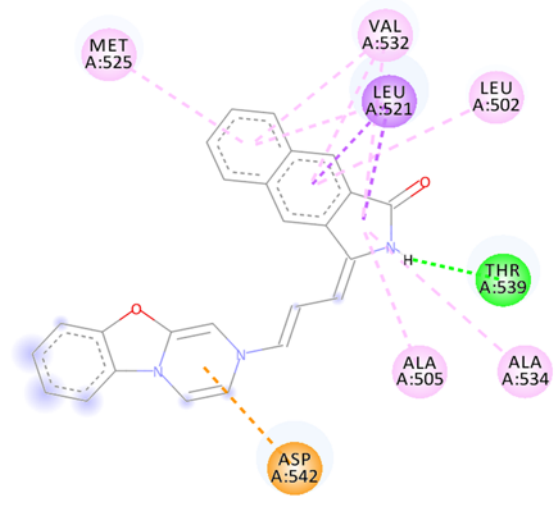

Table IV: Residues of BmrA interacting with 3 ligands selected from first top 1000 ligands of Chimiothèque Nationale Library based on first strategy. (These ligands obeyed all drug-likeness rules) (Continue).

Ligand Name	Binding Energy (Kcal/mol)	Region	Interacting Residues
CN52946	-9.3	Left	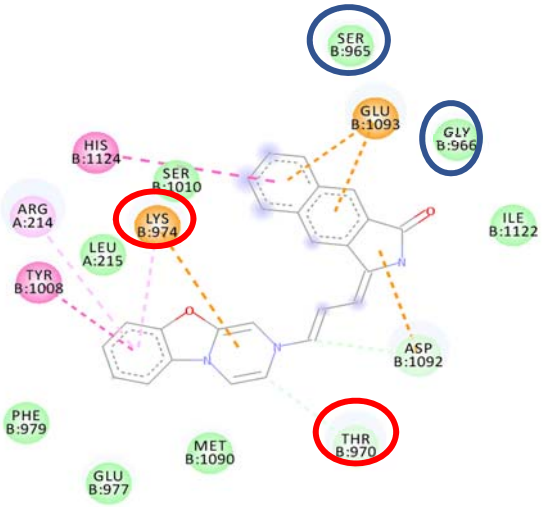
CN53203	-10.93	Cavity	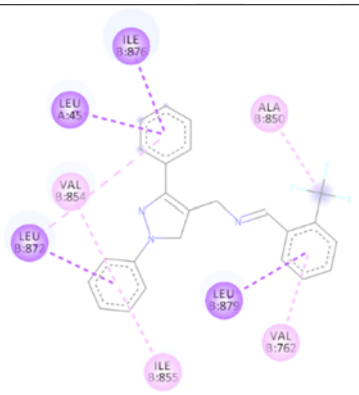
CN53203	-8.9	Right	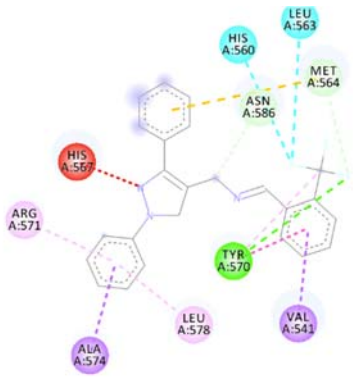

Table IV: Residues of BmrA interacting with 3 ligands selected from first top 1000 ligands of Chimiothèque Nationale Library based on first strategy. (These ligands obeyed all drug-likeness rules) (Continue).

Ligand Name	Binding Energy (Kcal/mol)	Region	Interacting Residues
CN53203	-8.3	Left	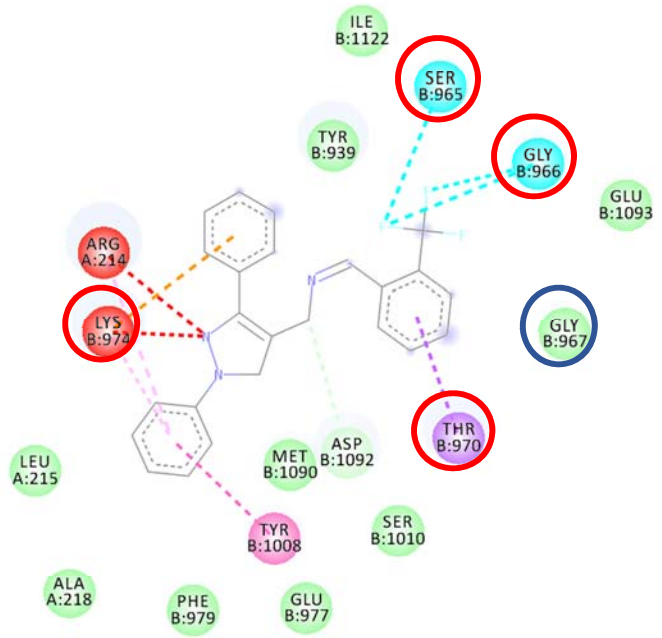
CN52560	-10.92	Right	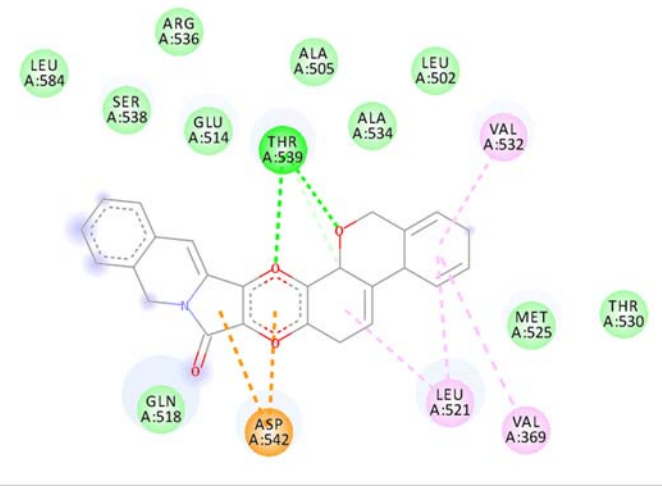

Table IV: Residues of BmrA interacting with 3 ligands selected from first top 1000 ligands of Chimiothèque Nationale Library based on first strategy. (These ligands obeyed all drug-likeness rules) (Continue).

Ligand Name	Binding Energy (Kcal/mol)	Region	Interacting Residues
CN52560	-10.13	Cavity	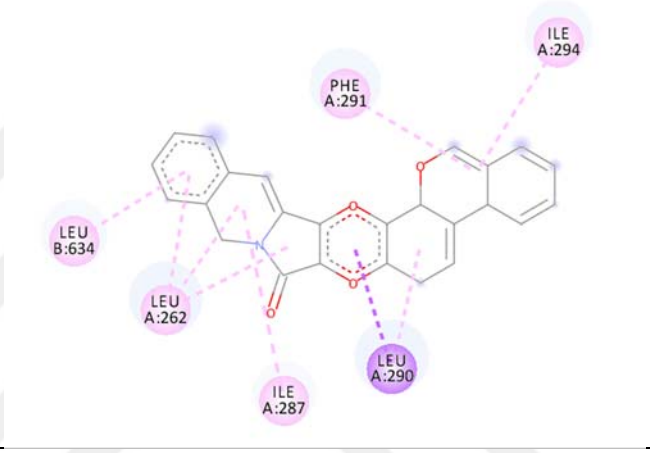
CN52560	-9.54	Left	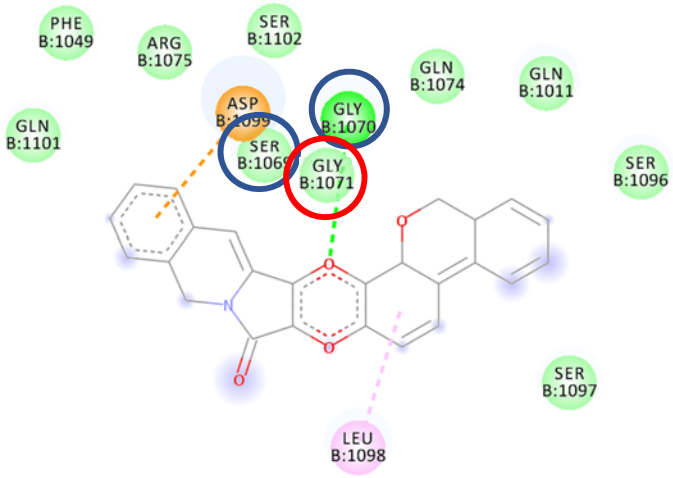

Table V: Residues of BmrA interacting with 5 ligands selected from first top 1000 ligands of Chimiothèque Nationale Library based on first strategy. (These ligands obeyed all drug-likeness rules except for MDDR-like).

Ligand Name	Binding Energy (Kcal/mol)	Region	Interacting Residues
CN50498	-11.3	Cavity	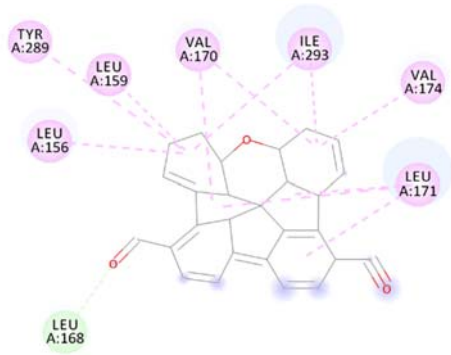
CN50498	-9.7	Right	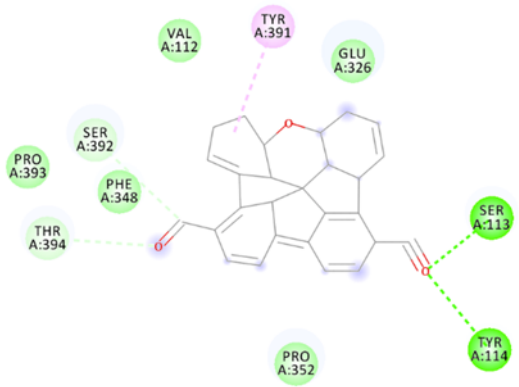
CN50498	-9.44	Left	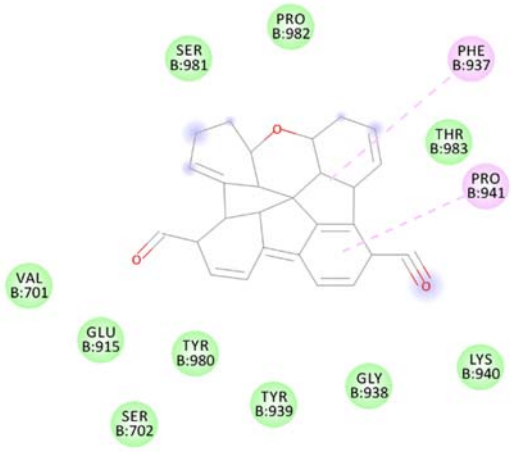

Table V: Residues of BmrA interacting with 5 ligands selected from first top 1000 ligands of Chimiothèque Nationale Library based on first strategy. (These ligands obeyed all drug-likeness rules except for MDDR-like) (Continue).

Ligand Name	Binding Energy (Kcal/mol)	Region	Interacting Residues
CN51357	-11.27	Cavity	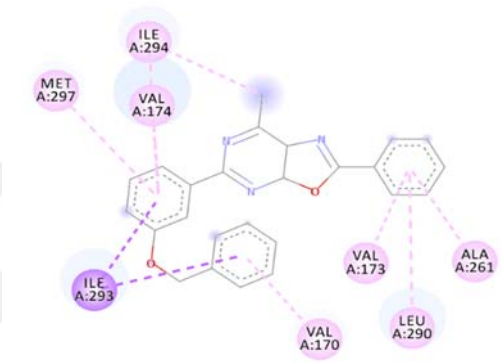
CN51357	-9.72	Right	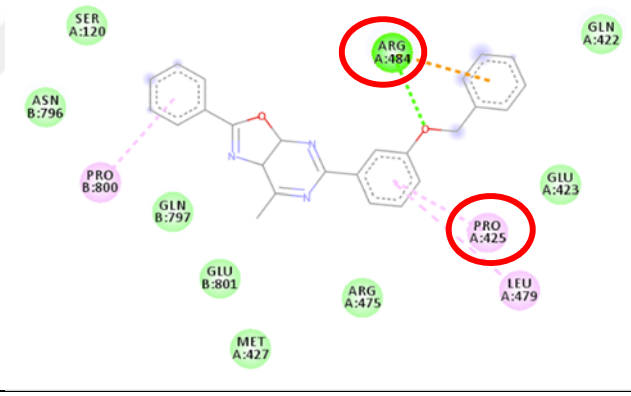
CN51357	-9.08	Left	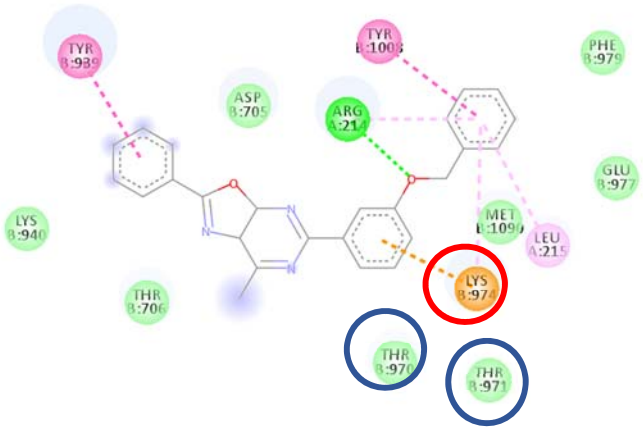

Table V: Residues of BmrA interacting with 5 ligands selected from first top 1000 ligands of Chimiothèque Nationale Library based on first strategy. (These ligands obeyed all drug-likeness rules except for MDDR-like) (Continue).

Ligand Name	Binding Energy (Kcal/mol)	Region	Interacting Residues
CN52148	-11.16	Right	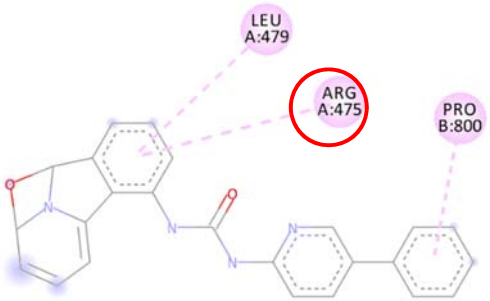
CN52148	-10.67	Cavity	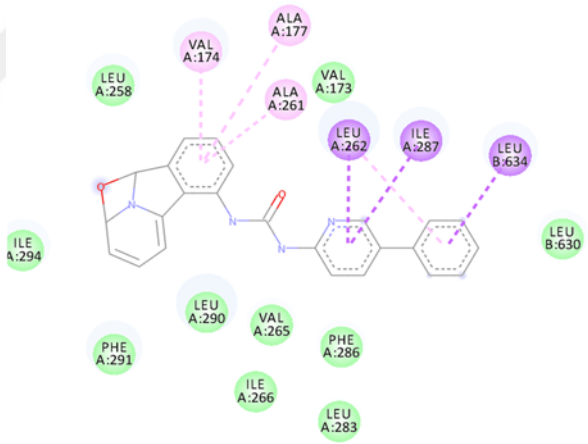
CN52148	-9.14	Left	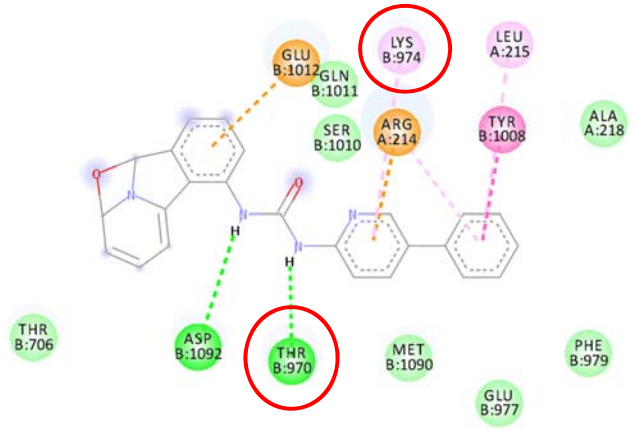

Table V: Residues of BmrA interacting with 5 ligands selected from first top 1000 ligands of Chimiothèque Nationale Library based on first strategy. (These ligands obeyed all drug-likeness rules except for MDDR-like) (Continue).

Ligand Name	Binding Energy (Kcal/mol)	Region	Interacting Residues
CN53019	-11.1	Cavity	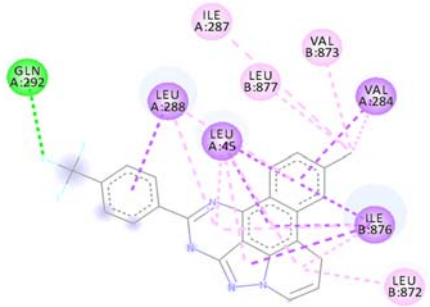
CN53019	-9.86	Right	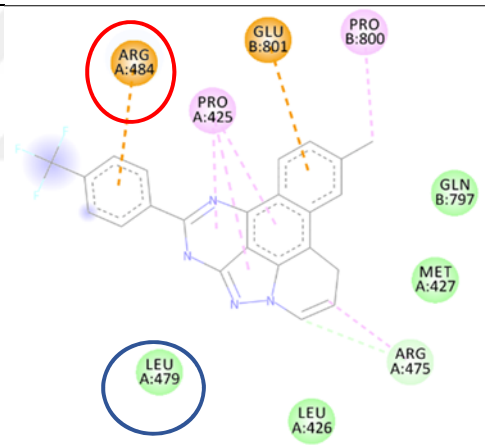
CN53019	-9.26	Left	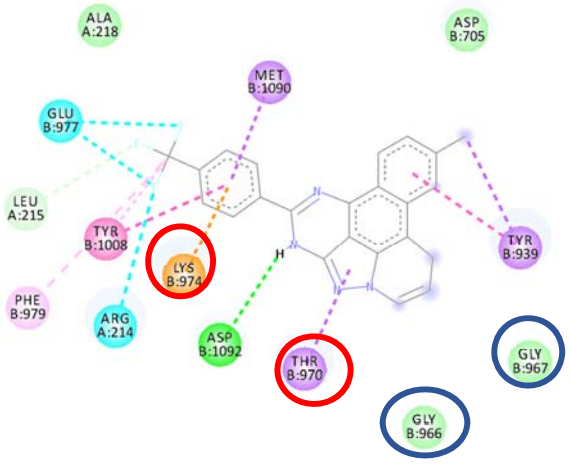

Table V: Residues of BmrA interacting with 5 ligands selected from first top 1000 ligands of Chimiothèque Nationale Library based on first strategy. (These ligands obeyed all drug-likeness rules except for MDDR-like) (Continue).

Ligand Name	Binding Energy (Kcal/mol)	Region	Interacting Residues
CN52716	-11.06	Right	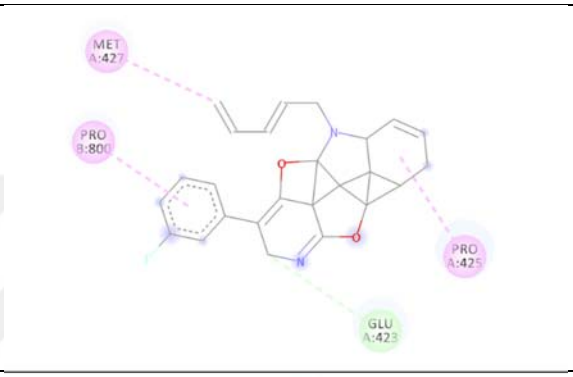
CN52716	-10.33	Cavity	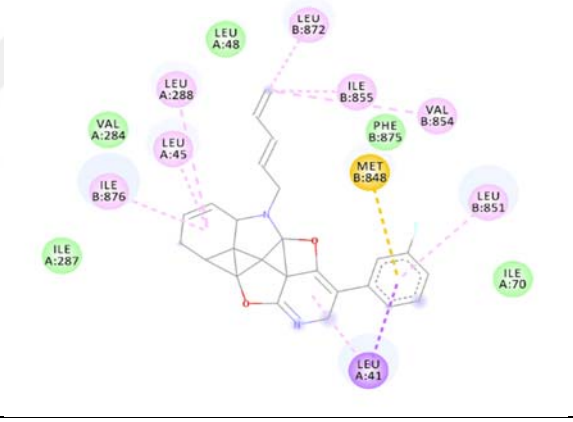
CN52716	-8.46	Left	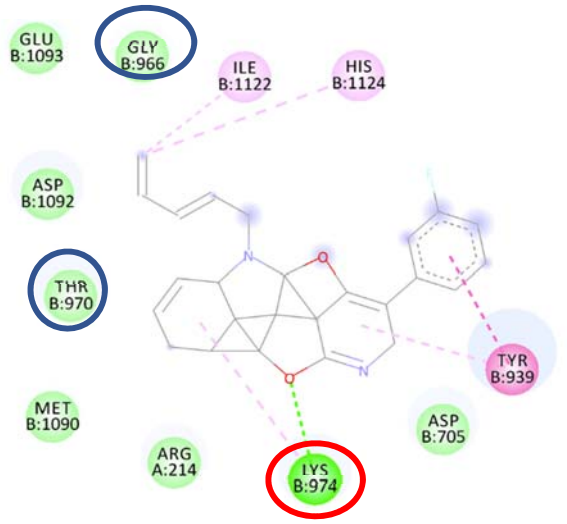

Table VI: Residues of BmrA interacting with the ligands whose binding energy difference is 0 kcal/mol, selected based on the second strategy (These ligands obeyed all drug-likeness rules).

Ligand Name	Binding Energy (Kcal/mol)	Region	Interacting Residues
CN53952	-8.18	Right	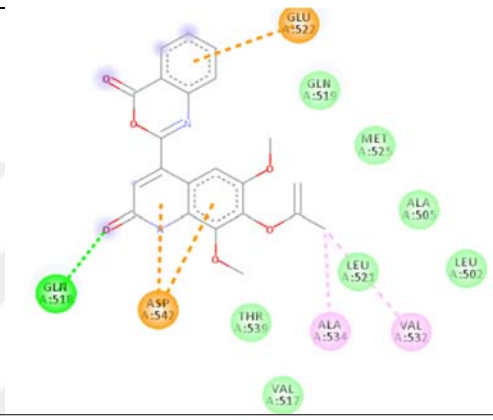
CN53952	-8.18	Left	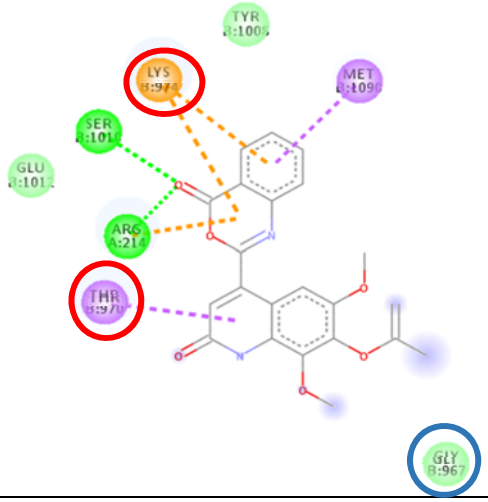

Table VI: Residues of BmrA interacting with the ligands whose binding energy difference is 0 kcal/mol, selected based on the second strategy (These ligands obeyed all drug-likeness rules) (Continue).

Ligand Name	Binding Energy (Kcal/mol)	Region	Interacting Residues
CN54578	-7.94	Right	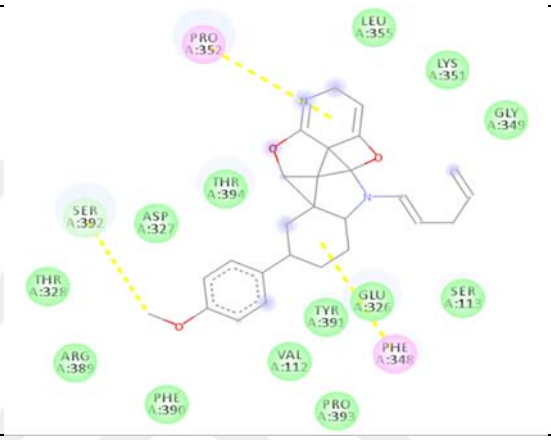
CN54578	-7.94	Left	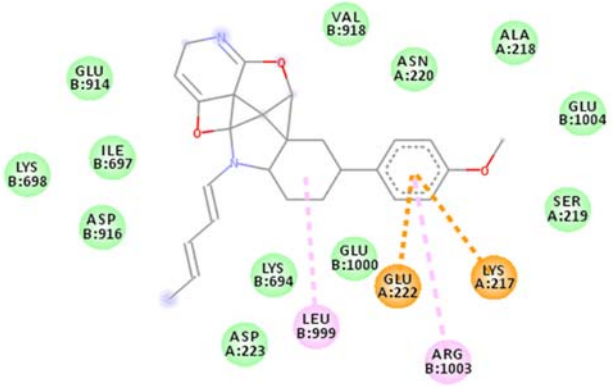

Table VII: Residues of BmrA interacting with the ligands whose binding energy difference is 0 kcal/mol, selected based on the second strategy (These ligands obeyed all drug-likeness rules except for MDDR-like rule).

Ligand Name	Binding Energy (Kcal/mol)	Region	Interacting Residues
CN52150	-9.5	Right	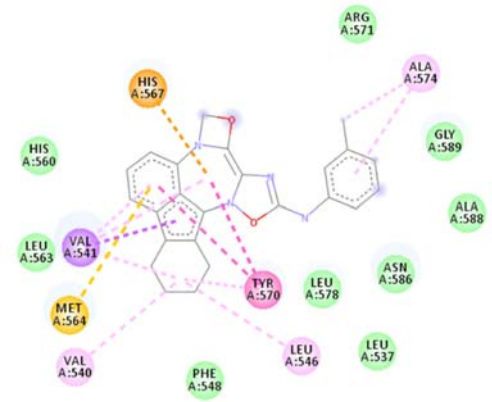
CN52150	-9.5	Left	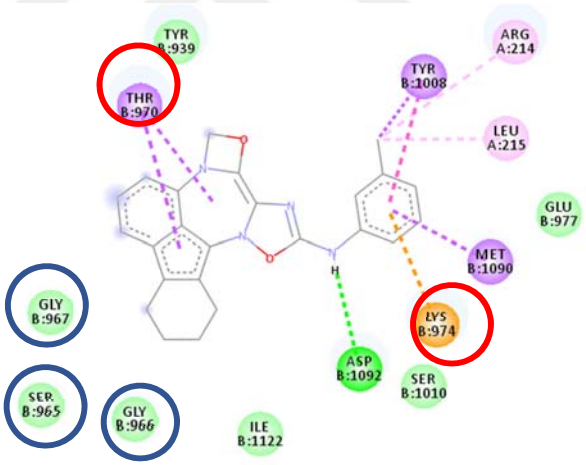
CN55373	-8.9	Right	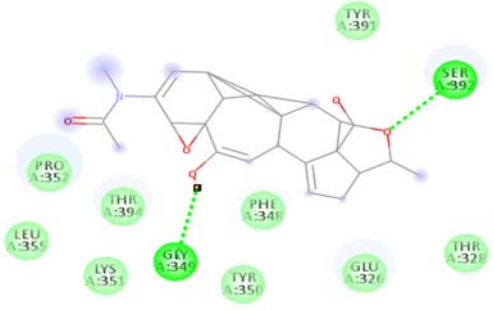

Table VII: Residues of BmrA interacting with the ligands whose binding energy difference is 0 kcal/mol, selected based on the second strategy (These ligands obeyed all drug-likeness rules except for MDDR-like rule) (Continue).

Ligand Name	Binding Energy (Kcal/mol)	Region	Interacting Residues
CN55373	-8.9	Left	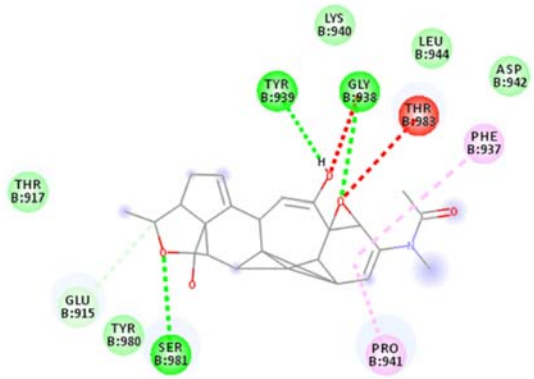
CN50901	-8.6	Right	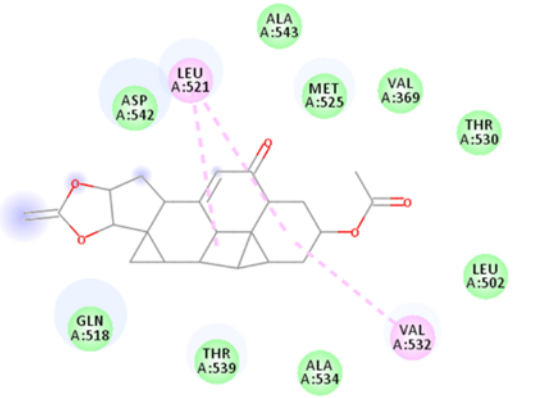
CN50901	-8.6	Left	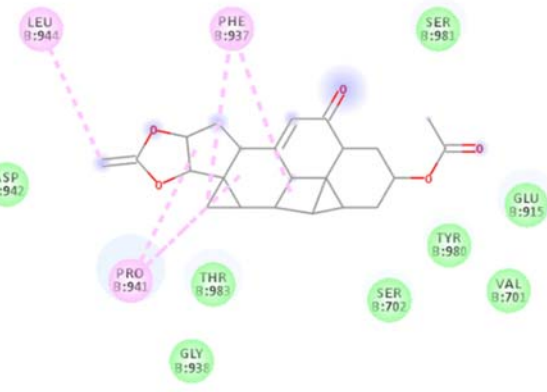

Table VII: Residues of BmrA interacting with the ligands whose binding energy difference is 0 kcal/mol, selected based on the second strategy (These ligands obeyed all drug-likeness rules except for MDDR-like rule) (Continue).

Ligand Name	Binding Energy (Kcal/mol)	Region	Interacting Residues
CN51977	-8.3	Right	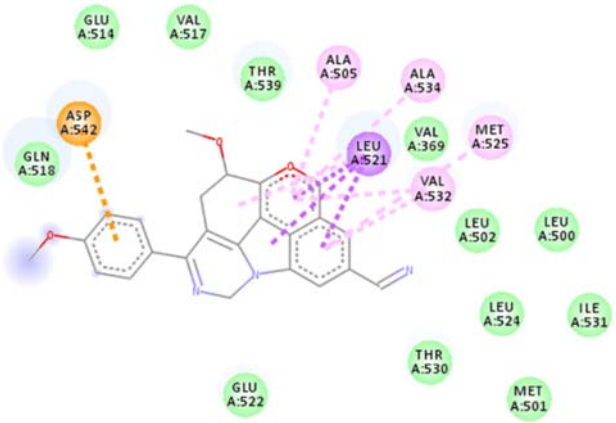
CN51977	-8.3	Left	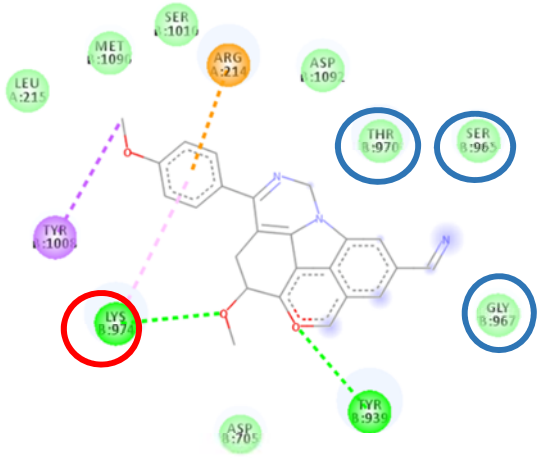
CN53545	-8.14	Right	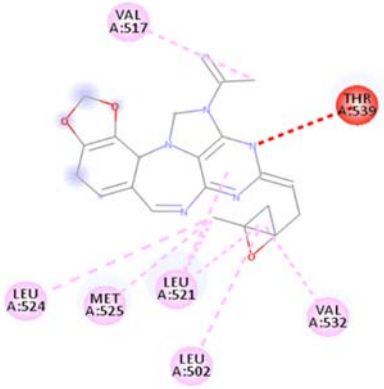

Table VII: Residues of BmrA interacting with the ligands whose binding energy difference is 0 kcal/mol, selected based on the second strategy (These ligands obeyed all drug-likeness rules except for MDDR-like rule) (Continue).

Ligand Name	Binding Energy (Kcal/mol)	Region	Interacting Residues
CN53545	-8.14	Left	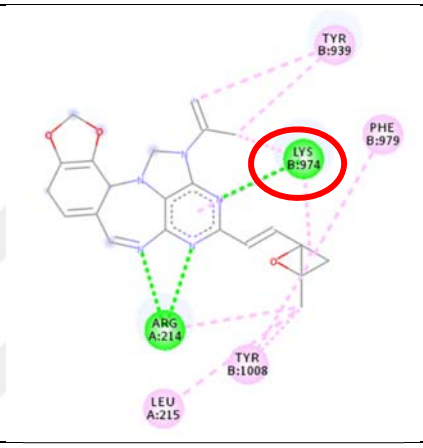
CN48004	-8.1	Right	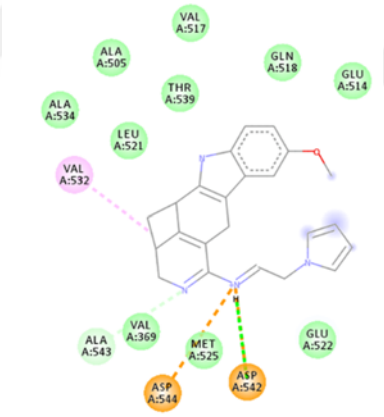
CN48004	-8.1	Left	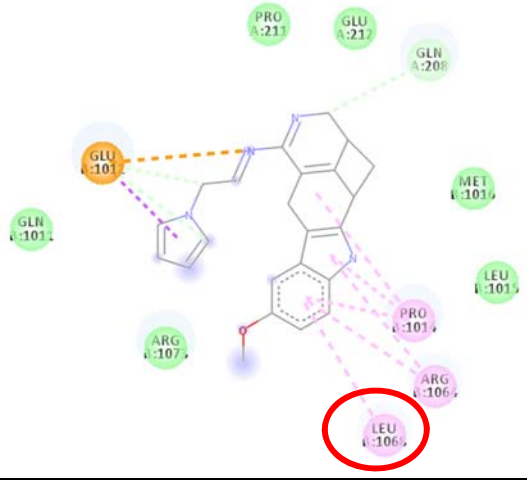

Table VIII: Residues of BmrA interacting with the ligands whose binding energy difference is between 0 kcal/mol and 0.02 kcal/mol, selected based on the second strategy (These ligands obeyed all drug-likeness rules).

Ligand Name	Binding Energy (Kcal/mol)	Region	Interacting Residues
CN54268	-9.22	Right	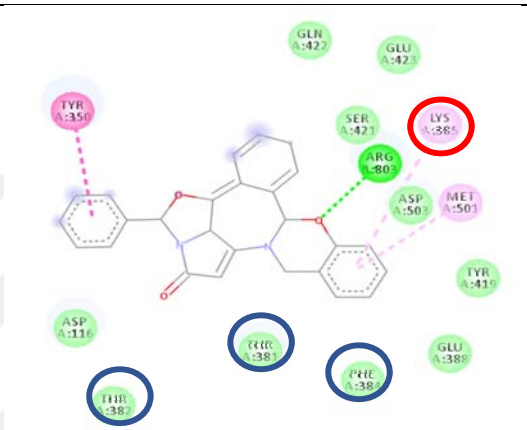
CN54268	-9.2	Left	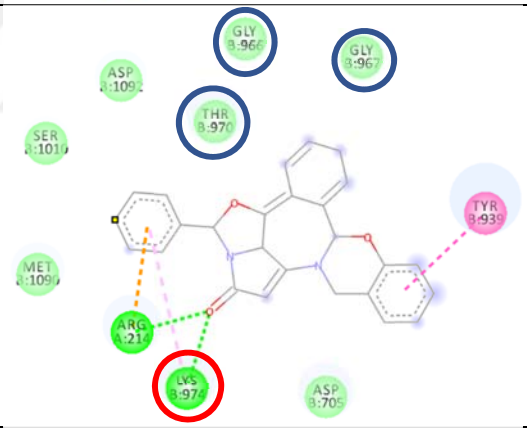
CN52559	-8.86	Right	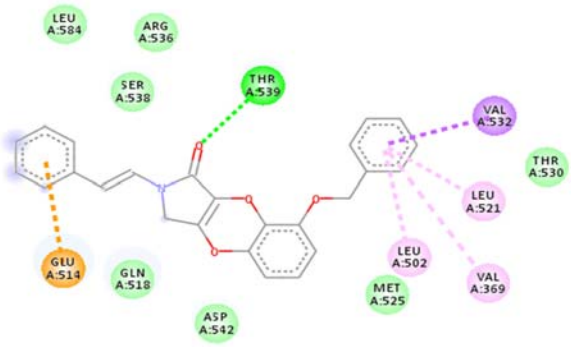

Table VIII: Residues of BmrA interacting with the ligands whose binding energy difference is between 0 kcal/mol and 0.02 kcal/mol, selected based on the second strategy (These ligands obeyed all drug-likeness rules) (Continue).

Ligand Name	Binding Energy (Kcal/mol)	Region	Interacting Residues
CN52559	-8.84	Left	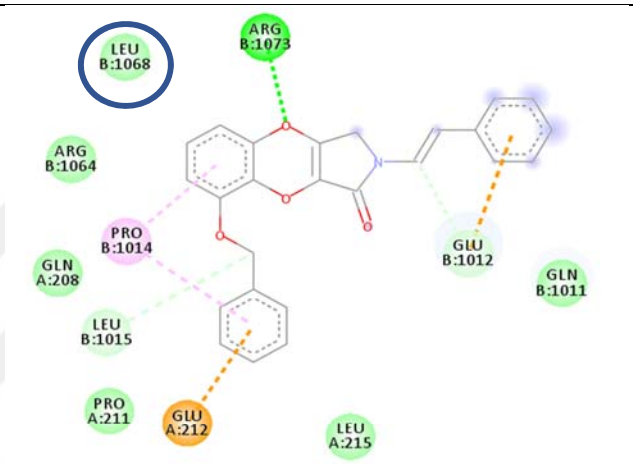
CN53648	-8.7	Right	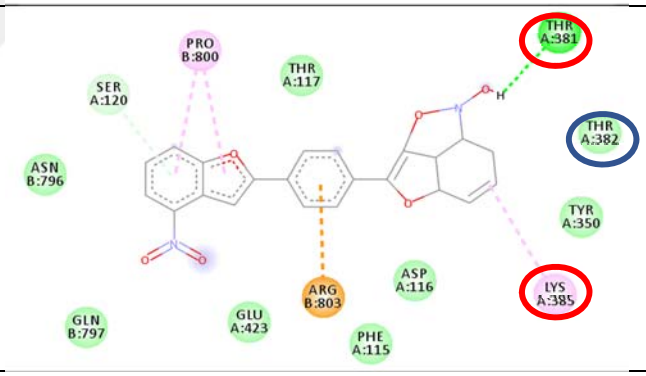
CN53648	-8.67	Left	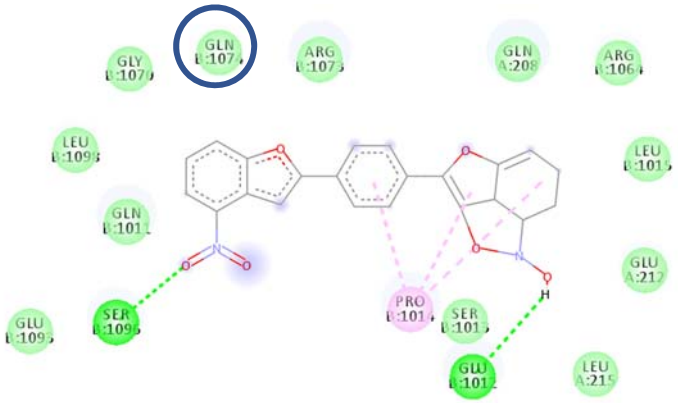

Table VIII: Residues of BmrA interacting with the ligands whose binding energy difference is between 0 kcal/mol and 0.02 kcal/mol, selected based on the second strategy (These ligands obeyed all drug-likeness rules) (Continue).

Ligand Name	Binding Energy (Kcal/mol)	Region	Interacting Residues
CN53428	-8.5	Right	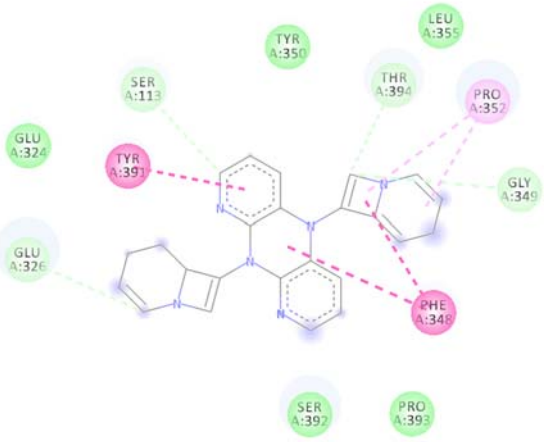
CN53428	-8.48	Left	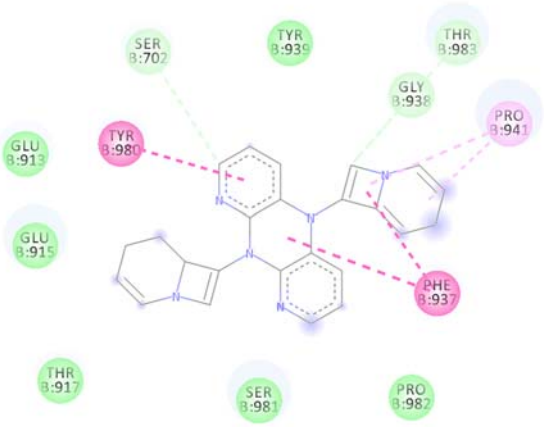

Table IX: Residues of BmrA interacting with the ligands whose binding energy difference is between 0 kcal/mol and 0.02 kcal/mol, selected based on the second strategy (These ligands obeyed all drug-likeness rules except for MDDR-like rule).

Ligand Name	Binding Energy (Kcal/mol)	Region	Interacting Residues
CN51349	-9.48	Right	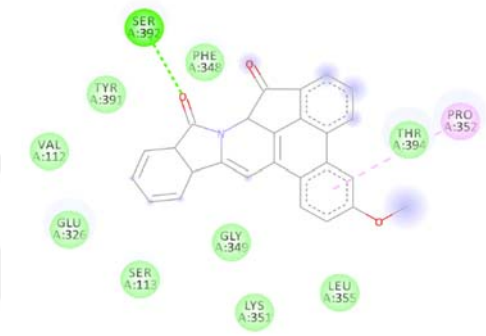
CN51349	-9.5	Left	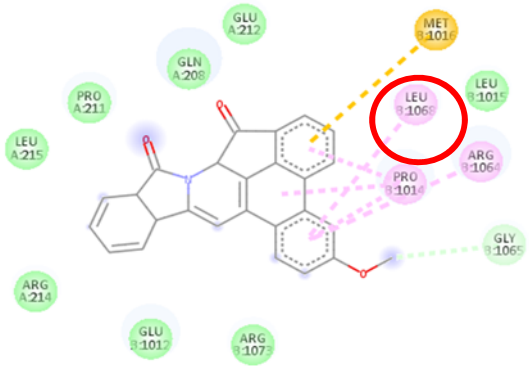
CN54733	-9.3	Right	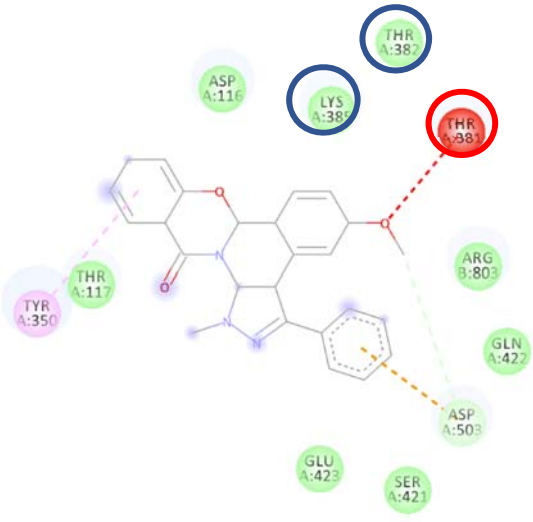

Table IX: Residues of BmrA interacting with the ligands whose binding energy difference is between 0 kcal/mol and 0.02 kcal/mol, selected based on the second strategy (These ligands obeyed all drug-likeness rules except for MDDR-like rule) (Continue).

Ligand Name	Binding Energy (Kcal/mol)	Region	Interacting Residues
CN54733	-9.32	Left	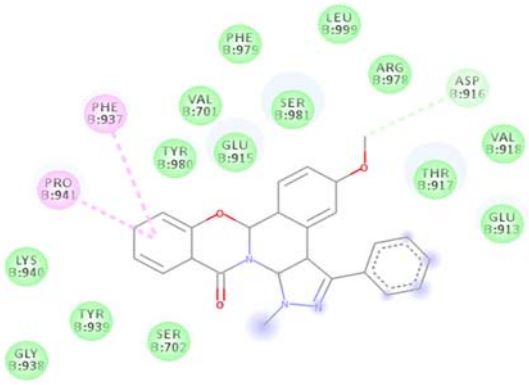
CN52909	-8.92	Right	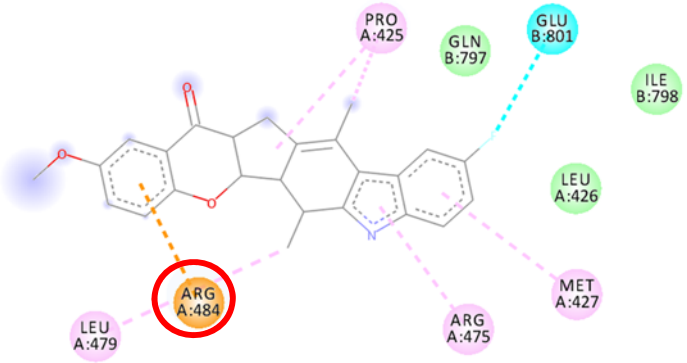
CN52909	-8.90	Left	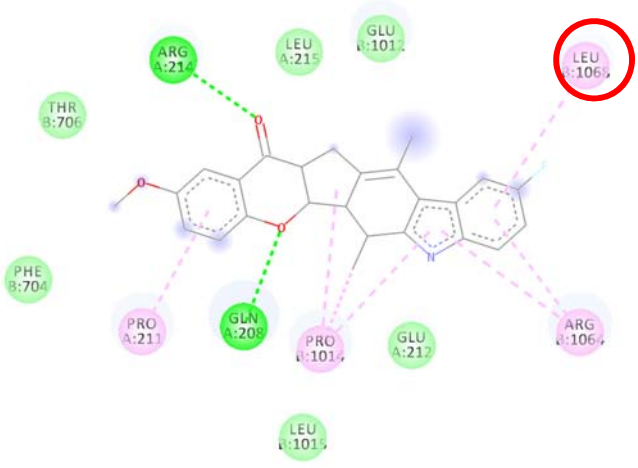

Table IX: Residues of BmrA interacting with the ligands whose binding energy difference is between 0 kcal/mol and 0.02 kcal/mol, selected based on the second strategy (These ligands obeyed all drug-likeness rules except for MDDR-like rule) (Continue).

Ligand Name	Binding Energy (Kcal/mol)	Region	Interacting Residues
CN52713	-8.42	Right	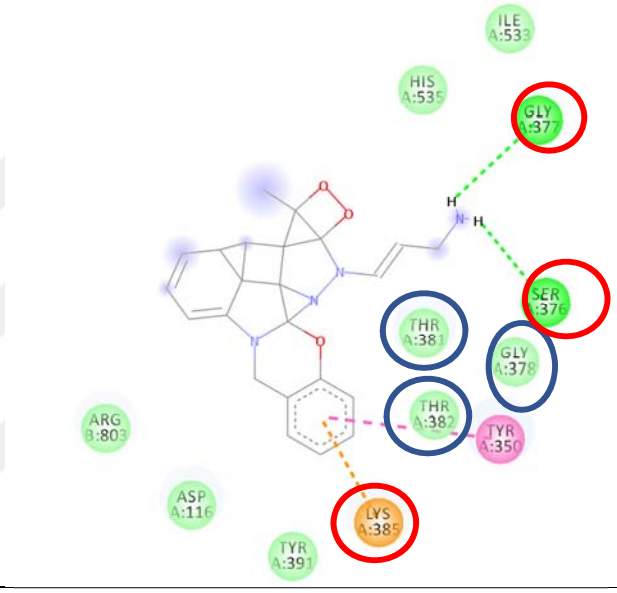
CN52713	-8.40	Left	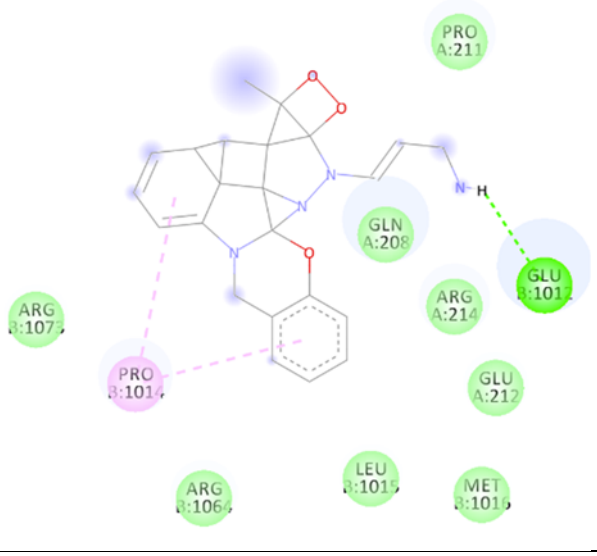

Table IX: Residues of BmrA interacting with the ligands whose binding energy difference is between 0 kcal/mol and 0.02 kcal/mol, selected based on the second strategy (These ligands obeyed all drug-likeness rules except for MDDR-like rule) (Continue).

Ligand Name	Binding Energy (Kcal/mol)	Region	Interacting Residues
CN54281	-8.3	Right	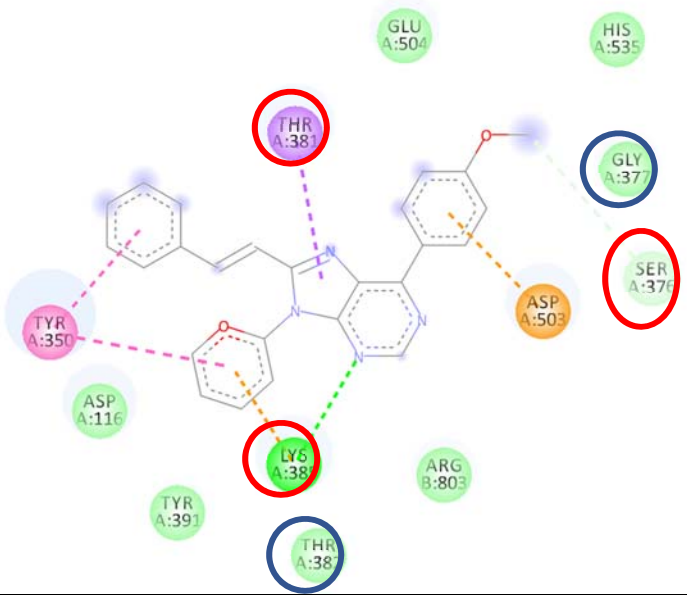
CN54281	-8.28	Left	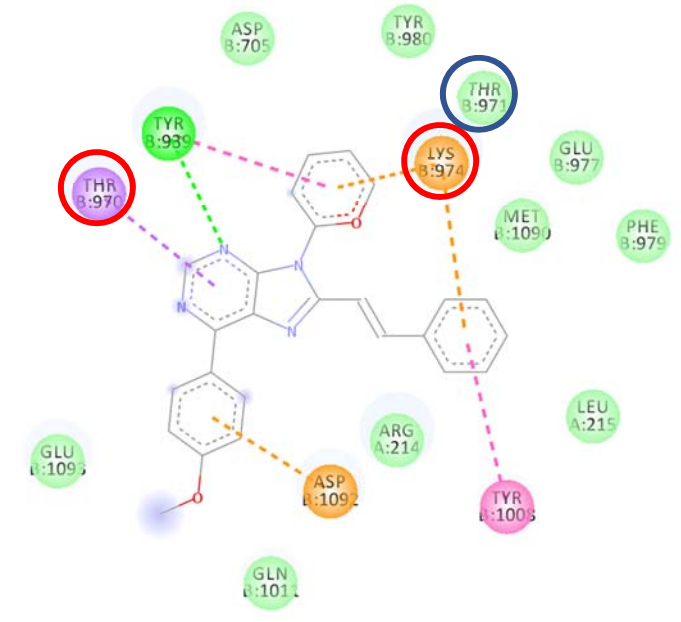

Table IX: Residues of BmrA interacting with the ligands whose binding energy difference is between 0 kcal/mol and 0.02 kcal/mol, selected based on the second strategy (These ligands obeyed all drug-likeness rules except for MDDR-like rule) (Continue).

Ligand Name	Binding Energy (Kcal/mol)	Region	Interacting Residues
CN53219	-7.88	Right	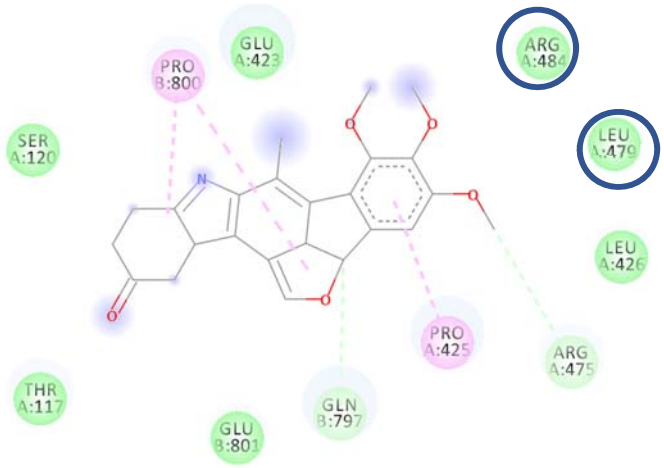
CN53219	-7.86	Left	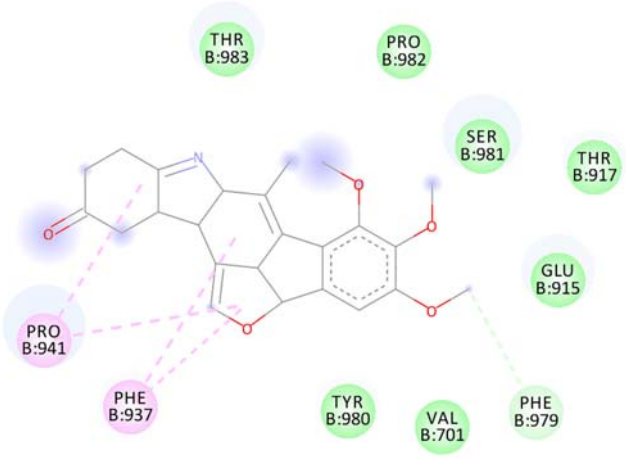

Table X: Residues of BmrA interacting with the ligands whose binding energy difference is between 0.02 kcal/mol and 0.04 kcal/mol, selected based on the second strategy (These ligands obeyed all drug-likeness rules).

Ligand Name	Binding Energy (Kcal/mol)	Region	Interacting Residues
CN52562	-9.10	Right	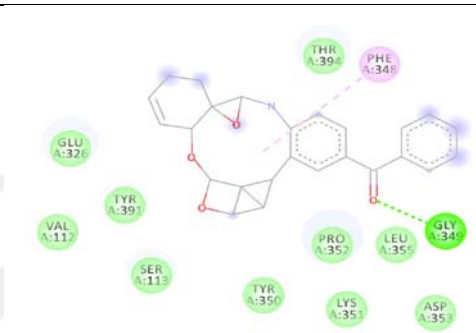
CN52562	-9.14	Left	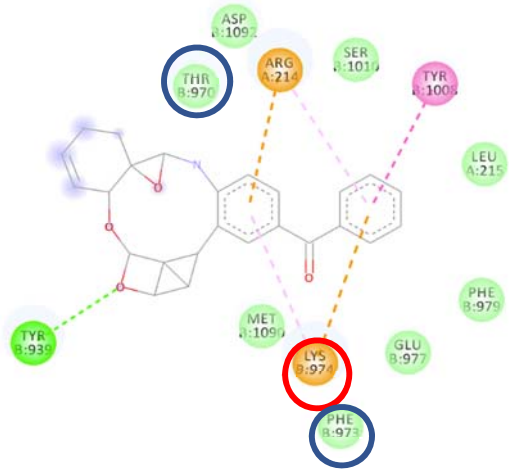
CN53026	-8.56	Right	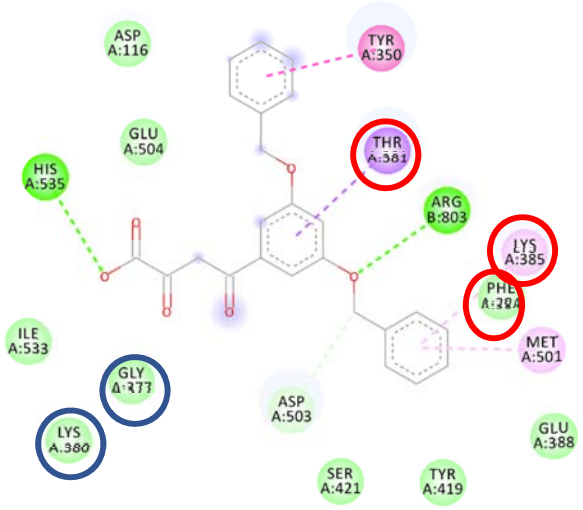

Table X: Residues of BmrA interacting with the ligands whose binding energy difference is between 0.02 kcal/mol and 0.04 kcal/mol, selected based on the second strategy (These ligands obeyed all drug-likeness rules) (Continue).

Ligand Name	Binding Energy (Kcal/mol)	Region	Interacting Residues
CN53026	-8.52	Left	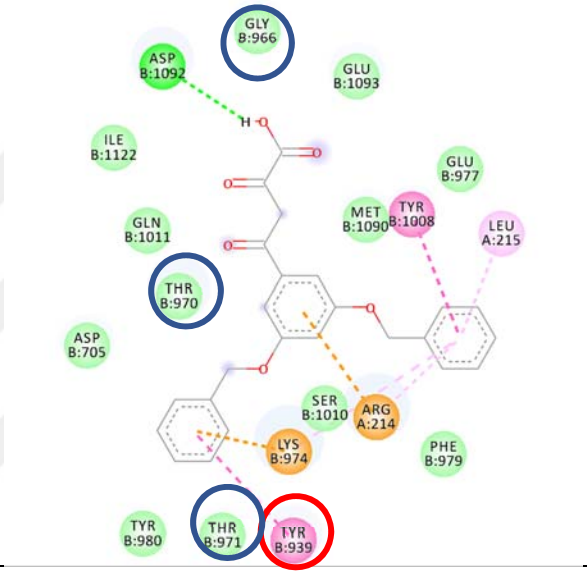
CN53196	-8.16	Right	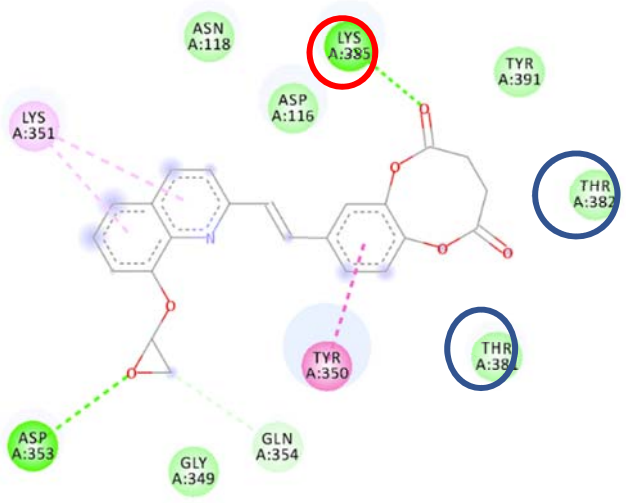

Table X: Residues of BmrA interacting with the ligands whose binding energy difference is between 0.02 kcal/mol and 0.04 kcal/mol, selected based on the second strategy (These ligands obeyed all drug-likeness rules) (Continue).

Ligand Name	Binding Energy (Kcal/mol)	Region	Interacting Residues
CN53196	-8.12	Left	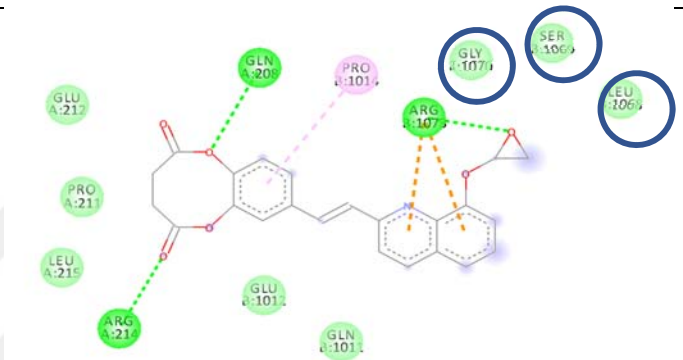
CN50557	-8.1	Right	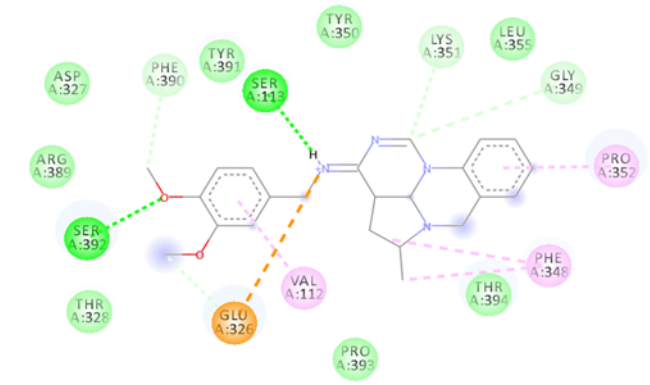
CN50557	-8.06	Left	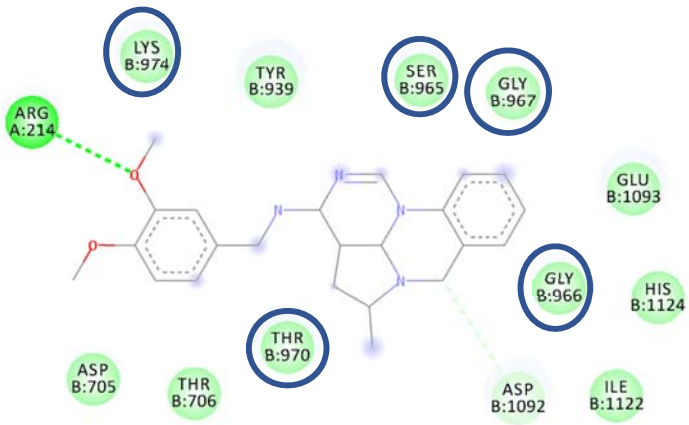

Table XI: Residues of BmrA interacting with the ligands whose binding energy difference is between 0.02 kcal/mol and 0.04 kcal/mol, selected based on the second strategy (These ligands obeyed all drug-likeness rules except for MDDR-like rule).

Ligand Name	Binding Energy (Kcal/mol)	Region	Interacting Residues
CN52318	-8.56	Right	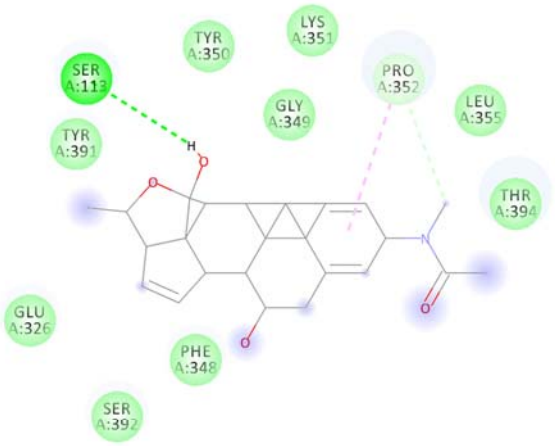
CN52318	-8.52	Left	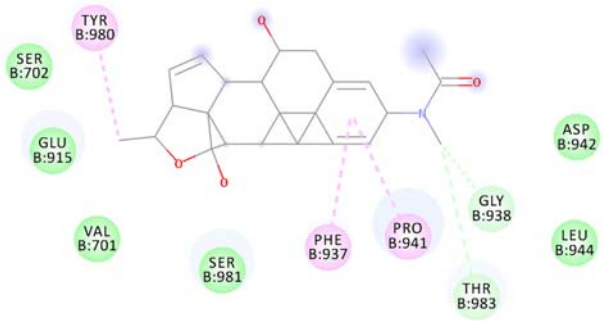
CN43483	-8.54	Right	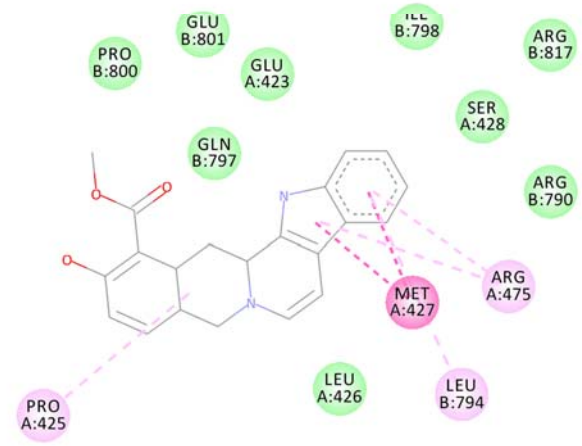

Table XI: Residues of BmrA interacting with the ligands whose binding energy difference is between 0.02 kcal/mol and 0.04 kcal/mol, selected based on the second strategy (These ligands obeyed all drug-likeness rules except for MDDR-like rule) (Continue).

Ligand Name	Binding Energy (Kcal/mol)	Region	Interacting Residues
CN43483	-8.5	Left	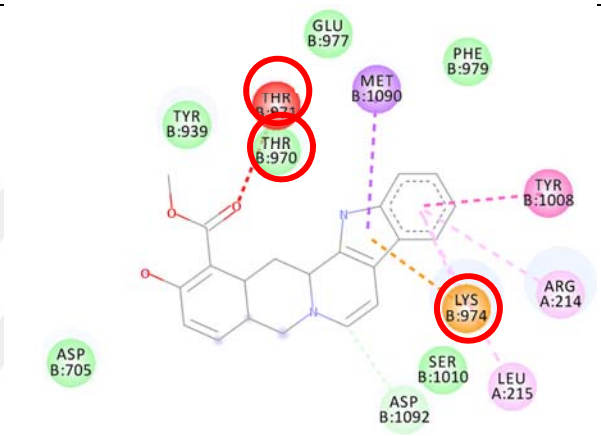
CN54231	-8.08	Right	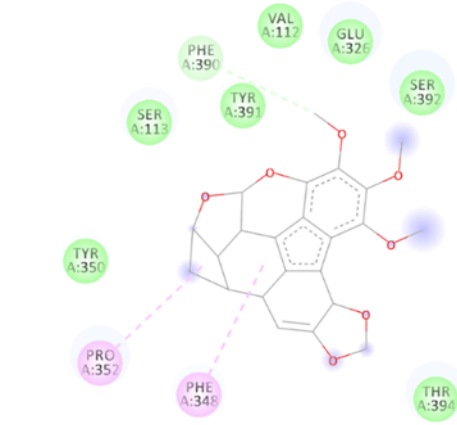
CN54231	-8.04	Left	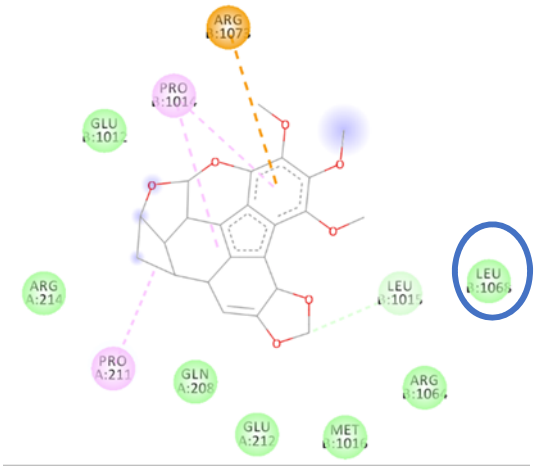

AUTOBIOGRAPHY

Name Surname **:** Duygu ŞENTÜRK KARAGÖZ

Place and Date of Birth **:** Istanbul / 14.08.1993

Foreign Language **:** English

E-mail **:** bioeng.duygusenturk@gmail.com

EDUCATION

Degree	Department / Program	University / High School	Graduation Year
High School	Science	Istanbul Uskudar Anatolian High School	2011
Bachelor of Science	Bioengineering	Marmara University	2016

PRESENTATIONS

1. Berna SARIYAR AKBULUT, Duygu ŞENTÜRK KARAGÖZ, Onur SERÇİNOĞLU, Pemra ÖZBEK SARICA, Cedric ORELLE, Jean-Michel JAULT, "Virtual Screening of Chemotheca for The BmrA Pump", MuTaLig COST Annual Meeting, Valletta / Malta, October 2018.
2. Duygu ŞENTÜRK KARAGÖZ, Onur SERÇİNOĞLU, Berna SARIYAR AKBULUT, Pemra ÖZBEK SARICA, Cedric ORELLE, Jean-Michel JAULT, "Virtual Screening for Inhibitors of The BmrA Pump", 11th International Symposium on Health Informatics and Bioinformatis, Antalya / Turkey, October 2018.

3. Duygu ŞENTÜRK KARAGÖZ, Onur SERÇİNOĞLU, Berna SARIYAR AKBULUT, Pemra ÖZBEK SARICA, Cedric ORELLE, Jean-Michel JAULT, “Novel Inhibitors of The BmrA Pump With Virtual Screening”, 6th International BAU Drug Design Congress, Istanbul / Turkey, December 2018.